ABSTRACT

Title of Dissertation:	REGULATION OF GENE EXPRESSION BY FC RECEPTOR CROSS-LINKING IN PRIMARY HUMAN MACROPHAGES
	Elizabeth Ryland Dalby, Doctor of Philosophy, 2017
Dissertation directed by:	Dr. David M. Mosser, Professor Department of Cell Biology & Molecular Genetics

Macrophages can adopt an anti-inflammatory phenotype through exposure to TLR ligands together with immune complexes (IC). However, a thorough investigation of this phenotype in human macrophages has not yet been performed. In this work, we sought to characterize IC-induced regulatory activation in primary human macrophages (R-Mϕ-IC). Analysis of the transcriptome and secretome revealed broad suppression of inflammatory molecules, and an upregulation of molecules involved in angiogenesis and the resolution of inflammation. RNAscope and flow cytometry analysis identified MMP-10 and DC-STAMP, among others, as potential biomarkers for this activation state. Pathway analysis predicted the activation of the Akt and ERK signaling pathways, which further studies confirmed were activated in these cells. Inhibition of

Akt and ERK led to a suppression of R-Mϕ-IC gene transcription, with Akt inhibition having a greater effect. Since GSK3 is a direct substrate of Akt, activation of this kinase was also investigated. The addition of IC to cells stimulated with lipopolysaccharide (LPS) significantly prevented the entry of GSK3 into the nucleus, while small-molecule inhibition of GSK3 phenocopied IC co-stimulation. To determine if GSK3 inhibition had anti-inflammatory activity, mice were injected intraperitoneally with macrophages treated with LPS and GSK3β-specific inhibitor. Compared to mice injected with macrophages stimulated only with LPS, the mice in the test group were slightly protected from lethal endotoxemia, but these results were not statistically significant (p-value = 0.063). Together these data are consistent with an anti-inflammatory role for Fc receptor cross-linking, and highlight the importance of the Akt/GSK3 signaling pathway in this activity.

REGULATION OF GENE EXPRESSION BY FC RECEPTOR CROSS-LINKING
IN PRIMARY HUMAN MACROPHAGES

by

Elizabeth R. Dalby

Dissertation submitted to the Faculty of the Graduate School of the
University of Maryland, College Park, in partial fulfillment
of the requirements for the degree of
Doctor of Philosophy
2017

Advisory Committee:
 Professor David M. Mosser, Chair
 Professor Jeffrey DeStefano
 Professor Najib El-Sayed
 Professor Wenxia Song
 Professor Xiaoping Zhu

Dedication

This thesis is dedicated to my son Bruce.

Acknowledgements

First of all, I owe huge thanks to Dr. Mosser, who gave me the independence I needed to get my project started, and the guidance I needed to get it finished. I can't thank him enough for remaining patient with me these past five years. I thank my parents and my partner Carlos for their invaluable love and support, and my friend Andrew for making me laugh when I really needed to. I owe thanks to Bryan and Rahul for their advice and technical guidance as I was first learning the ropes, and Andy Stewart for his advice when I was first navigating my way through the early stages of my project. I must also thank Gail and Jared Gerhart for their contribution; they worked hard and sacrificed a lot to be there for Bruce as I went through this process, and I could not have done it without them. Finally, I would like to thank my friend Prabha Chandrasekaran, whose cheery attitude, impressive research skills, and unbelievable generosity helped me graduate even under tremendous stress.

Table of Contents

List of Tables

List of Figures

List of Illustrations

List of Abbreviations

AP-1	Activator protein 1
APC	Allophycocyanin
ATP	Adenosine triphosphate
BCA	Bicinchoninic acid
bFGF	Basic fibroblast growth factor
bp	Base pairs
BMDMs	Bone marrow-derived macrophages
cAMP	cyclic adenosine monophosphate
CCL	C-C chemokine ligand
CD	Cluster of differentiation
cDNA	Complementary deoxyribonucleic acid
CREB	cAMP response element
CXCL	C-X-C chemokine ligand
DAMPs	Damage-associated molecular patterns
DC-STAMP	Dendritic Cell-Specific Transmembrane Protein
DEG	Differentially expressed gene
DNA	Deoxyribonucleic acid
dsDNA	Double-stranded DNA
ECM	Extracellular matrix
EGF	Epidermal growth factor
ELISA	Enzyme-linked immunosorbent assay
ERK	Extracellular signal-regulated kinases

FcR	Fc (fragment crystallizable region) receptor
FACS	Fluorescence activated cell sorting
FC	Flow cytometry
FDR	False discovery rate
FFPE	Formalin-fixed paraffin-embedded
FITC	Fluorescein isothiocyanate
FBS	Fetal bovine serum
G-CSF	Granulocyte colony stimulating factor
GSEA	Gene set enrichment analysis
GSK3	Glycogen synthase kinase 3
HB-EGF	Heparin-binding EGF-like growth factor
HMDMs	Human monocyte-derived macrophages
IC	Immune complex
IFN	Interferon
Ig	Immunoglobulin
IL-	Interleukin
IKK	IκB kinase
Inhb	Inhibitor
IP	Intraperitoneal
IPA	Ingenuity Pathway Analysis
IRAK	Interleukin 1 Receptor Associated Kinase
IRF	Interferon regulatory factor
ITAM	Immunoreceptor tyrosine-based activation motif

ITIM	Immunoreceptor tyrosine-based inhibition motif
JNK	c-Jun N-terminal kinase
kb	Kilobase
KEGG	Kyoto Encyclopedia of Genes and Genomes
LIF	Leukemia inhibitory factor
LPS	Lipopolysaccharide
Mϕ	Macrophage
Mϕ-LPS	Macrophages stimulated with LPS
Mϕ-NS	Macrophages that are not stimulated
MAPK	Mitogen activated protein kinase
M-CSF	Macrophage colony stimulating factor
MEK	Mitogen-activated protein kinase kinase
MFI	Mean fluorescence intensity
mL	milliliter
mg	milligram
mM	millimolar
μM	micromolar
MMP	matrix metalloproteinase
mRNA	messenger ribonucleic acid
MyD88	Myeloid differentiation primary response gene 88
mTORC	Mammalian target of rapamycin complex
nM	nanomolar
NES	Normalized enrichment score

NF-κB	Nuclear factor κB
ng	Nanogram
NK cells	Natural killer cells
PAMPs	Pathogen-associated molecular patterns
PBMCs	Peripheral blood mononuclear cells
PBS	Phosphate buffered saline
PCA	Principal component analysis
PCR	Polymerase chain reaction
PE	Phycoerythrin
PGE2	Prostaglandin E2
PI3K	Phosphatidylinositol-4,5-bisphosphate 3-kinase
PM	Plasma membrane
PRR	Pattern recognition receptor
qRT-PCR	Quantitative real time polymerase chain reaction
R-Mϕ	Regulatory macrophages
R-Mϕ-IC	Regulatory macrophages induced by immune complexes
Raf	Rapidly Accelerated Fibrosarcoma
RFU	Relative fluorescence units
RIPA	Radioimmunoprecipitation assay
RNA	Ribonucleic acid
RNA-seq	RNA-sequencing
RPKM	Reads per kilobase per million
SEM	Standard error of the mean

Sp1   Specificity protein 1

STAT   Signal transducers and activators of transcription

sTLR   Soluble toll-like receptor

Syk   Spleen tyrosine kinase

TBK1   Serine/threonine-protein kinase

Th1   T helper 1 type response

Th2   T helper 2 type response

TLR   Toll-like receptor

TM4SF1   Transmembrane 4 L6 family member 1

TNF   Tumor necrosis factor

TRAF   TNF receptor associated factor

TREM1   Triggering Receptor Expressed On Myeloid Cells 1

TRIF   TIR domain-containing adaptor protein inducing IFNβ

TSC1   Tuberous sclerosis 1

μl   Microliter

VEGF   Vascular endothelial growth factor

WCL   Whole cell lysate

XIRP1   Xin actin-binding repeat-containing protein 1

Acknowledgement of Assistance

Chapter 1: Introduction

1.1 Innate Immunity

Innate immunity refers to the non-adaptive branch of the immune system and broadly refers to any cell, tissue or fluid in the body that serves to defend the host against foreign organisms, and that does not have an adaptive component[1]. This therefore includes anatomical barriers such as skin, tears and mucous, and digestive enzymes, as well non-cellular systems such as inorganic chemicals and the complement cascade. It is thought that this system developed earlier in our evolutionary history than did the adaptive arm of the immune system, as it is present in most invertebrates, whereas the adaptive response is mainly expressed in higher vertebrate species[2]. The cells that make up the innate immune system include neutrophils, dendritic cells, macrophages, mast cells, eosinophils, basophils and NK cells. These cells are important in initiating inflammation, and are equipped with an array of pattern recognition receptors that recognize danger signals in order to activate an appropriate immune response[3]. Although these receptors are able to detect a wide variety of pathogen-associated molecular patterns (PAMPs)[4], this system is unable to develop memory or specificity for particular antigens. It has the advantage of triggering a rapid response that includes cytokine production, recruitment of other immune cells, destruction of pathogens, and antigen presentation to T cells[5], the latter of which makes innate immunity indispensable for initiation of the adaptive immune response.

1.1.1 Macrophages

Macrophages are phagocytic white blood cells of the innate immune system that have a heightened capacity for digestion. These cells were first discovered in 1884 by Russian zoologist Élie Metchnikoff, who won the Nobel Prize in 1908 for his contribution to the understanding of immunity[6]. They are ubiquitous in the body in a resting state, and are known for taking on specialized roles depending on which tissue they inhabit[7]. Beyond the clearance of dead cells and tissue debris[8], macrophages are sentinel cells that can activate an immune response upon exposure to pathogens. Macrophages demonstrate a remarkable level of tissue diversity and an impressive ability to produce cytokines and other secreted factors in response to environmental cues. They are activated through exposure to pathogen- and damage-associated molecular patterns (PAMPS and DAMPs), at which point they drastically increase expression of chemokines, cytokines, leukotrienes and prostaglandins; these molecules orchestrate the host immune response and recruit other immune cells to the area[9]. Far from being relevant only during infection and damage, macrophages also reside under normal circumstances in the tissues where they have been found to be indispensable in maintaining homeostasis of the brain, bone, liver, gut, connective tissue, lung, lymph nodes, and spleen[10].

Macrophages were mainly thought to be derived from circulating blood monocytes that migrate into the tissues[11] where they differentiate via exposure to macrophage-colony stimulating factor (M-CSF). More recently, however, it has been reported that some resident tissue macrophages are derived from tissue-resident stem cells originating from the yolk sac component of the embryonic tissue[12]. Monocyte-

derived macrophages are triggered to migrate into tissue during infection and damage[13], at which point they can remain in the tissues for the remainder of their lifespan as tissue-resident macrophages.

1.2 Macrophage Functions

Macrophages have diverse roles in the body, including clearance of debris, recognition and destruction of pathogens, iron recycling, bone resorption, iron storage, cytokine production, immune regulation, wound healing, antigen presentation, ingestion of neutrophils, ingestion of cholesterol, muscle regeneration after exercise[14], angiogenesis, thermoregulation[15], and neuronal trimming[16]. The versatility of macrophages is made possible by its tissue heterogeneity; specifically, the specialization of the macrophage is determined by exposure to tissue-specific molecules during the macrophage's differentiation. This effect is mediated through the activation of a tissue-specific enhancer regions, which preferentially promote transcription of certain genes dependent on exposure to factors in the extracellular milieu. The tissue-specific mediators also trigger the expression of transcription factors that function together with the lineage-determining transcription factor PU.1 to establish these enhancer regions[17], setting the stage for the macrophages' genetic responses throughout its lifespan.

1.2.1 Phagocytosis

The ability to engulf and digest pathogens and particles is a function of great practical importance[18]. The macrophage is especially equipped for this task, as its amoeboid characteristics allow it to move easily through tissue and engulf even very

large objects. It is known as a "professional phagocyte", due to its expression of FcRs and complement receptors[19,20]. These receptors allow macrophages to recognize and respond appropriately to its target. Furthermore, its arsenal of digestive enzymes, free radicals and other chemicals serves to give it superior digestive capabilities. For this reason, macrophages are considered important not only for janitorial purposes, but also as pathogen killers.

1.2.2 Cytokines and chemokines

Macrophages are a potent and important producer of cytokines and chemokines. These small and relatively unstable proteins are important mediators for intracellular communication, not only among immune cells, but also between immune cells and tissue cells. Ligation of TLRs or other pattern recognition receptors (PRRs) activates several cytosolic signaling molecules such as NFκB, ERK, p38, and interferon regulatory factors (IRFs), covered in more detail in subsequent sections. These molecules lead to upregulation in gene expression of potent inflammatory molecules such as TNFα, IL-1β IL-6, IL-12, and an array of chemokines such as CXCR6, which serve to recruit other immune cells to the area. The type, total amount, and proportions of these proteins that macrophages secrete can profoundly influence the behaviors of surrounding cells. This flexibility and plasticity allows the macrophage to orchestrate a sophisticated response appropriate to the pathogen or damage at hand.

Macrophages are also an important source of IL-10, a cytokine with broad immunosuppressive activity that plays a pivotal role in the suppression of inflammation[21,22]. Knockout mice lacking this important immune regulator have a higher basal level of IL-1 and IFNγ[23], and an increased susceptibility to LPS-induced

4

sepsis[24], colon carcinoma[23], and parasitic infections[25]. IL-10 knockout mice also develop spontaneous enterocolitis[26], the mechanism for which appears to be dependent on the production of IL-1[27], a proinflammatory cytokine that is powerfully inhibited by IL-10[28]. More than a dozen transcriptional regulators have been confirmed as redundantly involved in IL-10 transcription, with NFκB, STAT3, Sp1, and CREB being among the best characterized thus far[29].

1.2.3 Matrix metalloproteinases

Activated monocytes and macrophages are considered among the most important producers of matrix metalloproteinases, enzymes involved in tissue remodeling and angiogenesis. Matrix metalloproteinases (MMPs) were first discovered in 1962 in cultured tadpole tissue[30]. These proteases are secreted by endothelial cells, epithelial cells, and immune cells, and although they are not expressed under normal physiological conditions, they are collectively indispensable for tissue remodeling and angiogenesis[31]. Different types of MMPs are capable of degrading various types of extracellular matrix components such as collagen, elastin, and fibronectin, but have also been found to degrade and thus inactivate bioactive molecules including cytokines[32–35]. Monocytes and macrophages can produce high levels of various types of MMPs in inflammatory or other activating conditions, which contributes to tissue remodeling and angiogenesis necessary for tissue repair following infection[36,37]. The immunological activity of MMPs is still being studied, but knockout studies suggest that MMPs play a complex role that is both inflammatory and anti-inflammatory. For example, upon initial exposure to inflammatory stimuli, macrophages secrete MMPs, which then release TNFα from a membrane-bound inactive precursor[38]. These same

MMPs will later cleave chemokines, not only rendering them inactive but also able to act as chemokine receptor antagonists[34]. The diverse role of MMPs in both inflammation and healing makes them an exciting topic of research.

1.3 Macrophage polarization

1.3.1 Classical Activation

A "classically activated" macrophage is defined as one that has been primed with INFγ and stimulated with lipopolysaccharide, initially defined by their ability to kill intracellular pathogens. These cells undergo a drastic change in protein expression characterized by inflammatory cytokine secretion, cellular adhesion, and production of reactive oxygen species that destroy phagocytized pathogens[39]. Lipopolysaccharide (LPS) is a molecule found on the outer membrane of gram-negative bacteria and ligates TLR4 (along with CD14, LPS binding protein), initiating MYD88- and TRIF-dependent signaling cascades that eventually leads to the activation of transcription factors such as NFκB[40–42]. NFκB and other activated transcription factors trigger production of inflammatory cytokines such as TNFα and interleukin 1 (IL-1)[43], leading to generalized inflammatory activity. Simultaneously, LPS that leaks into the cytosol from vacuoles can directly bind caspase 11, triggering the assembly of the inflammasome complex necessary for activation of IL-1[44]. The priming of the macrophage with IFNγ greatly increases the strength and duration of the cytokine response to LPS[43]; furthermore, it leads to the induction of IRFs through the activation of the STAT1 transcription factor[45], which are important for the immune response against intracellular pathogens such as viruses[46]. Interestingly, IFNγ has the effect of

6

suppressing activity of the mTORC pathway, which is thought to be involved in the limiting of inflammatory responses after TLR ligation[47]. This mechanism could explain the ability for IFNγ priming to amplify the inflammatory response.

1.3.2 M1/M2 paradigm

In the 1990's the work of Siamon Gordon found that an "alternative" activation state of macrophages could be induced through stimulation with IL-4[48]. Treatment of macrophages with IL-4 upregulates mannose receptors and increases arginase production[49], with little to no production of nitric oxide or inflammatory molecules. These macrophages have been found to be highly important in host defense against helminthic parasites[50], homeostasis of adipose tissue[51], and in the later stages of wound healing[52]. These studies helped develop the paradigm of bimodal macrophage activation, wherein activated macrophages are thought to be polarized along a continuum, ranging from inflammatory (M1) to anti-inflammatory (M2). Classically activated macrophages, as well as those stimulated with PAMPs, DAMPs, and inflammatory cytokines, are all classified as M1, whereas all other activation states are classified as M2. Unfortunately, this model is an oversimplification. Although the introduction of this classification system contributed a great deal to the understanding of macrophage plasticity, enthusiastic attempts to fit all observations into this bipolar model have been problematic. Macrophages with any anti-inflammatory features have been incorrectly classified as subsets of M2, despite being physiologically quite distinct, and in some cases more closely resembling M1 macrophage activation[39,53]. It is for this reason that Mosser et al. introduced the color wheel model for macrophage

activation[39], in which a wide range of macrophage activation states exist (Illustration 1), covered in more detail in the following section.

1.3.3 Regulatory macrophages

A third activation state, known as regulatory macrophage (R-Mϕ) activation, has been identified and characterized[53]. These macrophages are stimulated with a TLR ligand (typically LPS) along with a second "reprogramming" signal that modulates the actions of the TLR ligand, leading to an anti-inflammatory phenotype. Several of these reprogramming signals have been characterized, including, but not limited to, immune complexes, prostaglandin E2, adenosine, and apoptotic cells. An effective reprogramming signal suppresses the inflammatory cytokine response induced by LPS, while upregulating anti-inflammatory and immunoregulatory proteins such as IL-10. The discovery of this macrophage phenotype led to an updated model of macrophage activation that is represented by a color wheel[39]. The blending of the primary colors to produce the entire color spectrum is meant to indicate that an infinite number of activation states are possible, with the three primary colors being the polarized extremes. An imbalance in these activation states may lead to excessive or chronic inflammation in the case of classically activated macrophages, whereas excessive regulatory activation is detrimental to a robust immune response to infection.
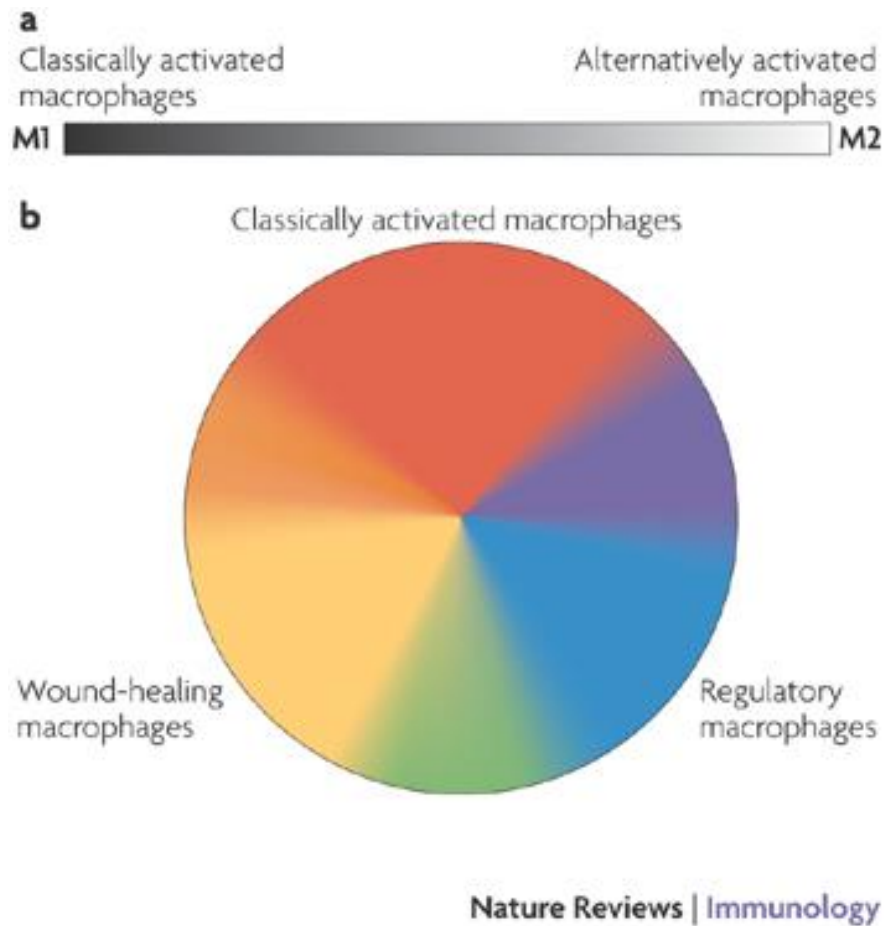
Illustration 1. Color wheel model of macrophage activation. (A) M1/M2 model of macrophage activation first proposed in the 1990's. (B) An updated model represented by a color wheel that includes regulatory macrophages as a distinct phenotype, with the many intermediate phenotypes designated by the secondary colors. Reprinted by permission from Macmillan Publishers Ltd: Nature Reviews Immunology, "Exploring the full spectrum of macrophage activation", David M. Mosser & Justin P. Edwards, 8, 958-969, copyright 2008.

The study of regulatory macrophage activation first began when Mosser and colleagues observed that macrophages treated with opsonized bacteria produced less IL-12 than macrophages infected with non-opsonized bacteria[54]. Later, it was found that the same response could also be induced by antibody-coated sheep's red blood cells[55], and immune complexes[56], both of which induce Fcγ receptor cross-linking. These dual signals synergize to induce increased production of IL-10 and the EGF receptor ligand HB-EGF[57], even when cells were primed with IFNγ. The IL-10 response was found to be dependent on Fcγ chain signaling[54] and could not induced by treatment with immune complexes alone. In the M1/M2 model of macrophage activation, this activation state has been (incorrectly) designated "M2b", despite being genetically more similar to M1 macrophages[53]. Whereas M2a macrophage activation is known to involve STAT6 signaling, this is not the case with M2b macrophages. Rather, a transient ERK hyper-phosphorylation increases IL-10 transcription through transient chromatin remodeling at the IL-10 promoter[58]. Because of the decrease in inflammatory cytokines and increase in IL-10 and growth factors with this treatment, it is hypothesized that these cells play an important role in the tissue repair and the dampening of inflammation associated with the resolution of infection. Indeed, injection of mice with R-Mφ-IC can rescue mice from lethal endotoxemia[53]. Almost all research studies on R-Mφ-IC thus far have been carried out in mice. No comprehensive studies have been done to characterize this activation state in primary human macrophages.

1.3.4 Transcriptomic analysis of polarized macrophages

Since the widespread availability of next-generation sequencing has enabled whole-transcriptome analysis of cell populations, there has been an overwhelming surge in information on macrophage polarization in both mouse and human cells. Previously, microarray techniques were frequently utilized to catalog global transcript changes, and this technique facilitated the relative quantification of thousands of genes. However, this method has several disadvantages: (1) because probes had to be designed for each transcript, the method restricts analysis to the number of probes that have been designed, in contrast to RNA-seq which can provide information on every gene expressed in the sample. (2) Microarray is unable to provide a comprehensive profile of transcript variants and unknown genes. (3) Microarray is unable to provide information about total transcript abundance, and (4) has limited sensitivity due to high background, reducing its ability to quantify low-abundance transcripts. As massive parallel sequencing technology became more accessible to researchers, there came to be a great increase in the amount of data that could be gleaned from one experiment. Currently, the entire transcriptome of a cell population can be characterized from only a small sample of RNA, providing a snapshot of the transcriptional activity of the cell. Although changes in RNA don't necessarily lead to equal changes at the protein level[59], through this analysis we can predict not only the way in which these changes could have physiological effects, but also which signaling pathways could give rise to these changes in gene expression. In the context of macrophage activation, high throughput studies have slowly led to the understanding that macrophages are highly sophisticated in their response to external stimuli, and produce fine-tuned and specific genetic

programs dependent on the exact environment to which they are exposed. In 2014, this diversity in gene expression was thoroughly profiled using RNA sequencing analysis on all known macrophage activation states in human cells[60]; the authors found that when looking at global changes in gene expression, macrophage activation states do not fall neatly along the M1/M2 bimodal continuum, but rather, selectively modify their gene expression upon exposure to different stimuli. This study illustrated that the complexity of macrophage activation states is best appreciated by looking at both global and functional analyses.

1.4 Toll-like receptor signaling

1.4.1 Toll-Like Receptors

Cells of the innate immune system express an array of receptors known as pattern recognition receptors (PRRs). These receptors bind pathogen-associated molecular patterns (PAMPs) and damage-associated molecular patterns (DAMPs), which activate an inflammatory immune response[61]. PRRs are present both in the plasma membrane, facing either the extracellular environment or the internal side of endosomes, and are also present in the cytosol. One subset of the membrane bound PRRs is the toll-like receptor (TLR). TLRs are named after the drosophila homolog "toll", which was discovered by Christiane Nüsslein-Volhard[62], and further characterized by Bruno Lemaitre in 1996 when it was found to be necessary for host defense[63]. It was soon found that the requirement for innate immunity to trigger a robust adaptive immune response is explained largely by the action of toll-like receptors, which leads to upregulation of costimulatory molecules necessary for T helper cell

activation. This discovery led to a revolution in the understanding of innate immunity and its interaction with the adaptive immune system[5].

There are eleven TLRs in humans, numbered accordingly, which have a leucine-rich repeat in their extracellular portion capable of binding molecules associated with pathogens[64]. PAMPs associated with viral infection, such as dsRNA and unmethylated DNA, bind to receptors TLR-3[65], TLR-7/8[66], and TLR-9[67]. These receptors signal through TRAF3 leading to the activation of interferon regulatory factors[68], transcription factors that are important for driving the cell-mediated immune response most appropriate for intracellular cytosolic pathogens. TLRs that bind to components of bacteria, such as flagellin (TLR-5), peptidoglycan (TLR-1/2), bacterial lipopeptides (TLR-2/6) or lipopolysaccharide (TLR-4), initiate a broad inflammatory response appropriate for host defense against extracellular pathogens; this includes the production of antibody to increase efficiency of phagocytosis and accelerated killing of gram-negative bacteria through complement fixation. The ability for the immune system to tailor its immune response toward a particular pathogen originates in the PRR-specific genetic responses observed in antigen-presenting cells upon first encountering a pathogen. This flexibility and specificity in response allows the host to minimize collateral damage while maximizing host defense.

1.4.2 TLR signaling pathways

TLR ligation leads to activation of several signaling cascades, broadly classified into MYD88- and TRIF-dependent pathways[69]. Ligation leads to conformational changes in the intracellular portion of the receptor, allowing the adaptor molecule MYD88 to bind. MYD88 recruits IRAK-1, -2, and -4, which then activate

TRAF6. All of the TLRs signal through MYD88 with the exception of TLR3, which signals only through TRIF[61]. MYD88 activation primarily leads to activation of NFκB and the MAPK cascade, both heavily involved in the transcriptional control of cytokines, chemokines, and immunoreceptors. The MAP kinases include ERK, p38, and JNK, all of which activate Sp1 and the AP-1 family of transcription factors, contributing to transcription of genes related to inflammation and cell survival. TRIF is another TLR-associated adaptor molecule that is activated by both TLR3 and TLR4 ligation. Less is known about the downstream signaling of TRIF, but it was found to be essential for the IRF3 activation necessary for IFNβ transcription[70], and is also able to activate NFκB through cleavage of caspases 8 and 10[71].

Besides transcriptional changes, activated macrophages undergo profound alterations in metabolism, translation efficiency, and post-translational modification of intracellular signaling proteins. These changes coincide with several mechanisms of negative regulation that exert control over the cellular response and allow the cell to return to a resting state. For example, activation of Akt, TBK1, and IKKε by TLR ligation leads to increased activity of the glycolytic pathway[72]. This in turn increases intracellular ATP, which is released into the extracellular environment in small amounts. This released ATP is then converted by ectonucleotidases into adenosine, which activates adenosine receptors, thus suppressing the cytokine response[73]. Other mechanisms of feedback inhibition include the LPS-induced production of decoy receptors such as sTLR4 and sTLR2, release of PGE2, inhibitory microRNAs that target pro-inflammatory transcripts for degradation, phosphatases that remove phosphorylation sites on activated signaling molecules, and E3 ubiquitin-protein

14

ligases that target TLR signaling mediators for proteasomal degradation[74]. This broad collection of self-limiting mechanisms at all levels of regulation emphasizes the importance of autoregulation in the inflammatory response, and the potential harm that inevitably stems from unchecked inflammation.

1.4.3 NFκB

Nuclear factor kappa-light-chain-enhancer of activated B cells (NFκB) is a well-characterized transcription factor responsible for driving a cellular response to TLR ligands[41] and any receptor which acts through the adaptor molecule MyD88[75]. It can also be activated by oxidative stress, cytokine signaling, and DNA damage[76]. It has a profound effect on many genes, particularly cytokines, and can be activated in less than half an hour after the cell has encountered a triggering stimulus[77]. There are five NFκB proteins separated into two classes. In class I are p50 (NF-KB1) and p52 (NF-KB2) which both contain ankyrin repeats in their C-termini which have transrepression activity. Class II members include RelA (p65), RelB, and c-Rel, differentiated from those in class I by the presence of a transactivation domain in their C-termini. In the canonical model of transcriptional activation, NFκB forms a heterodimer composed of p50 and p65[78] which, under resting conditions, is prevented entry into the nucleus by its binding to nuclear factor of kappa light polypeptide gene enhancer in B-cells inhibitor alpha (IκBα)[79]. Upon activation of TLR ligands or cytokine receptors, IκBα is degraded by IκB kinase, allowing NFκB to enter the nucleus and control gene transcription. The various subunits can associate in different ways to perform distinct functions, including transcriptional suppression. For example, the p50 molecule can

form a homodimer which drives transcription of the anti-inflammatory cytokine IL-10[80]. Thus, while NFκB is highly important for cytokine response in macrophages, it is involved in transcription of both inflammatory and anti-inflammatory genes[81]. Thus, efforts to develop anti-inflammatory therapies by targeting NFκB may have unpredictable effects[81].

1.4.4 Akt

More recently it was discovered that the Akt/mTOR pathway plays a complex but highly important role in the regulation of the cytokine response. Akt (also known as protein kinase B) is a 60 kDa serine threonine protein kinase that acts as a sensor for the health and nutritional status of the cell, as well as a central regulator in the growth factor signaling cascade. It is known to phosphorylate dozens of substrates and lies upstream of several important cellular processes including gene regulation, cell growth and proliferation, utilization of nutrients, regulation of metabolism, and cell survival (Illustration 2). One of its most well-known activators is PI3K, which directly activates Akt through phosphorylation, and which itself is known to be activated by Fc receptor activation[82]. Akt is then able to phosphorylate dozens of substrates, and indirectly leads to activation of mammalian target of rapamycin (mTOR) through inhibition of TSC1. mTOR is itself a central modulator of metabolic signaling, including the well-known increase in glycolytic flux observed after activation of macrophages. This increase in glycolysis allows a rapid albeit inefficient production of high levels of ATP necessary for fueling a robust immune response.
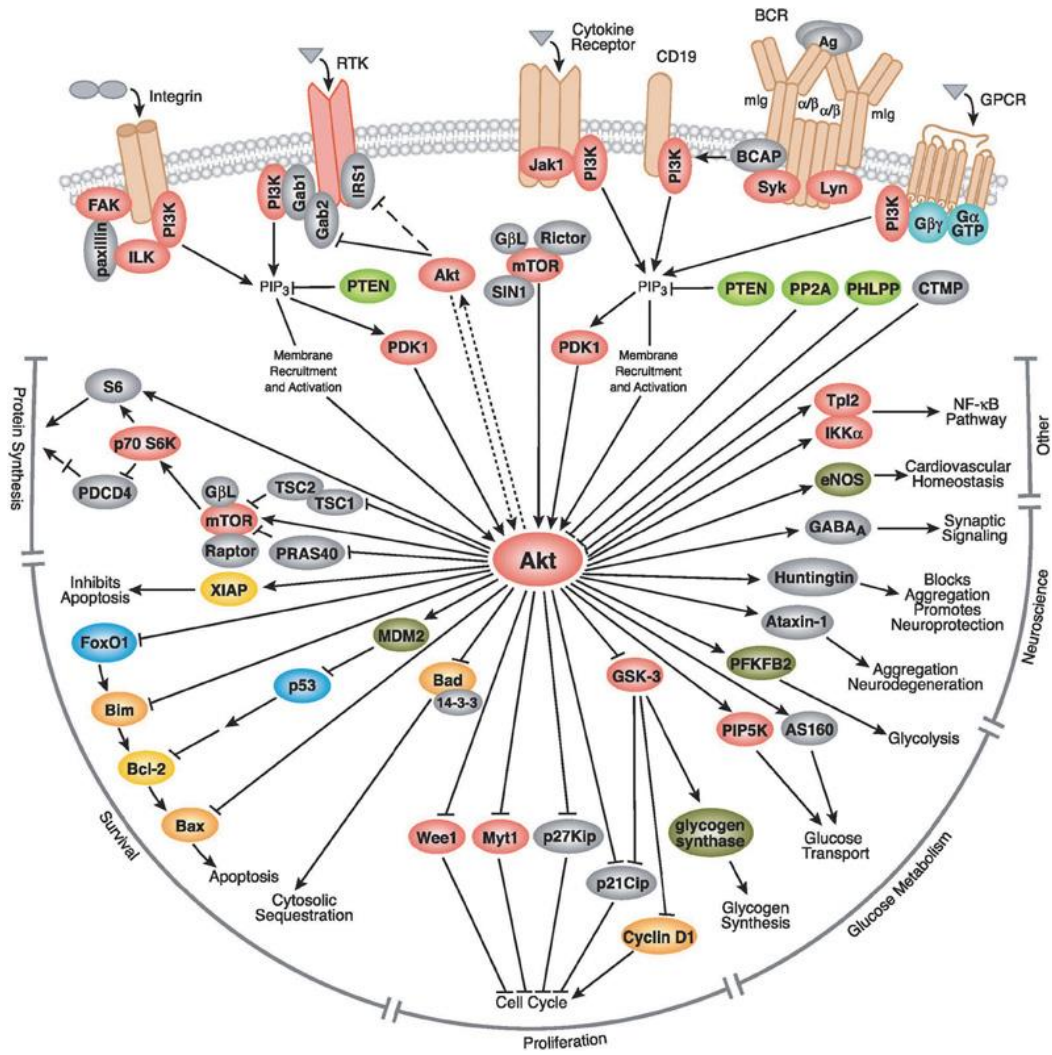
Illustration 2. Overview of Akt pathway. Illustration courtesy of Cell Signaling Technologies Inc., www.cellsignal.com.

LPS has been observed to activate Akt and downstream pathways through activation of PI3K, but the degree and effects of this activation appear to be context-specific. Akt1 is the isoform that can be activated by TLR ligation, which has been found to be necessary for the production of anti-inflammatory microRNAs such as let-7e[83]. Systemically, Akt appears to plays a role in negative regulation of inflammation, as Akt1-specific knockout mice are more susceptible to lethal endotoxemia and have higher levels of several inflammatory cytokines[84]. However, because Akt is so readily effected by nutritional status of the cell and exposure to growth factors present in serum, the effect of TLR ligation on phosphorylation of Akt varies considerably.

1.4.5 ERK

Also known as the Ras-Raf-MEK-ERK signaling pathway, the MAPK cascade is an important and prominent chain of cytosolic signaling events involved in extracellular signal transduction and leads to widespread effects on transcriptional regulation. It is one of the most well-characterized downstream mediators of growth factor signaling, and is highly upregulated in active tumors[85]. In murine macrophages, the MAPK/ERK pathway is involved in proliferation triggered by FcR mediated phagocytosis[86], and acts to upregulate IL-10 through chromatin modification at the IL-10 promoter[58]. Although LPS alone can increase in ERK activation in macrophages, cross-linking of Fc receptors by immune complexes leads to hyperphosphorylation of ERK within the first half hour following stimulation. ERK phosphorylates a myriad of substrates both in the cytosol and in the nucleus, leading to extensive changes in gene

transcription. In macrophages, it is involved in the regulation of both inflammatory and anti-inflammatory cytokines through its activation of the transcription factor AP-1.

1.5 Other signaling pathways in activated macrophages

1.5.1 FC receptors

Fc receptors are a class of cell-surface receptors belonging to the immunoglobulin gene family and recognize the Fc portion of antibodies. These receptors are expressed on the surface of hematopoietic cells, and trigger physiological functions specific to the cell type. There are several classes of FcR, designated with a greek symbol corresponding to the antibody isotype that they recognize. The Fcγ receptor is specific for IgG antibody, and in humans is found in three isoforms: FcγRI (CD64), FcγRII (CD32), and FcγRIII (CD16). FcγRI and FcγRIII associate with the common γ-chain, encoded by FCER1G, which contains an immunoreceptor tyrosine-based activation motif (ITAM) in the intracellular region[87]. FcγRIIA does not associated with the common gamma chain, but signals through an ITAM contained in the intracellular portion of the receptor. FCγRIIB is similar to FcγRIIA in structure, except that it contains an ITIM motif which leads to inhibitory signaling (Illustration 3).

Exposure of the FcRs to immune complexes or opsonized particles leads to aggregation of the FcR ITAMs, which enables them to be phosphorylated by Src family kinases[88]. The phosphorylation of these ITAMs is necessary for the recruitment and subsequent phosphorylation of spleen tyrosine kinase (Syk)[89], a molecule necessary for enhanced phagocytosis[90], cell activation[91], and activation of respiratory burst[92] in

	Activating Fc receptors					Inhibitory Fc receptor

Mouse

Structure

Name	FcγRI	FcγRIII	FcγRIV	FcγRIIB
Affinity	High	Low to medium	Low to medium	Low to medium

Human

Structure

Name	FcγRI	FcγRIIA	FcγRIIC	FcγRIIIA	FcγRIIIB	FcγRIIB
Affinity	High	Low to medium	Low to medium	Low to medium	Low to medium	Low to medium
Alleles		FcγRIIA^{131H} FcγRIIA^{131R}		FcγRIIIA^{158V} FcγRIIIA^{158F}	NA1 NA2	FcγRIIB^{232I} FcγRIIB^{232T}

Nature Reviews | Immunology

Illustration 3. Properties of Fcγ receptors in mouse and human. Reprinted by permission from Macmillan Publishers Ltd: Nature Reviews Immunology, "Fcγ receptors as regulators of immune responses", Falk Nimmerjahn & Jeffrey V. Ravetch, 8, 34-47, copyright 2008.

macrophages. Because of the nature of its activating mechanism, Fc receptor ligation in the absence of cross-linking does not induce the same signaling cascades[55], preventing cellular activation by antibody in the absence of bound antigen.

The physiological effect of Fc receptor ligation is context specific, and is often associated with increased inflammation by neutrophils[93,94] and NK cells[95]. In macrophages, cross-linking of Fc receptors by opsonized pathogens potentiates a powerful signaling cascade initiated by the phosphorylation of Syk[89], leading to activation of the MAPK pathway, actin remodeling, and Ca+ mobilization[96], all enabling the macrophage to phagocytose the opsonized particles. Kinetics studies of macrophages treated with immune complex confirmed that the clustering of many Fc receptors gives rise to recruitment and subsequent phosphorylation of Syk[97]. The molecular mechanisms involved in the induction of phagocytosis are complex, and require phosphorylation of PI3K and activation of the MAPK pathway through Ras and Raf. Phosphorylation of PI3K leads to BTK and PLCγ activation, subsequently increasing cytosolic calcium levels[98]. Although Syk is critical for FcγR-mediated phagocytosis by macrophages[99], inhibition of Syk is also associated with upregulation of inflammatory cytokine production in macrophages[100].

1.5.2 GSK3

Glycogen synthase kinase 3 is an unusual signaling protein that typically inactivates its substrate upon phosphorylation rather than activating it. Furthermore, unlike most other signaling molecules this kinase is inactivated when it is itself phosphorylated because the phosphate group physically blocks substrate binding[101]. The kinase was first discovered in 1980[102] and as its name suggests, was thought to be

mainly a regulator of glycogen synthesis. Since then, over 100 substrates for this molecule have been proposed, most of which are transcription factors[103]. Research into GSK3 increased dramatically after it was found to be relevant in neurobiology, as it is thought to be responsible for the effects of lithium on bipolar disorder. More recently GSK3 has also been found to be important in the regulation of inflammation[104], with GSK3 inhibition associated with a down-regulation of inflammatory responses. Specifically, it was found that Akt activation is able to induce activation of AP-1 and CREB through inactivation of GSK3, which normally has a suppressive effect on these transcription factors [105]. This release of AP-1 and CREB leads to an increase in IL-10 transcription, explaining one mechanism by which Akt activation can contribute to IL-10 production in human macrophages. This observation was replicated in a study examining the effect of Leishmania infection on IL-10, where they found that Akt2 led to phosphorylation of GSK3 at serine 9. The resulting inhibition of GSK3 nuclear translocation allowed CREB to promote IL-10 transcription[106]. GSK3 inhibition has also been found to be involved in angiogenesis[107,108], but the mechanism for this is still unknown.

1.6 Sepsis

1.6.1 Incidence and Cost

Sepsis is one of the most widespread and costly conditions treated in hospitals in the United States. In fact, deaths from sepsis outnumber mortality due to both breast and prostate cancer combined[109]. Sepsis is ranked the top most expensive condition in U.S. hospitals; in 2011 treatment for sepsis cases came to a cost of over $20 billion and

rises every year by about 12%[110]. Furthermore, incidence of sepsis deaths has increased in recent years, and is expected to increase as the population ages.

1.6.2 Etiology

Risk of sepsis is associated with old age, as well as lifestyle factors such as smoking and alcohol use. It is also strongly associated, likely causally, with chronic diseases such as heart disease, diabetes, stroke, and hypertension. Immunosuppressed individuals such as those being treated with chemotherapy for cancer, can develop infection leading to sepsis. Other risk factors include long-term catheter use, surgical procedures, recreational drug use, burns, long-term steroid use, and pregnancy. The majority of infections leading to sepsis begin in the lungs, so any condition or injury that leads to pneumonia also increases risk of sepsis[111].

1.6.3 Physiology

Although death is ultimately caused by the patient's immune response[112], poor immunity is a risk factor for the development of sepsis because a sensitive and responsive immune system is able to prevent widespread infection upon initial exposure to the pathogen[113]. Upon widespread dissemination of the pathogen, the host's production of TNF and IL-1 is often (but not always) the ultimate cause of multiple organ failure and death, which is likely why anti-TNF therapies have been effective in reducing sepsis mortality if administered early[114]. In recent years, gram-positive bacteria account for 50% of sepsis cases, but sepsis can also be caused by viruses and fungi, typically in immunosuppressed individuals[115].

23

The role of macrophages in the pathophysiology of sepsis is multi-faceted. On the one hand, a poor initial immune response or excessive tolerization to endotoxin leaves the patient vulnerable to the infectious agent. On the other hand, the inflammatory cytokines that ultimately lead to vascular leakage and multiple organ failure are produced mainly by macrophages; a hyperactive immune response in this respect can increases risk of mortality before antibiotic treatment has the opportunity to clear the infection. In human patients, the presence of M1 markers of macrophage activation such as IL-1β and IL-6 predicts imminent mortality[116]. In baboons, mortality was correlated with M1 markers secreted from monocyte isolated during infection, whereas a mixed M1/M2 phenotype predicted resistance to bacterial sepsis[117]. For this reason, the macrophage response is considered crucial in the understanding of immunological management of the disease.

1.6.4 Current Treatments

Sepsis is an extremely dangerous condition that requires intensive hospital care. Constant monitoring is necessary to detect and respond to potentially fatal changes in blood pressure, respiration and heart rate. In the case of bacterial septicemia, appropriate antibiotics, usually of multiple types, are administered intravenously. In the case of a hyperinflammation, low doses of corticosteroids are used to dampen the cytokine response. IV fluids and vasopressors are used to prevent a lethal drop in blood pressure[118]. Given the 38% mortality rate despite these measures[119], the need for more effective treatment remains.

Summary

In a descriptive study of several M2 macrophage polarization states, Fleming et al. revealed that IC has a potent anti-inflammatory phenotype in murine macrophages, and that this phenotype is similarly observed in primary human macrophages. In this study, we intend to thoroughly examine this activation state in human monocyte-derived macrophages (HMDMs) in order to explore its molecular regulation and functional significance. The effect and control of the R-Mϕ-IC phenotype is yet to be thoroughly characterized in human macrophages, and no biomarkers exist to identify this activation state in human tissue. Here we intend to use a multi-omics approach to characterize M2b macrophages and identify key regulators of gene expression. We have examined the transcriptome and secretome of regulatory macrophages, which has provided us with a global picture of the behavior and function of these cells. We propose that these studies could be applicable to a wide range of disease states where immune responses are dysregulated.

Chapter 2: Materials and Methods

2.1 Differentiation of human monocyte-derived macrophages

Human monocyte-derived macrophages (HMDMs) were either purchased from
HemaCare Corporation (Van Nuys, CA) or differentiated in house. PBMCs were
obtained from 50 milliliters of human blood by Ficoll-paque density gradient
centrifugation. Pure unlabeled monocytes were isolated from PBMCs using the pan
monocyte isolation kit from Miltenyi Biotec (San Diego, CA) and cultured for 7-10
days in X-VIVO^{TM} 15 serum-free media (Lonza, Walkersville, MD) containing 1%
penicillin-streptomycin, 1% L-glutamate (Gibco, Gaithersburg, MD), and 30 ng/mL
recombinant human M-CSF (Peprotech, Rocky Hill, NJ). The night before stimulation,
M-CSF-containing media was removed and replaced with X-VIVO^{TM} 15 media
containing 2.5% fetal bovine serum (Atlanta Biologicals, Flowery Branch, GA). For
some experiments (noted in figure legends) macrophages were purchased from
HemaCare, (product PBM2-MON; M-CSF-differentiated) and plated upon arrival in
X-VIVO^{TM}15 medium with 2.5% FBS and stimulated the following day. All studies
on human monocyte-derived macrophages were approved by the University of
Maryland, Institutional Review Board. A signed informed consent was obtained from
each healthy volunteer who donated blood.

2.2 Cell culture and stimulation

LPS-stimulated macrophages (LPS-Mϕ) were generated by adding 30 ng/ml
Ultra-pure LPS from Escherichia coli K12 (Invivogen, San Diego, CA). Regulatory
macrophages (R-Mϕ-IC) were generated by culturing HMDMs in the presence of 30

ng/ml LPS and 80 µl OVA-IC per million macrophages (designated as LPS+IC in text). Immune complexes were prepared by combining 1 mg/ml ovalbumin (Worthington, Lakewood, NJ) with 10 mg/ml anti-ovalbumin (Polysciences, Warrington, PA) at a 1:20 v/v ratio and incubating at room temperature for 30 minutes before use.

2.3 RNA-sequencing sample preparation

After 4 hours of stimulation, media was removed and the RNA was extracted from the cells using the mirVANA kit by Ambion (ThermoFisher Scientific, Waltham, MA) according to the manufacturer's protocol. PolyA-enriched cDNA libraries were generated using the Illumina TruSeq RNA sample prep kit (Illumina, SanDiego, CA).

2.4 RNA-seq data generation, pre-processing, and quality trimming

Paired end reads (100 bp) were obtained from the Illumina HiSeq 1500 platform (Illumina, SanDiego, CA). Trimmomatic was used to remove any remaining Illumina adapter sequences from reads and to cut off bases with quality score less than 20 [120]. Sequence quality metrics were assessed using FastQC (http://www.bioinformatics.babraham.ac.uk/projects/fastqc/). Mapping cDNA fragments to the reference genome, abundance estimation, and data normalization. Reads were aligned to the human genome (hg19/GRCh37.62.v3) obtained from the UCSC genome browser[121] (http://genome.ucsc.edu) using TopHat (v 2.0.13)[122]. Two mismatches per read were allowed and reads were allowed to map only to a single locus. The abundance of reads mapping to each gene feature was determined using HTSeq (http://www-huber.embl.de/users/anders/HTSeq/).

2.5 RNA-sequencing data quality assessment by statistical sample clustering and visualization

Multiple approaches were used to evaluate replicates and to visualize sample-sample distances. Those included Pearson correlation, Box Plots, Principal Component Analysis (PCA) and Euclidean distances-based hierarchical clustering. All components of the statistical pipeline, named cbcbSEQ, can be accessed on GitHub (https://github.com/kokrah/cbcbSEQ/).

2.6 RNA-sequencing differential expression analysis

Non-expressed and weakly expressed genes, defined as having less than 1 read per million in n of the samples, where n is the size of the smallest group of replicates[123] (here n=3), were removed prior to differential expression analysis. A quartile normalization scheme was applied to all samples[124]. Following log2 transformation of the data, Limma (a Bioconductor package) was used to conduct differential expression analyses. Limma utilizes a standard variance moderated across all genes using a Bayesian model and produces p values with greater degrees of freedom[125]. The voom module was used to transform the data based on observational level weights derived from the mean-variance relationship prior to statistical modeling. Experimental batch effects were adjusted by including experimental batch as a covariate in our statistical model. Differentially expressed genes were defined as genes with a Benjamini-Hochberg multiple-testing adjusted P value of < 0.05.

2.7 RNAscope

RNAscope probes for Interleukin 10 (IL-10), leukemia inhibitory factor (LIF), and matrix metalloproteinase 10 (MMP10) were custom designed by Advanced Cell Diagnostics (Newark, CA), accession numbers: NM_000572 (IL10), NM_002421 (MMP1), NM_002309 (LIF). HMDMs were cultured and stimulated in 4-well chamber slides for 4 hours. Supernatants were removed, cells were washed and then fixed for 30 minutes in 4% paraformaldehyde, dehydrated and stored in 100% ethanol. Slides were then rehydrated and staining was done according to manufacturer's protocol (RNAscope Multiplex Fluorescent Reagent Kit v2 User Manual, http://www.acdbio.com/support/technical-doc). After staining, slides were mounted with Fluoromount-G™ with DAPI (ThermoFisher Scientific, Waltham, MA). Slides were imaged using the Zeiss LSM710 confocal Laser microscope (Carl Zeiss Microscopy GmbH, Jena, Germany) and fluorescence was quantified using Zen software by Zeiss.

2.8 Flow cytometry

Human monocytes were cultured and stimulated in ultra-low attachment plates for a week to obtain macrophages for flow cytometry. Staining for surface or intracellular protein expression was performed following standard protocols recommended by the antibody manufacturer. FITC conjugated CD274, CD68; PE-conjugated CD93, CXCR4, CD66b, TM4SF1, MMP-1, IL-6, IP-10 and APC conjugated DC-STAMP, CD49b, LIF, NOTCH-2 antibodies were used for flow cytometry. The antibodies for NOTCH-2 and DC-STAMP (cat # FAB7824A) were purchased from R&D systems (Bio-techne, Minneapolis, MN); CD93 and CD68 from

eBioscience (San Diego, CA); and IP-10, CD49b from Biolegend (San Diego, CA). All other antibodies were purchased from BD Biosciences (Franklin Lakes, NJ). Data acquisition was carried out in FACSCanto II (BDbiosciences, Franklin Lakes, NJ USA), and analyses were done on FlowJo version 10.

2.9 SOMAscan™ assay

Cell culture supernatants were collected from human macrophages 24 hours after stimulation (NS, LPS, and LPS+IC), flash frozen at -80° C, and were analyzed using the SOMAscan™ proteomic assay (SOMAscan Assay 1.1k; SomaLogic; Boulder, CO). SOMAscan is a protein biomarker discovery platform that utilizes SOMAmers (Slow Off-rate Modified Aptamers), single-stranded DNA aptamers with modified nucleotides, that bind to specific proteins in the sample and are subsequently quantified. SOMAmers were mixed with samples to allow binding; sample concentrations of 40%, 1%, and 0.005% were used to allow measurement of protein concentrations at ~8 log range. Unbound SOMAmers were then washed away. Protein-bound SOMAmers were eluted and quantified using a DNA microarray. In this way, protein concentrations in the supernatant were transformed into a corresponding signature of DNA aptamer concentrations followed by a fluorescence signal on the DNA microarray. Values are reported in relative fluorescence units (RFU). The SOMAscan assay quantified relative levels of 1,129 proteins in each sample. For some analyses, intracellular proteins were excluded from the analysis to leave only secretory proteins (subcellular localization information was gathered from GeneCard).

Prior to analysis, RFU values from SOMAscan™ assays were normalized against hybridization control sequences to correct for any systematic effects introduced

during hybridization. Median normalization was performed across samples within an array. Finally, calibration was performed based on calibrator samples in each array to allow comparison of samples across runs. To reduce heteroscedasticity, values were log2 transformed. Group comparisons were performed using Bayesian modified linear model using the Limma package in R[126]. Default parameters were used, except the "proportion" parameter was set to 0.05. Between groups, comparisons were assessed using contrast and the p-values of the moderated-t-test were adjusted by the Benjamini–Hochberg procedure which controls the false discovery rate (FDR). Differentially expressed proteins were defined as those with fold change (FCH) ≥1.5 and FDR ≤0.05.

2.10 ELISA

Human IL-10 and IL-12p40 were detected by use of ELISA kits purchased from eBioscience (San Diego, CA, USA). ELISA kits for the remaining analytes were purchased from R&D (Minneapolis, MN).

2.11 Cyclic AMP measurement

A direct colorimetric cAMP ELISA kit was purchased from Enzo Life Sciences (Farmingdale, NY) and used according to manufacturer's instructions to analyze HMDM cell lysates 2 minutes after stimulation.

2.12 Bioinformatics Analyses

Ingenuity Pathway Analysis (IPA) software[127] was used to predict diseases and functions associated with LPS and LPS+IC stimulated macrophages, and to predict upstream regulators responsible for LPS+IC phenotypic changes. Data used for the

31

analysis included genes that showed at least a two-fold up-regulation or down-regulation (p-value <0.05) when compared to macrophages stimulated with LPS alone.

For the Upstream Regulators Analysis, the resulting predicted regulators list was limited to members of intracellular signaling pathway members by restricting them to those located in the cytosol (molecule types included: kinase, group, enzyme, complex, and other). Regulators with a low number of known targets were removed (cutoff = 10) to limit false positive findings.

Gene Set Enrichment Analysis (http://www.broadinstitute.org/gsea/index.jsp) was performed using the GSEA software using $\log_2$ transformed RPKM values in LPS and LPS+IC, to assess overlap with datasets in the Molecular Signature Database (MSigDB). Specifically, data were compared to collections C2 and C3, containing curated gene sets and transcription factor targets respectively[128,129].

2.13 Antibody array

The PathScan Akt Signaling Antibody Array Kit (Cell Signaling Technologies, Danvers, MA) was used to assess the relative differences of 16 phosphorylated signaling molecules within the Akt signaling pathway. Whole cell lysates were obtained 20 minutes after stimulation as described in 'Cell culture and stimulation' section, and a BCA assay (Pierce Biotechnology, Waltham, MA) was used to determine protein concentration of the samples. The array was performed according to the manufacturer's instructions and the density was quantified using Image J software[130].

2.14 Western blotting

Protein samples for western blotting were prepared by lysing the cells with radioimmunoprecipitation assay (RIPA) buffer containing protease and phosphatase inhibitors (ThermoFisher Scientific, Waltham, MA). For blots in which nuclear and cytosolic fractions were isolated, the NE-PER nuclear extraction kit (ThermoFisher Scientific, Waltham, MA) was used with sonication prior to centrifugation of nuclear debris. Protein lysates were incubated for 2 hours at 4°C with protein agarose A (Santa Cruz Biotechnology, Inc., Dallas, Texas) to clear the lysate of any residual anti-ovalbumin from macrophage stimulation. Antibodies for phospho-ERK 1/2, phospho-Akt, cofilin, phospho-GSK3β, GSK3β, histone H3 were purchased from Cell Signaling Technologies (Danvers, MA); the antibody for phospho-GSK3α/β was purchased from R&D Systems (Minneapolis, MN); the actin antibody was purchased from Santa Cruz (Dallas, Texas). To reduce cross-reactivity of secondary antibody with anti-ovalbumin in the protein isolate, a conformation-specific anti-rabbit IgG (Cell Signaling Technologies, Danvers, MA) was used as the secondary antibody against those primary antibodies derived from rabbit.

2.15 Luminex assay

A magnetic bead Luminex kit with a custom set of analytes was purchased from R&D Technologies (Minneapolis, MN). The Luminex assay was run according to manufacturer's instructions using supernatants from HMDMs that had been stimulated for 16 hours. Beads were quantified using a Luminex MagPix^{TM} instrument (Austin, TX), and data were analyzed using xPonent® software.

2.16 Quantitative Real-time PCR (qRT-PCR)

RNA for qRT-PCR was isolated using the Trizol method (ThermoFisher Scientific, Waltham, MA). Complementary DNA was synthesized from 2 µg equivalent of RNA using Superscript® Vilo^{TM} cDNA synthesis kit (ThermoFisher Scientific, Waltham, MA). Relative quantification of RNA was done using SYBR-Green based real time PCR (ThermoFisher Scientific, Waltham, MA). The samples were run in Roche Light Cycler® 480, in a 384 well plate, each well containing 10 ng of cDNA, 1.5 µl each of sense and anti-sense primers (5 pmol), 6 µl of nuclease free water and 10 µl of 2X Sybr-Green PCR master mix. For data analysis, the comparative threshold cycle (CT) value for beta actin was used to calculate relative differences. The fold induction of RNA was calculated using $2^{\wedge(-\Delta\Delta CT)}$[131]. Sequences used for primer pairs are listed in Table 1.

2.17 Inhibitors

The Akt inhibitor MK-2206 2HCl, GSK3 inhibitor sb415286, and ERK inhibitor U0126 were purchased from ApexBio (Houston, TX), Cayman Chemicals (Ann Arbor, MI) and Cell Signaling Technologies (Danvers, MA) and were used at 20-, 20- and 10- µM concentrations, respectively.

2.18 Endotoxemia

Female C57bl/6 mice (between 9 and 11 weeks old) were injected with $2x10^5$ HMDMs that had been stimulated for 60 minutes with 30 ng/mL LPS, or LPS and 10 µM GSK3β inhibitor (AZD2858), 2 hours prior to IP injection with 15 mg/kg of LPS.

Mice were checked every 12 hours for survival. In each independent experiment, one group of littermates was used which were co-housed.

2.19 Statistics

Non-parametric t tests were performed to calculate the significance of the observed differences. A p value of <0.05 was considered to be significant in all the analyses. The data in the graphs represent mean ± standard error of the mean (SEM).

Accession number	Gene	Sequence
NM_000572.2	**IL10**	
	Forward primer	5'-ACGGCGCTGTCATCGATTT-3'
	Reverse primer	5'-CAGAGCCCCAGATCCGATTTT-3'
NM_001101.3	**ACTB**	
	Forward primer	5'-GCCGCCAGCTCACCAT-3'
	Reverse primer	5'-TCGATGGGGTACTTCAGGGT-3'
NM_002192.3	**INHBA**	
	Forward primer	5'-GGGGACCAGAAAGAGAATTTGC-3'
	Reverse primer	5'-CCTCTCAGCCAAAGCAAGGG-3'
NM_002422.4	**MMP3**	
	Forward primer	5'-GTCCCTCTATGGACCTCCCC-3'
	Reverse primer	5'-AGGGATTTGCGCCAAAAGTG-3'
NM_139314.2	**ANGPTL4**	
	Forward primer	5'-CTTGGGACCAGGATCACGAC-3'
	Reverse primer	5'-AAACCACCAGCCTCCAGAGAG-3'
NM_002426.5	**MMP12**	
	Forward primer	5'-GGCCCGTATGGAGGAAACAT-3'
	Reverse primer	5'-GGAAGTCTCCATGAGCTCCAC-3'
NM_000759.3	**CSF3**	
	Forward primer	5'-TGAGTGAGTGTGCCACCTACAA-3'
	Reverse primer	5'-TGGTAGAGGAAAAGGCCGCT-3'
NM_000602.4	**SERPINE1**	
	Forward primer	5'-GACCGCAACGTGGTTTTCTC-3'
	Reverse primer	5'-GCCATGCCCTTGTCATCAAT-3'
NM_002421.3	**MMP1**	
	Forward primer	5'-CCTGGAAAAATACTACAACCTGAAG-3'
	Reverse primer	5'-TTCAATCCTGTAGGTCAGATGTGT-3'
NM_004591.2	**CCL20**	
	Forward primer	5'-TCAGAAGCAGCAAGCAACTTT-3'
	Reverse primer	5'-GATTTGCGCACACAGACAACT-3'
NM_002425.2	**MMP10**	
	Forward primer	5'-GGATCTTGCCCAGCAATACCTA-3'
	Reverse primer	5'-GTCAGGAACTCCACACCTGGAAAA-3'

Chapter 3: Results

3.1 Transcriptomic analysis of Human Macrophages with a Regulatory Phenotype

In our previous studies we identified a population of murine macrophages with an immuno- regulatory phenotype, capable of inhibiting inflammatory responses[53]. We named these cells regulatory macrophages (R-Mϕ). We further demonstrated that R-Mϕs were transcriptionally and functionally different from alternatively activated M2a macrophages and began to identify potential candidate biomarkers for mouse R-Mϕs. In the present study, we set out to study the transcriptome of human monocyte-derived macrophages with an immunoregulatory phenotype, and to characterize global changes in gene expression in these cells upon stimulation. RNA-sequencing analysis was performed on non-stimulated resting macrophages (NS-Mϕ), M1 macrophages stimulated with lipopolysaccharide (LPS-Mϕ), and R-Mϕs stimulated with LPS in the presence of immune complexes (R-Mϕ-IC). RNA samples were collected four hours after stimulation to capture the "first wave" of gene expression following stimulation. This early analysis avoids potential complications due to secondary effects, such as those associated with autocrine action of secreted cytokines.

3.1.1 Basic analyses of RNA-sequencing results

We first examined the variations in individual gene transcripts by plotting all log transformed reads per kilobase per million (RPKMs) that meet minimal expression criteria (arbitrary threshold cutoff <0.1 RPKMs averaged across all samples). RPKMs were calculated using the edgeR package in R and resulting values were plotted to visualize gene expression levels. Hierarchical clustering analysis of RPKMs revealed

samples from the same treatment group clustering together, and provided visual representation for LPS or LPS+IC-driven changes in gene expression (Figure 1A). Next, to determine total degree of variance among datasets, principal component analysis (PCA) was performed (Figure 1B). As shown in the PCA plot, samples grouped together according to treatment conditions, indicating minimal variance among donors. Principal component 1 explained 75% of the variance in global gene expression, separating resting cells from those stimulated with LPS. Principal component 2 segregated LPS-Mϕ from R-Mϕ-IC by a 13% variance (Figure 1B). These analyses indicate that the presence of LPS accounts for a greater amount of variance in global gene expression than does the addition of IC.

3.1.2 Analysis of differentially expressed genes

Next, differentially expressed genes (DEGs) were identified with the Limma package in R, using a fold change cutoff of 2 and a p-value of <0.05. Stimulation with LPS resulted in numerous changes in gene expression, as previously reported[132,133]. Over 4,500 genes were differentially expressed in response to LPS, accounting for approximately 38% of all detectable genes in the transcriptome as defined by a minimum of 1 count in each sample (Figure 2A).

To compare gene changes among the conditions, a scatterplot was made to show all fold change values in LPS-Mϕ and R-Mϕ-IC, both compared to baseline levels in resting cells (Figure 3A). The positive correlation observed in the plot is assumed to be due to the presence of LPS in both groups. The divergence from this linear correlation indicates the effect of the IC; genes that are differentially regulated to a significant degree in R-Mϕ-IC vs LPS-Mϕ are colored in blue. The top ten differentially expressed

38
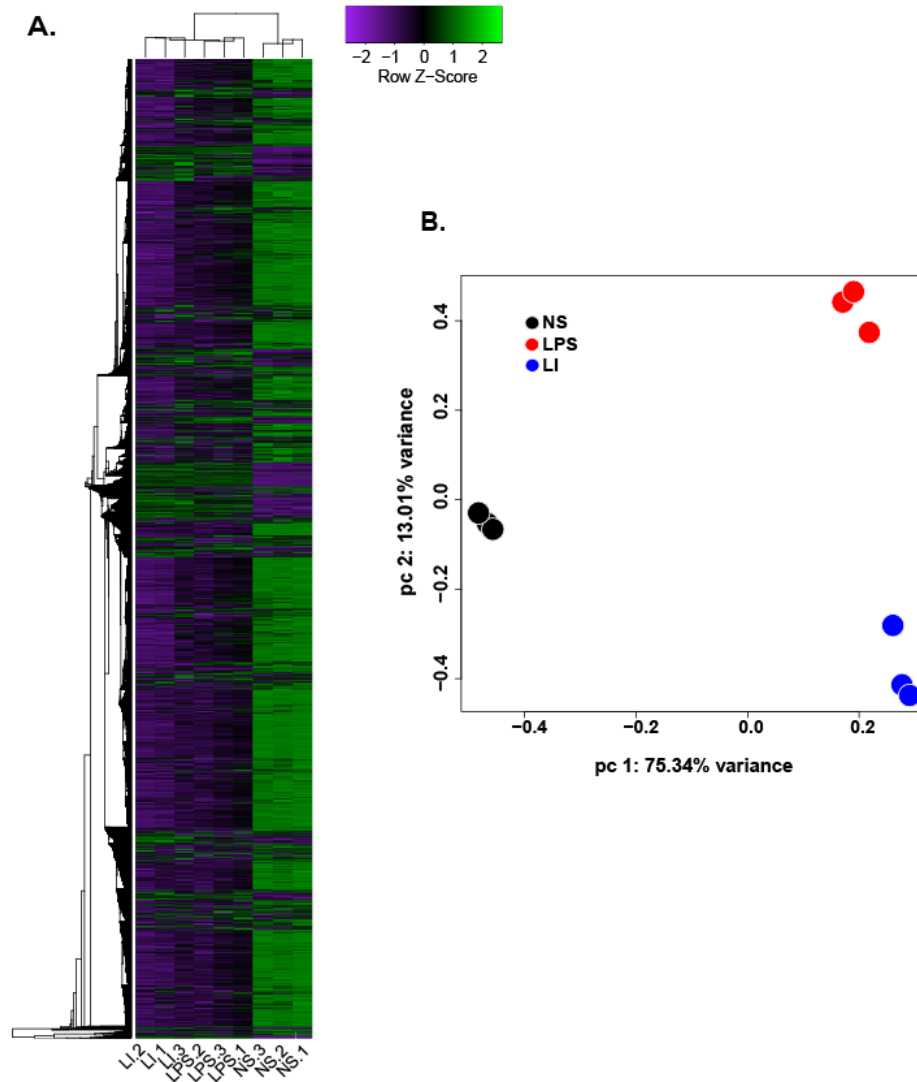
Figure 1. Basic analysis of RNA-sequencing results for LPS-Mϕ and R-Mϕ-IC. Human monocyte-derived macrophages purchased from HemaCare were stimulated with LPS (LPS) or LPS with immune complexes (LI) for 4 hours and total mRNA was isolated and sequenced on an Illumina platform. (A) Heatmap of RPKMs in each sample tested, threshold cutoff 0.1, uses Euclidean distance and complete agglomeration method for clustering. Numbers following sample name denote the donor from which the sample was obtained. (B) Principal component analysis to visualize variance among samples. Data for figures were generated with assistance from Stephen Christensen and Jingya Wang.

39
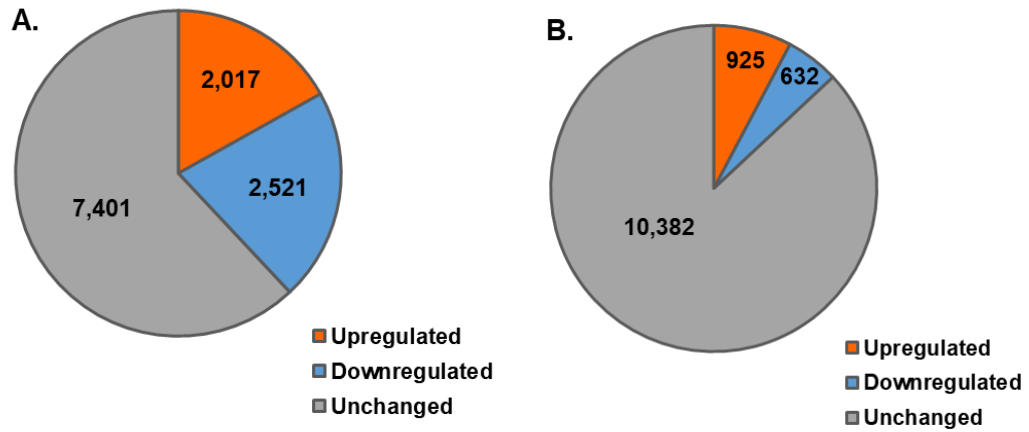
Figure 2. Differentially expressed genes. Pie graphs illustrating the DEGs in LPS-Mϕ vs NS-Mϕ (A), or R-Mϕ-IC vs LPS-Mϕ (B), as a percentage of total detectable genes in the transcriptome. The criterion for a "detectable gene" is one for which at least one count was detected in each sample.

A.
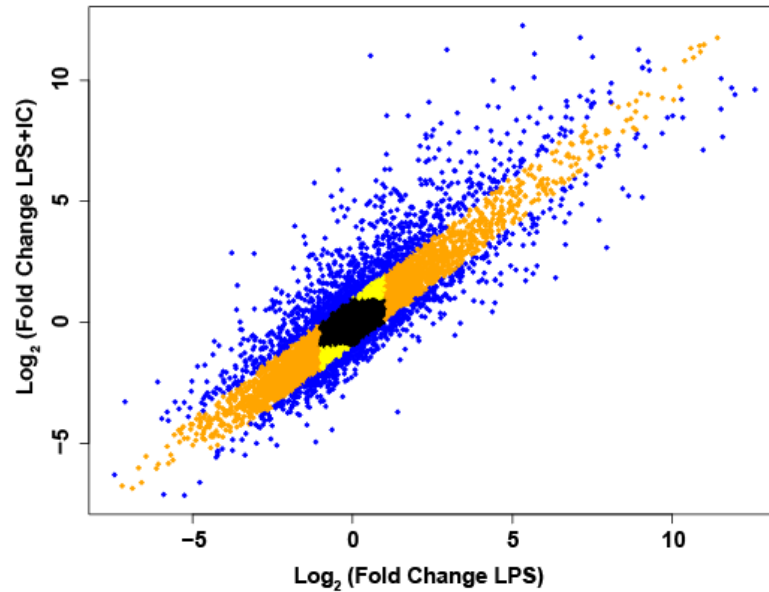
B.
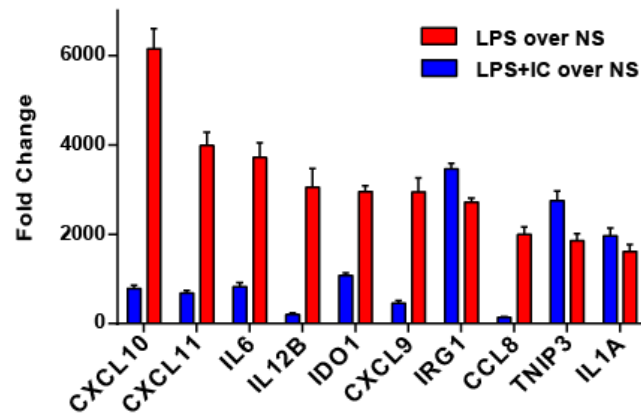
Figure 3. IC modulates the effect of LPS, suppressing genes involved in inflammation and host defense. (A) Gene changes for LPS (x axis) and LPS+IC (y axis) compared to resting cells. Data points for genes that are differentially regulated between LPS and LPS+IC are indicated in blue. (B) The top 10 most highly upregulated transcripts following LPS stimulation for 4 hours. Values for corresponding genes in LPS+IC phenotype were included for comparison.

genes in LPS-Mϕ are presented in Figure 3B. Consistent with previous reports [132,134], LPS stimulation leads to increased production of inflammatory mediators such as the chemokines CXCL9, -10, and -11 and the cytokines IL-6 and IL-12B. Indolamine dioxygenase, an enzyme that limits tryptophan availability, was also highly expressed in human macrophages in response to LPS stimulation (Figure 3B, red). Treatment with LPS+IC resulted in an immune-regulatory phenotype in macrophages as observed by the downregulation of several of the LPS-induced inflammatory mediators (Figure 3B, blue).

Analysis of LPS+IC-driven changes in gene expression showed 1,557 genes were differentially expressed compared to LPS-stimulation alone, equaling 13% of total detectable genes in the transcriptome (Figure 2B, Figure 4A). IC also differentially regulated many genes compared to resting cells that were not changed in LPS-Mϕ, numbering 1,497 genes in total (Figure 3A). Among the most significantly upregulated genes induced in R-Mϕ-IC (Figure 4A, magnified in the volcano subset box) were several proteins with known immunomodulatory and angiogenic functions, highlighted in red for emphasis. IL-10 appeared in this subset, which was previously observed to be upregulated in murine R-Mϕ-IC and found to have anti-inflammatory activity in mice[53]. Also highlighted is amphiregulin, a member of the EGF family of growth factors which can bind to EGFR to promote cell growth[135]. Figure 4B lists the top 10 differentially upregulated and downregulated genes of R-Mϕ-IC compared to LPS-Mϕ. Among the 10 most upregulated genes were the matrix metalloproteinases MMP1, MMP3, and MMP10, which are known to be involved in tissue remodeling, angiogenesis, and extracellular cytokine regulation[136,137]. These 10 genes are also

42
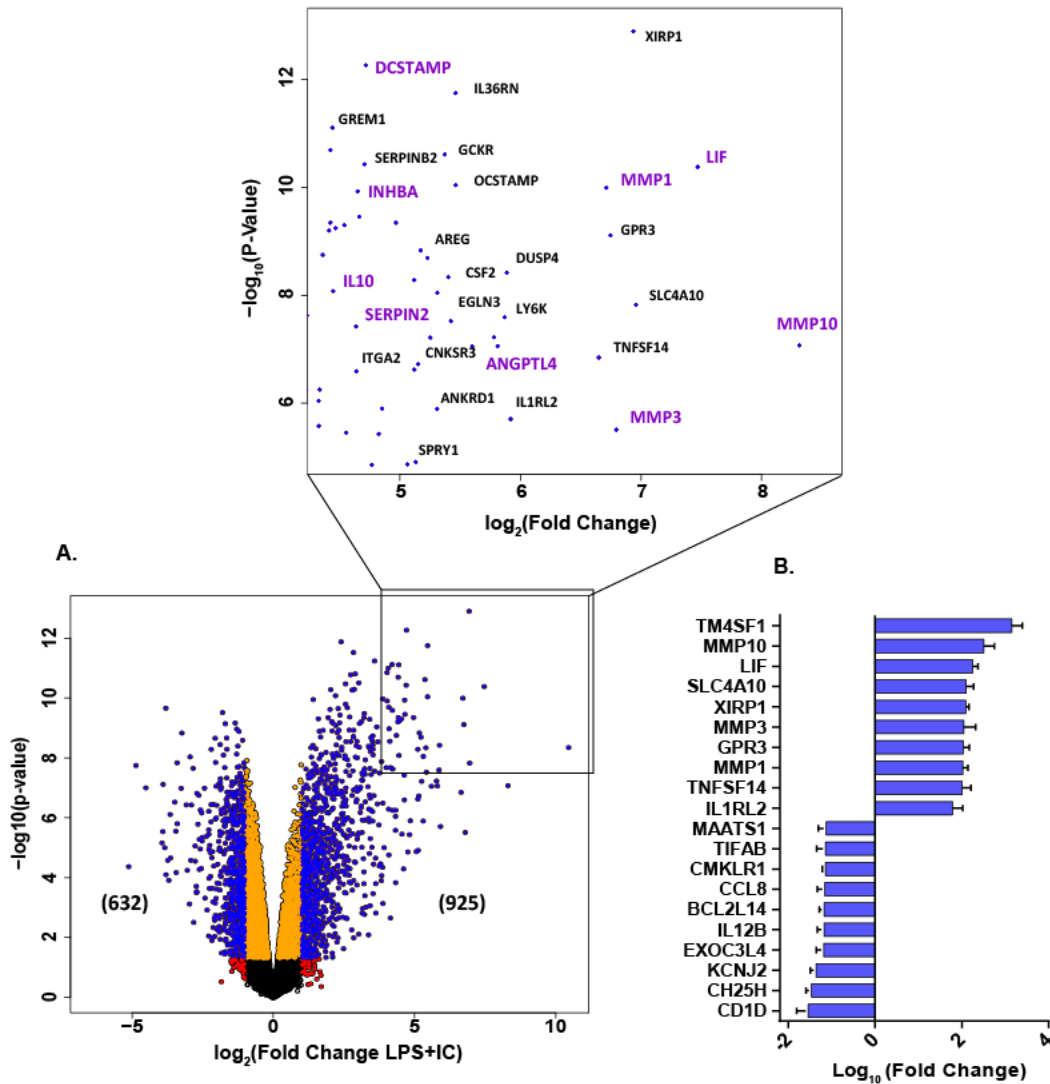
Figure 4. The addition of IC results in significant changes in global gene expression compared to LPS-Mϕ. (A) Volcano plot of RNA-seq values in LPS+IC condition as compared to LPS condition. In parentheses are the number of genes regulated above or below 2-fold change with a z-score < 0.05. Highlighted in the box are the top most highly and significantly upregulated genes with their respective identities, sorted by log fold change (x-axis) and log p value (Y axis). (B) The top 10 most highly upregulated and downregulated transcripts in LPS+IC stimulated macrophages relative to LPS alone.

43

upregulated significantly compared to resting cells. Within the 10 most down-regulated genes by R-Mϕ-IC were IL12B, a cytokine that induces Th1 responses, and CCL8, a chemokine that attracts monocytes. Both of these genes appeared in the list of top 10 most upregulated genes in LPS-Mϕ (Figure 3B). Taken together, our data indicate that LPS stimulation triggers major gene expression variations in human macrophages. Addition of IC in conjunction with LPS leads to remarkable downregulation of inflammatory gene expression, shutting down the LPS-Mϕ markers and enhancing an array of immunoregulatory genes with probable roles in tissue modeling and angiogenesis.

3.2 RNA and cell-surface biomarkers of human regulatory macrophages

Markers for the identification of macrophages with regulatory functions in humans could be relevant to the discovery of prognostic markers for inflammatory diseases. For this reason, we employed three different approaches for the identification of potential biomarkers: (a) a fluorescence in situ hybridization method for the visual microscopic identification of R-Mϕ-IC, (b) flow cytometric identification of surface and intracellular markers, and (c) secretome analysis to define secreted markers.

3.2.1 Markers of R-Mϕ-IC for imaging

Three genes, IL-10, LIF, and MMP10, were chosen as potential RNA biomarkers based on their high fold-change in expression compared to both LPS-Mϕ and NS-Mϕ in the RNA-seq. Activated macrophages (NS, LPS, and LPS+IC) from three donors were fixed, and then stained using custom probes from Advanced Cell Diagnostics (Newark, CA). The increase in mean fluorescence intensity per cell of

44

LPS+IC stimulated HMDMs for all 3 markers was significantly higher than the change in MFI induced by LPS treatment alone (Figure 5). Resting cells showed little to no expression of these transcripts. Combined with a macrophage marker, this method may prove useful for identification of R-Mϕ-IC in human tissue.

3.2.2 Flow cytometry marker for R-Mϕ-IC

Flow cytometry is a powerful and sensitive measurement tool that allows the characterization of individual cells from both research animals and human patients. The development of a cell-surface biomarker of R-Mϕ-IC activation was thus a strong interest for us, as it would be useful as biomarker for flow cytometry and potentially for immunohistochemistry techniques for use in human tissue. Using the RNA-sequencing data we identified genes that met the following criteria: (1) upregulated significantly with a minimum fold change of 2 in R-Mϕ-IC compared to LPS-Mϕ, (2) classified as a plasma membrane protein according to the Ingenuity Pathway Analysis database, and (3) having an average expression of at least 1 read per sample. The resulting list was sorted according to fold change between LI and LPS, and the top resulting genes were measured with flow cytometry. Several markers were tested that produced insignificant results, including TM4SF1, CD93, CD68, NOTCH2, GPR-C5A, and CD49b (data not shown). Of the many proteins tested, CXCR4 (Figure 6A) and DC-STAMP (Figure 6B) were the most reliable predictors of R-Mϕ-IC activation. At 16 hours after activation of HMDMs, cells positive for CXCR4 increase significantly in R-Mϕ-IC over both LPS-Mϕ and NS-Mϕ (Figure 6C). For DC-STAMP both MFI and % positive cells increased significantly over LPS-Mϕ (p-value<0.05), with % positive cells increasing by an average of 14% (Figure 6C).
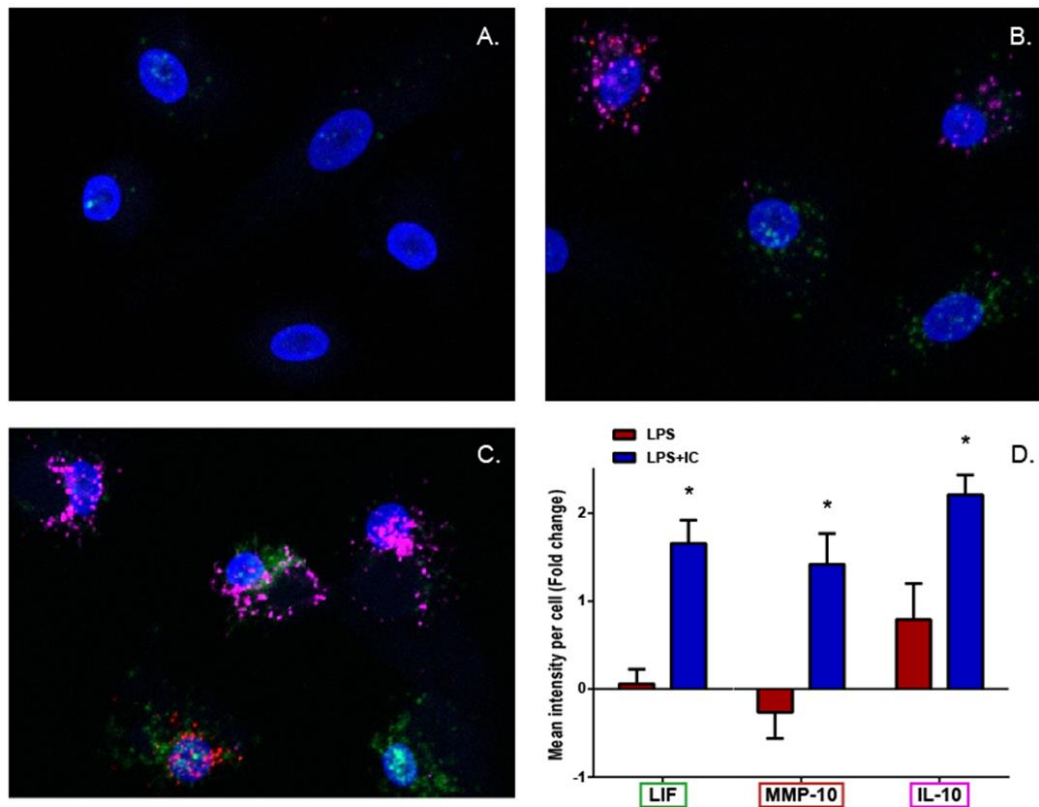
Figure 5. RNAscope can be used to identify R-Mϕ-IC. Mean fluorescence intensity per cell for 3 genes selected as potential RNA biomarkers using RNAscope, in Mϕ-NS (A), Mϕ-LPS (B) and R-Mϕ-IC (C). Sample RNAscope images with LIF in green, MMP10 in red, and IL-10 in magenta. Mean intensity per cell from 3 donors was quantified using Zen Software and is expressed as fold change compared to NS (p-value < 0.05).
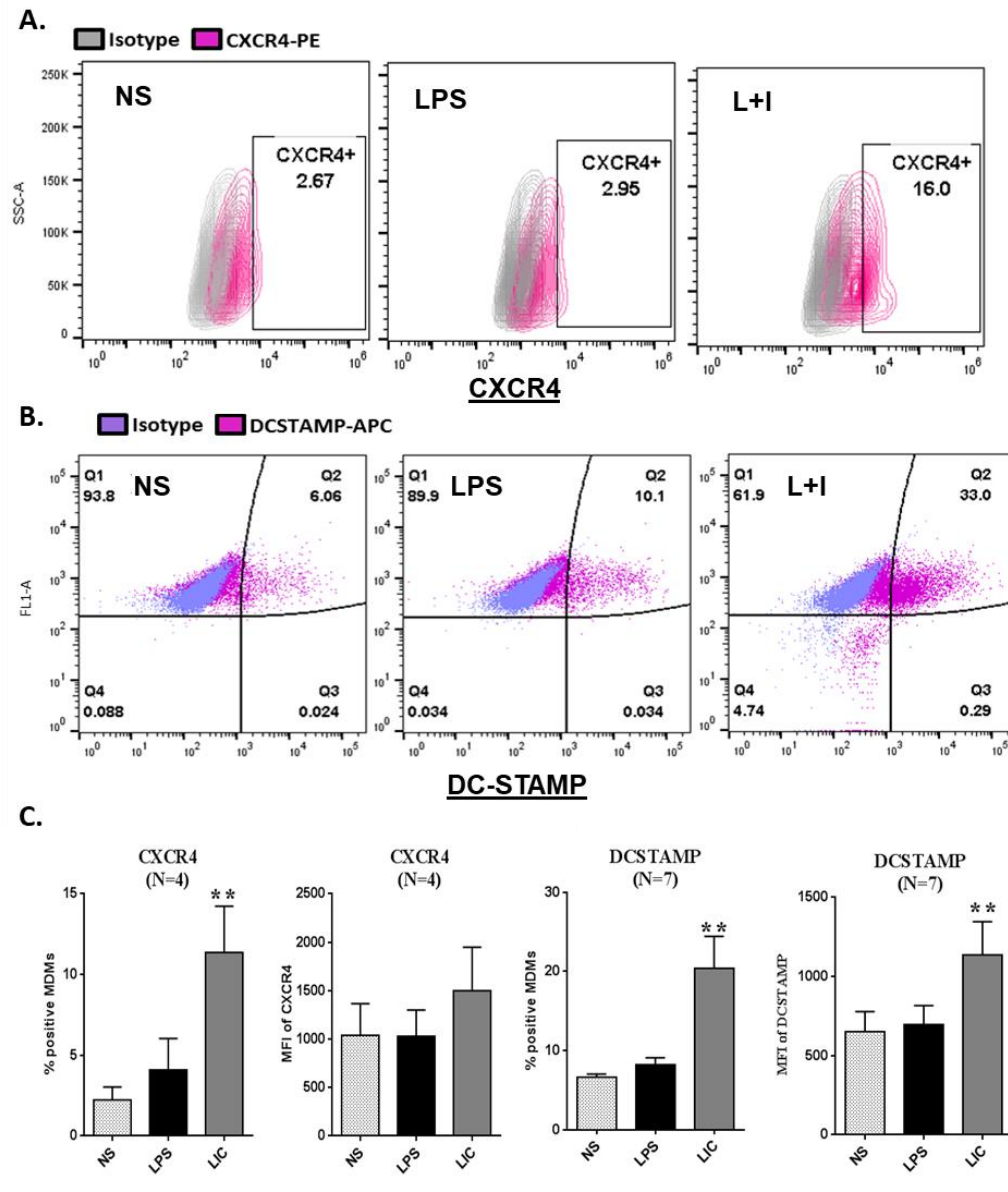
Figure 6. CXCR4 and DC-STAMP are potential cell surface biomarkers for R-Mφ-IC. HMDMs were stimulated with LPS with or without IC and collected 16 hours later for flow cytometry analysis of candidate biomarkers. Scatterplots are representative flow cytometry results for CXCR4 (A) and DC-STAMP (B). (C) % positive macrophages and MFI for both markers were calculated using data from multiple donors (n indicated in graphs; error bars are SEM, ** p-value<0.01). Figures were generated by Prabha Chandrasekaran.

These data indicate that CXCR4 and DC-STAMP are potential cell surface biomarkers for R-Mφ-IC.

In addition to upregulated transcripts, we also selected downregulated transcripts to test their potential as negative markers. Figure 7A shows the flow cytometry staining results for CD66b, also known as carcinoembryonic antigen-related cell adhesion molecule 8 (CEACAM8). Although LPS slightly downregulated this marker, LPS+IC significantly downregulated its expression compared to both LPS-Mφ and NS-Mφ (Figure 7B). Used together with CXCR4 and DC-STAMP upregulation, we proposed surface CD66b downregulation as a potential indicator of R-Mφ-IC activation.

3.2.3 Secretory protein markers of R-Mφ-IC

To characterize the secretome of R-Mφ-IC, a SOMAscan assay was performed on cell culture supernatants of HMDMs collected 24 hours following stimulation. As previously observed, IC was able to suppress the production of inflammatory mediators that were significantly upregulated with LPS treatment (Figure 8A). ELISA was performed to validate on proteins of interest. Whereas IL-6 and IL-12p40 were significantly downregulated (Figure 8B), CXCL11 was not detectable (data not shown). IL-12p40 did not appear on the SOMAscan panel, but it was measured as well because it was previously demonstrated to be down-regulated by IC[53]. The CC-chemokines CCL8, CCL15, CCL19 and CCL23, and CXC- chemokines CXCL11, CXCL13 were downregulated by IC, all of which have been demonstrated to be pro-inflammatory[138–140].
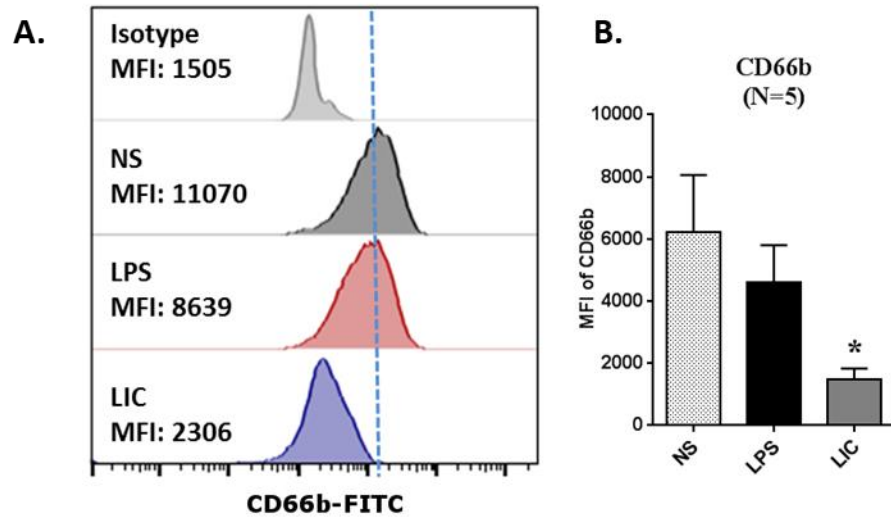
Figure 7. CD66b surface expression is suppressed by IC co-stimulation. HMDMs were stimulated with LPS with or without IC and collected 16 hours later for flow cytometry analysis of candidate biomarkers. (A) Representative histogram for CD66b staining from one donor. (B) MFI for CD66b was calculated using data from 5 donors (error bars are SEM, ** p-value<0.01). Figures were generated by Prabha Chandrasekaran.
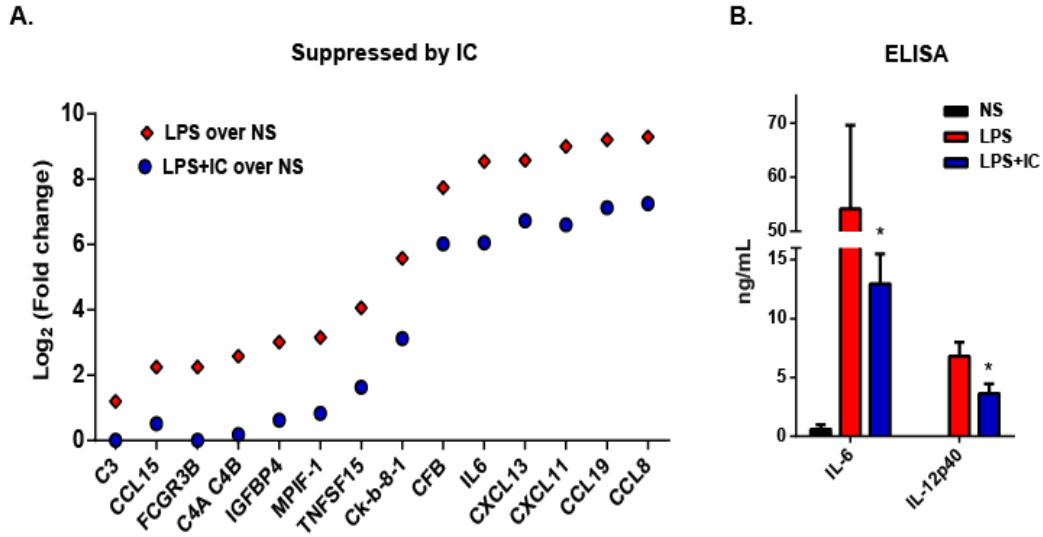
Figure 8. Treatment with immune complexes broadly suppresses the inflammatory actions of LPS. Cell culture supernatants were collected from NS, LPS, and LPS+IC stimulated HMDMs 24 hours after stimulation and differentially expressed proteins were identified using SOMAscan technology. (A) All extracellular proteins that were significantly upregulated in LPS-Mϕ compared to NS-Mϕ, but suppressed by R-Mϕ-IC treatment ($\log_2$ FC >1). (B) ELISA confirmation of inflammatory cytokines; IL-12p40 was included despite being absent from the SOMAscan panel. Data for figures were generated in collaboration with Stephen Christensen, Jingya Wang, Gary Sims, and Elizabeth Ward.

The proteins of the complement pathways C3, C4AC4B and CFB were also inhibited, indicating that addition of IC targets several pathways of inflammation for down regulation.

Cyclic AMP (cAMP) is a second messenger known to be produced following prostaglandin E2[141] and adenosine treatment[142], both of which induce regulatory activation in LPS-stimulated murine macrophages[53]. Because cAMP can suppress cytokine production, it was hypothesized that cAMP levels may be increased in R-Mϕ-IC as well. Measurement of cAMP with ELISA showed a significant increase in intracellular production of cAMP in macrophages stimulated with LPS+IC, with no detectable production apparent with LPS alone (Figure 9A). Attempts to block cAMP production using 3 different inhibitors of adenylyl cyclase were unsuccessful; however, treatment with forskolin (a drug that increases intracellular levels of cAMP) was able to suppress the LPS-induced production of inflammatory cytokines in HMDMs (Figure 9B).

To identify secreted proteins that are upregulated in R-Mϕ-IC, we followed two approaches (a) identify proteins that are specifically upregulated in R-Mϕ-IC and not under naïve or LPS stimulated conditions and (b) identify proteins that are >2 fold upregulated in R-Mϕ-IC compared to LPS stimulation (Figure 10A). Among the proteins upregulated >2 fold specifically by R-Mϕ-IC cells but not in LPS-stimulated cells were MMP-3, SPHK1, PRSS22, LBP and TNFRSF25. Secreted proteins that were triggered by LPS and are further upregulated by IC by >2 fold change include IL-10, MMP-12, INHBA, MMP-1 and CCL-20. In our analysis, it was not surprising that
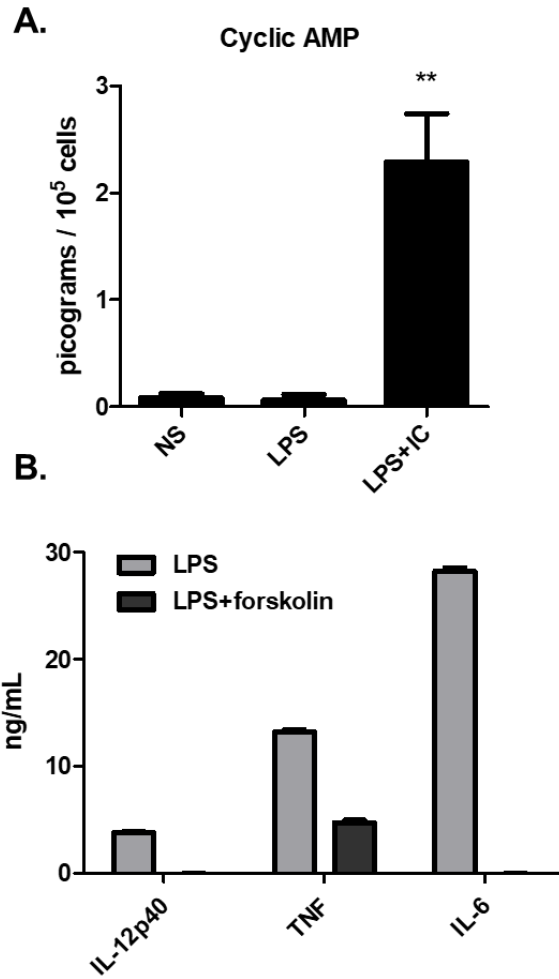
Figure 9. IC treatment increases intracellular cyclic AMP, which has a suppressive effect on inflammatory cytokines. (A) Activated HMDMs were lysed 2 minutes following stimulation, and intracellular cAMP was then measured using a direct ELISA colorimetric assay (n=3, p-value<0.01). (B) HMDMs were stimulated with 30 ng/mL LPS for 16 hours with or without forskolin, a small-molecule drug that increases intracellular cAMP. Cytokine levels were measured using ELISA.
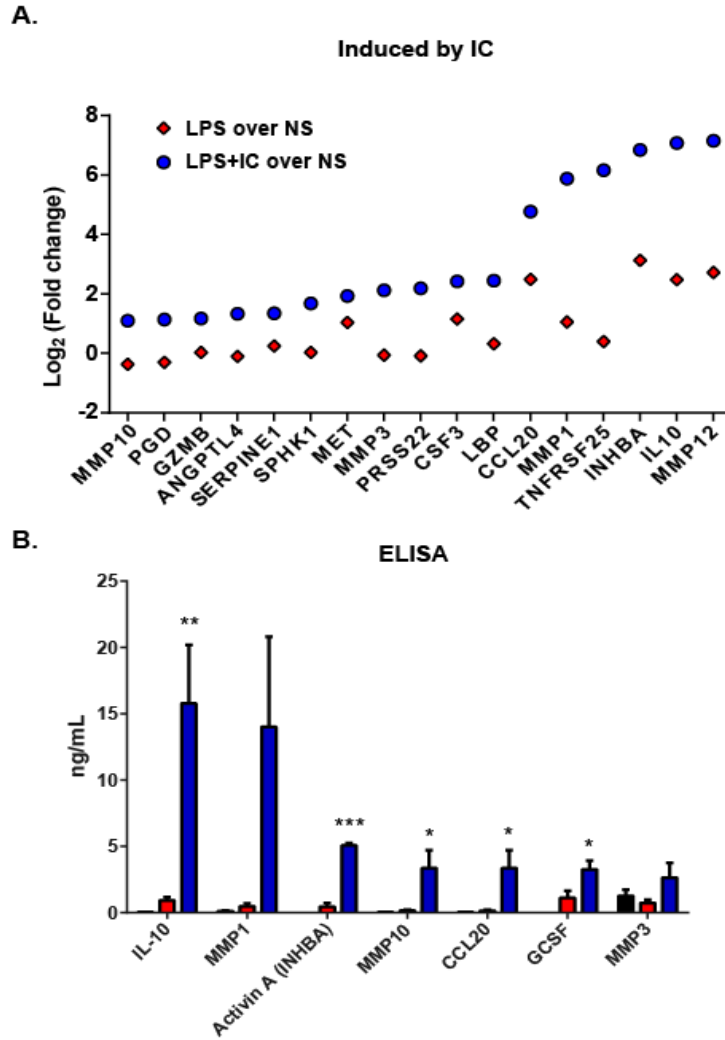
Figure 10. Treatment with LPS and IC leads to significant increase in several proteins implicated in immunoregulation, tissue remodeling, and angiogenesis. Cell culture supernatants were collected from NS-Mϕ, LPS-Mϕ, and R-Mϕ-IC HMDMs 24 hours after stimulation and differentially expressed proteins were identified using SOMAscan technology. (A) All extracellular proteins which were significantly upregulated in R-Mϕ-IC compared to both resting and LPS-Mϕ, with corresponding levels from LPS-Mϕ included for comparison. (B) ELISA confirmation of several of the gene changes observed in SOMAscan results (n=5, *p-value<0.05, **p-value<0.01, ***p-value<0.001). Data for figures were generated in collaboration with Stephen Christensen, Jingya Wang, Gary Sims, and Elizabeth Ward.

IL-10, a well-defined marker for R-Mϕ[39], was the second most highly upregulated of all proteins compared to LPS stimulation. For further verification, the expression of proteins that can serve as markers of secretory proteins of R-Mϕ-IC were validated by ELISA (Figure 10B) at 24 hours after stimulation.

Fold changes in protein levels from the SOMAscan were compared to the corresponding genes from the transcriptome to determine whether changes in secreted proteins corroborate the transcriptional changes observed in the RNA-seq (Figure 11). A general positive correlation was observed, although the genes differed in the degree of fold change ($r^2 = 0.46$). Nevertheless, the R value of 0.68 (p value $= 0.0001$) indicates a positive correlation between mRNA and protein regulation.

For qRT-PCR studies, a 7-hour time point was chosen rather than the previously chosen 4 hour time point (used for the RNA-sequencing) because gene induction in R-Mϕ-IC for the biomarker panel was higher at 7 hours. From the 16 LI-associated upregulated genes from the SOMAscan data, 10 genes were chosen based on their ability to meet the 3 following criteria: (1) upregulated compared to NS at the mRNA level, (2) not upregulated during general cellular stress, and (3) mainly secreted, as quantified by a confidence level of 5 for secreted/PM and 3 or less for all other locations according to the GeneCard database. Quantitative real-time PCR of these 10 genes (Figure 12) was performed to develop a panel as a readout for mechanistic studies. For this reason, certain data shown in Figure 12 is used again in future graphs.
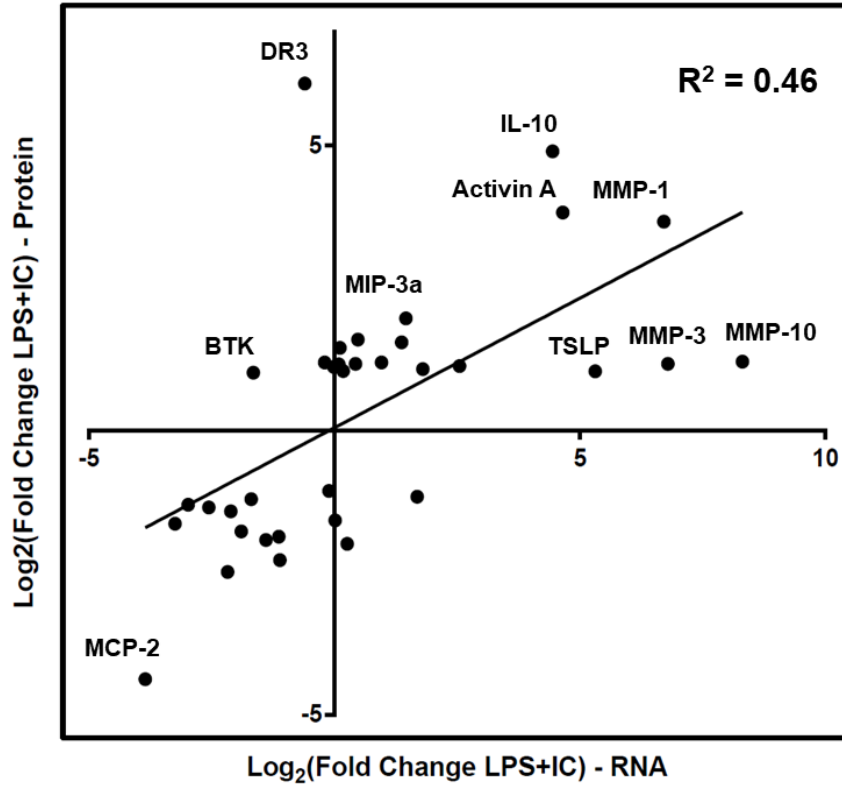
Figure 11. Correlation between protein and mRNA levels for differentially expressed proteins in R-Mɸ-IC. Fold changes of all differentially regulated proteins observed in SOMAscan results (LPS+IC vs LPS) plotted against fold changes observed in the RNA-seq for the corresponding genes. Spearman method was used to compute correlation.
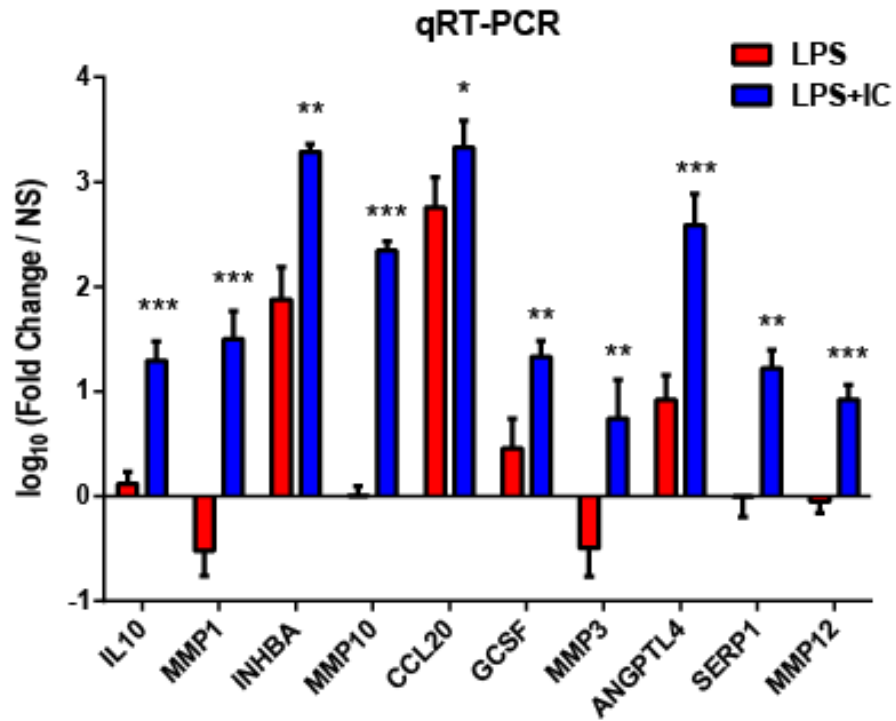
Figure 12. Quantitative real-time PCR validation of 10 chosen genes from the SOMAscan. qRT-PCR confirmed that 10 genes chosen for a R-Mφ-IC marker panel are reliably upregulated at the mRNA level at 7 hours after stimulation (n=6, *p-value<0.05, **p-value<0.01, ***p-value<0.001).

3.3 Bioinformatic analysis predicts MAPK-ERK, PI3K-Akt and AP1 complex as

upstream regulators

3.3.1 Ingenuity Pathway Analysis

Identifying key molecular regulators of transcriptional programs is important

for development of treatments that seek to activate the regulatory macrophage

phenotype _in vivo_. To identify the key pathways and master regulators involved in

generation of the R-Mϕ-IC phenotype, differentially expressed genes from RNA

sequencing (R-Mϕ-IC vs LPS-Mϕ) were analyzed using the Ingenuity Upstream

Regulators Analysis of the Ingenuity Pathway Analysis program (IPA). This analysis

uses information available in the literature to predict upstream regulators of the R-Mϕ-

IC differentially expressed genes (DEGs) by identifying the presence of targets for

specific regulators within the dataset. If there is significant overlap between the target

dataset and the R-Mϕ-IC DEGs, and the direction of gene change is consistent with the

action of the regulator, the regulator is predicted to be either activated or inhibited. The

results of this analysis predicted MAPK kinases and Akt signaling pathway members

to be probable regulators for the transcriptional gene changes in R-Mϕ-IC (Table 2).

3.3.2 Gene Set Enrichment Analysis

To complement the IPA analysis, we utilized GSEA to predict transcriptional

regulators likely to be involved in induction of R-Mϕ-IC genes. RPKMs from LPS+IC

and LPS RNA-seq samples were ranked according to difference between LI and LPS,

and compared to transcription factor target gene sets. Each set contains genes that share

a transcription factor binding site defined in the TRANSFAC database (version 7.4) in

Table 2. Ingenuity Pathway Analysis Upstream Regulators Report

Upstream Regulator	Molecule Type	z-score	p-value
ERK	group	4.451	1.20E-17
ERK1/2	group	3.977	2.15E-17
RAF1	kinase	5.084	5.86E-17
PI3K (complex)	complex	2.797	2.85E-12
Ras	group	3.299	1.53E-10
AKT1	kinase	2.826	2.40E-10
KRAS	enzyme	2.88	3.43E-10
MAP3K1	kinase	2.875	1.11E-09
Ap1	complex	2.763	4.62E-09
Pkc(s)	group	4.165	1.28E-08

Top 10 R-Mφ-IC-associated activated regulators ranked by p-value. Differentially regulated genes in LI vs LPS were uploaded and analyzed in IPA using the Upstream Regulators Analysis. Results were filtered by removing regulators with a low number of targets in its target dataset (<10). To identify regulators consistent with intracellular cytosolic signaling molecules, results were filtered according to ''molecule type' to include only groups, kinases, complexes, and enzymes (removed extracellular molecules, receptors, peptides, transcription factors, chemicals, microRNA, toxins and drugs).

the regions spanning up to 4 kb around their transcription start sites[129]. Listed in Table 3 are the top 10 transcription factors ranked by normalized enrichment score; AP-1, a direct target of ERK, dominated the list. GSEA of curated gene sets identified overlap of the R-Mϕ-IC associated genes with genes upregulated in cancer and hypoxic conditions, both associated with activation of the Akt pathway (Table 4). The curated data sets contain data from various sources such as online pathway databases, biomedical literature, and knowledge of domain experts; it includes chemical and genetic perturbations, all canonical pathways, BioCarta gene sets, KEGG gene sets and Reactome gene sets[128]. Further down the list, it was observed that R-Mϕ-IC genes also significantly overlap with genes upregulated in breast cancer cells expressing a constitutively active form of Akt1. In light of these results, the Akt/ERK pathways were chosen for further mechanistic studies on gene expression in R-Mϕ-IC.

3.4 Akt and ERK are activated in R-Mϕ-IC and contribute to immuno-regulatory gene induction

3.4.1 Akt pathway antibody array

To explore the results from the IPA Upstream Regulators Analysis, an antibody array for phosphorylated proteins in the Akt/ERK pathway was utilized on protein lysates from activated HMDMs 30 minutes after stimulation. LPS alone modestly activated several signaling proteins along this pathway, which were amplified by the addition of IC (Figure 13A). Figure 13B reveals the fold change compared to NS after densitometry analysis of the membrane data points (n = 3) for those molecules in the

Table 3. Gene Set Enrichment Analysis (C3: Transcription Factor Targets)

Transcription Factor	Name	Size	NES	FDR q-val
V$BACH2_01	BACH2	257	2.0635881	0
V$AP1_01	AP1	249	1.9047545	0.009461368
V$TATA_01	TATA	246	1.8897362	0.00872087
V$BACH1_01	BACH1	249	1.8852448	0.00712926
V$AP1_Q2_01	AP1	255	1.8239871	0.014296551
V$AP1_Q6	AP1	245	1.7120004	0.03983329
V$AP1_Q4	AP1	255	1.6929773	0.034499478
V$PBX1_02	PBX1	124	1.6775415	0.03656478
V$AP1_Q4_01	AP1	247	1.6308024	0.03817041
TGASTMAGC_V$NFE2_01	NFE2	183	1.6269499	0.05723352
V$RSRFC4_Q2	RSRFC4	199	1.6248336	0.05367498
V$ATF_B	ATF	184	1.6105359	0.050147545
V$ATF1_Q6	ATF1	222	1.6081342	0.05381274
V$AP1_Q6_01	AP1	255	1.5973284	0.051095504
V$AP1_C	AP1	259	1.5765415	0.054647822
V$AP1_Q2	AP1	250	1.5457755	0.06257205
V$AP1FJ_Q2	AP1	253	1.5270847	0.0778924
V$OCT1_02	OCT1	202	1.5193005	0.08692873
V$MEF2_Q6_01	MEF2	231	1.5178035	0.087893
V$TATA_C	TATA	271	1.5150462	0.08454026

Top 20 R-Mφ-IC-associated transcription factors ranked by normalized enrichment score (NES). Differentially regulated genes in LPS+IC vs LPS were analyzed in GSEA to predict transcriptional regulators likely to be involved in induction of R-Mφ-IC genes. DEGs were compared to transcription factor target gene sets. Each set contains genes that share a transcription factor binding site defined in the TRANSFAC database (version 7.4) to determine degree of overlap. "Size" refers to the number of DEGs that appear in the gene set. FDR refers to the False Discovery Rate. Analysis performed by Jingya Wang.

Table 4. Gene Set Enrichment Analysis (C2: Curated Gene Sets)

Name	Size	NES	FDR q-val
Upregulated in NRG1 signaling	170	2.726674	<0.0001
Upregulated by WT1	208	2.6159592	<0.0001
Upregulated by EGF	56	2.598476	<0.0001
Upregulated during hypoxia	125	2.5628119	<0.0001
Metastasis by ERBB2	43	2.476098	<0.0001
Downregulated by HIF1A and HIF2A	101	2.3819392	<0.0001
HRAS oncogenic signature	244	2.32088	<0.0001
Upregulated in hypoxia	163	2.3159282	<0.0001
Upregulated in TGFB1	194	2.2986596	<0.0001
Tumorigenesis	59	2.2963085	<0.0001
Degraded via KHSRP	97	2.2956862	<0.0001
Downregulated in adenovirus infection	40	2.292276	<0.0001
Upregulated in basal vs luminal breast	52	2.2745335	<0.0001
Peptide chain elongation	84	2.2740734	<0.0001
Downregulated by CDH1	56	2.27238	<0.0001
Methylated in breast cancer	35	2.262185	<0.0001
Associated with epithelial differentiation	66	2.2621262	<0.0001
Upregulated in hypoxia	47	2.2602153	<0.0001
Transiently induced by EGF	465	2.2463908	<0.0001
Upregulated by IL-2 signaling	109	2.2423522	<0.0001

Top 20 curated gene sets overlapping with the R-Mϕ-IC gene signature, ranked by normalized enrichment score. "Size" refers to the number of R-Mϕ-IC DEGs that match genes in the associated dataset. Names have been edited for ease of reading. Analysis performed by Jingya Wang.
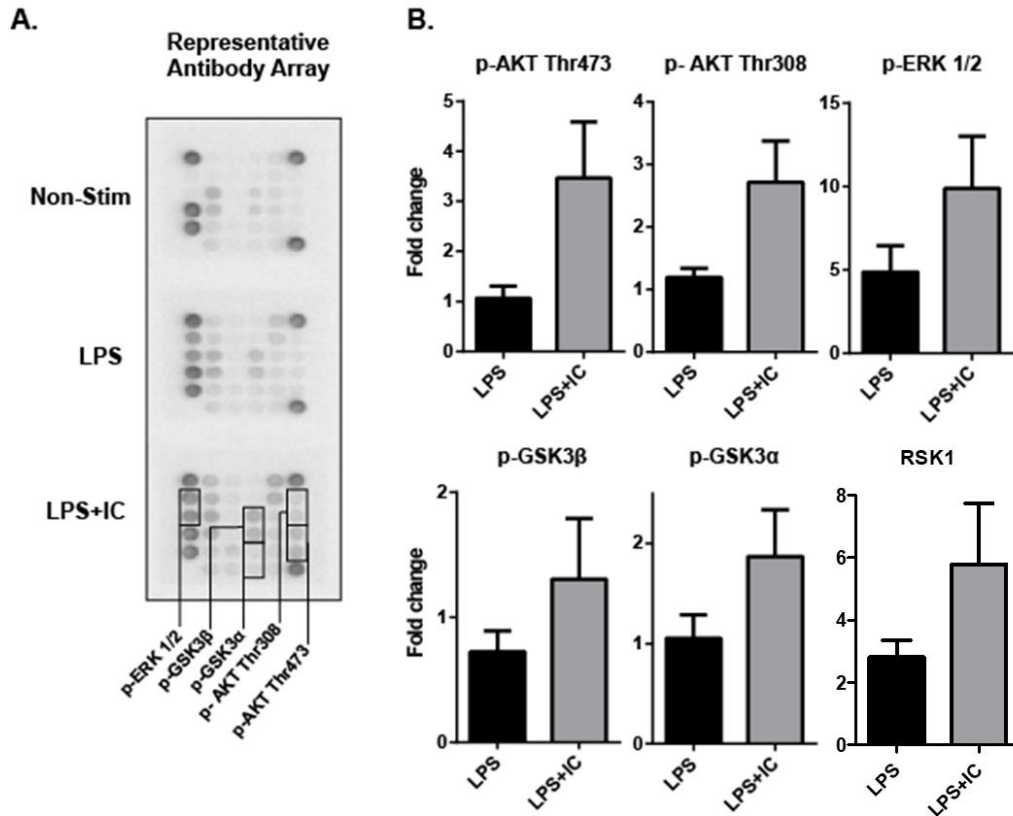
Figure 13. Immune complexes trigger increased phosphorylation of Akt, ERK, GSK3 and RSK1. (A) An Akt antibody array on whole cell lysates from HMDMs stimulated for 20 minutes containing antibodies against phosphorylated proteins of the Akt signaling pathway (Cell Signaling Technologies). (B) Densitometry was calculated using Image J software and compared to NS.

panel whose phosphorylation increased notably following co-stimulation with IC. Because Akt, ERK, GSK3α and GSK3β showed increased phosphorylation in R-Mφ-IC compared to LPS, they were selected for further analysis. Because RSK1 is directly downstream of ERK, its validation was delayed until it could be determined whether ERK or Akt were more potent regulators of the phenotype.

3.4.2 Involvement of ERK in R-Mφ-IC gene induction

Western blotting of ERK kinases were performed to confirm the results of the antibody array. Consistent with our previous observation in mouse[58], ERK 1/2 showed increased phosphorylation in LPS+IC treated cells (Figure 14A) with peak phosphorylation levels at 30 minutes (Figure 14B, n=3). Inhibition of ERK with U0126 suppressed four of the ten marker genes, with MMP1, MMP3, serpine 1, and MMP10 being significantly responsive to the effect of inhibition (Figure 14C). Because ERK only regulated a minority of the genes in the panel, the ERK substrate RSK1, despite displaying increased phosphorylation in the antibody array, was not chosen for further analysis.

3.4.3 Involvement of Akt in R-Mφ-IC gene induction

Western blotting of phosphorylated Akt was performed to confirm the results of the antibody array. Phosphorylation of Akt at Threonine 473 was higher under LPS+IC treated conditions (Figure 15A representative blot), with phosphorylation levels peaking at 30 min (Figure 15B, mean densitometry for 3 blots from independent experiments).
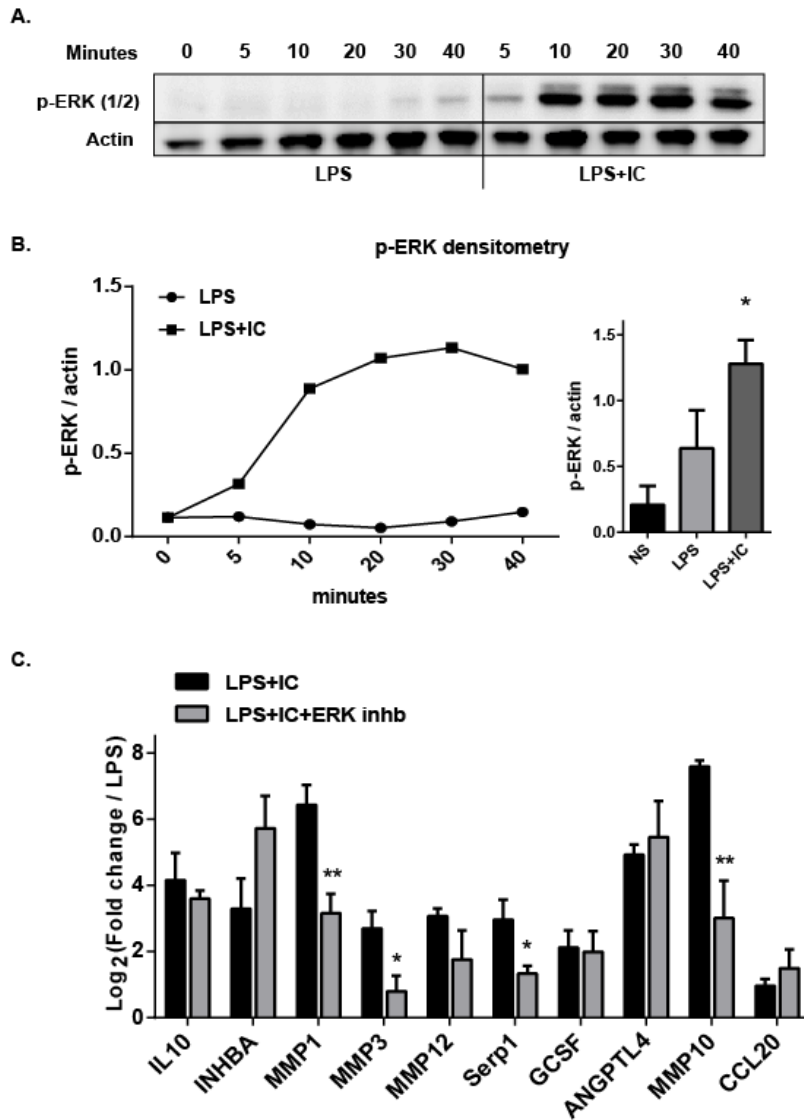
Figure 14. ERK is activated in R-Mφ-IC and contributes to expression of LI-induced genes.
(A) Western blot was used to confirm membrane array results in HMDM WCLs in the first 40 minutes after stimulation. (B) Densitometry was calculated using ImageJ software and normalized to loading control. Results from 3 blots at the 30 minute timepoint were averaged and statistics were performed to measure significance (n=3, p-value<0.05). (C) HMDMs were stimulated for 7 hours with LPS+IC, with or without a small molecule inhibitor of ERK (U0126, 10 µM). Gene expression was measured using qRT-PCR (n=4, *p-value<0.05, **p-value<0.01).
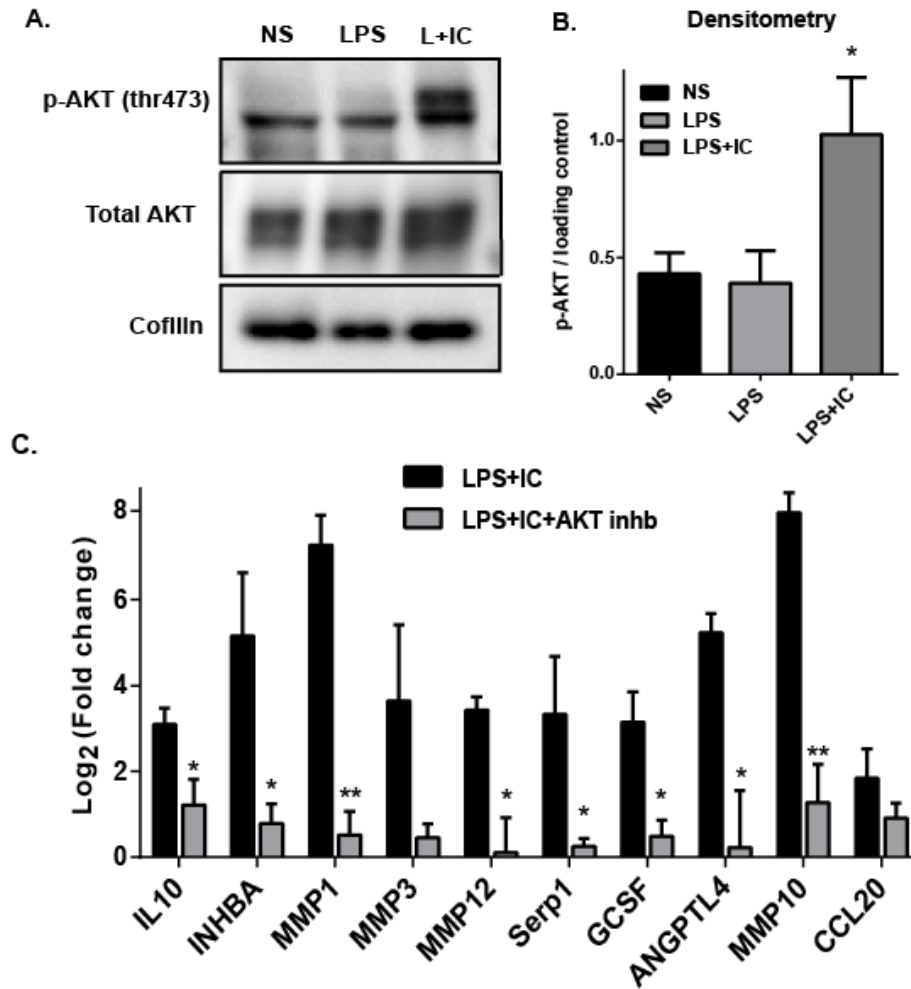
Figure 15. R-Mφ-IC display increased activation of Akt, which contributes to LI-induced gene changes. (A) Western blot was used to measure phosphorylation of Akt at thr473 30 minutes after stimulation with LPS+IC. (B) Densitometry on 3 replicate blots was calculated using Image J software and normalized to the loading controls. (C) R-Mφ-IC were treated with an inhibitor of Akt (MDS12384) before stimulation, and gene expression was measured at 7 hours using qRT-PCR (n=4, *p-value<0.05, **p-value<0.01, ***p-value<0.001.) Fold change was calculated using LPS and LPS+Akt inhb as the baselines for LPS+IC and LPS+IC+AKT inhb respectively.

To determine the involvement of the Akt pathway on gene expression in R-Mφ-IC, the macrophages were treated with an inhibitor of Akt and the mRNA levels of the R-Mφ-IC markers (see Figure 12) were quantified by qRT-PCR. Akt inhibition suppressed LI-induced expression of 8 of the 10 genes (Figure 15C). This was not likely due to any non-specific effects of the inhibitor, as inhibition of Akt led to varied effects on these genes in LPS-stimulated cells (Figure 16). Together, the data identify the MAPK-ERK and PI3K-Akt pathways as the primary pathways that drive regulatory phenotype in macrophages, with Akt being strongly influential.

3.5 GSK3 inhibition upregulates expression of R-Mφ-IC markers

Although GSK3 was not identified as one of the transcriptional regulators by GSEA analysis, the phosphorylation pattern of this protein was observed to be higher in the antibody array (Figure 13). Furthermore, the z-score for GSK3β from the IPA upstream regulators analysis was -1.862, indicating that its activity is predicted to be inhibited in these cells. Previous studies have demonstrated an inhibitory role for Akt on GSK3 signaling[143], and that GSK3 inhibition is known to increase IL-10 expression in primary human macrophages[105]. This led us to hypothesize that activation of Akt by IC should negatively regulate GSK3 and thus lead to higher IL-10 secretion.

3.5.1 GSK3 inhibition phenocopies IC co-stimulation

First, an ATP-competitive inhibitor of GSK3α/β was used in lieu of IC to determine if the GSK3 inhibition together with LPS stimulation could induce some of the transcripts that were induced in R-Mφ-IC cells.   Combined with LPS, the GSK3 inhibitor sb415286 consistently upregulated 9 out of the 10 genes tested in the panel of
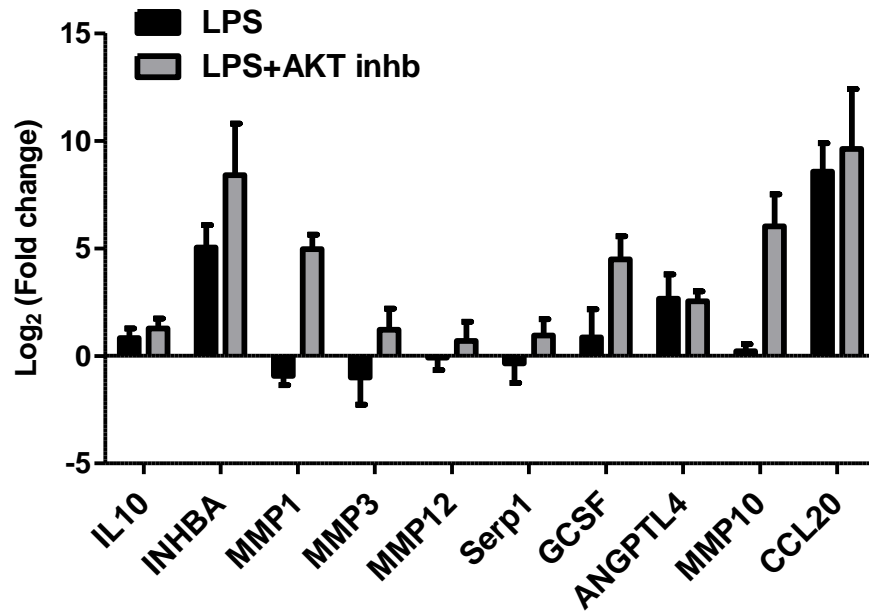
Figure 16. Akt inhibition has varied effects on M1 activation and does not broadly suppress gene expression. LPS-stimulated macrophages were treated with an inhibitor of Akt (MDS12384) 15 minutes prior to stimulation and gene expression was measured at 7 hours using qRT-PCR. Values are mean fold change over NS, n=4, error bars are standard error of the mean.

RNA markers for LPS+IC, 7 of which achieved statistical significance (Figure 17A).

Interestingly, the inhibitor did not affect expression of inflammatory cytokines (Figure

17B) indicating that GSK3 inhibition is important for inducing regulatory genes

expression, but is not sufficient for inhibiting LPS-triggered inflammatory response.

To determine if a GSK3β-specific inhibitor could also induce an anti-

inflammatory response, and if the response could be observed at the protein level, the

small-molecule inhibitor AZ2848 was used in combination with LPS to activate

HMDMs. ELISA analysis found that GSK3β-specific inhibition significantly

upregulated IL-10 and MMP10 in these cells (Figure 18). MMP-1 levels were also

upregulated, but this increase was not statistically significant due to extreme variability

in donor response. This variability for MMP-1 at the protein level was also observed in

response to LPS+IC (Figure 10B). LIF and MMP-12 were also measured by Luminex,

but neither one was detectable above threshold in most samples. Both genes had low

transcript numbers in the RNA-seq, which may explain why they were undetectable at

the protein level.

3.5.2 Co-stimulation with IC prevents entry of GSK3β into the nucleus

To validate the results of the antibody array, a western blot on phosphorylated

GSK3β was performed (Figure 19). Although phosphorylation of GSK3 was observed

after both LPS and LPS+IC stimulation, there was only a moderate increase for LPS+IC

above LPS, which was not significant (Figure 19A). Because GSK3β shuttles between

the cytoplasm and the nucleus, and active GSK3β has been shown to accumulate in

nucleus[144], we probed for GSK3β in cytoplasmic and nuclear fractions of R-Mϕ-IC
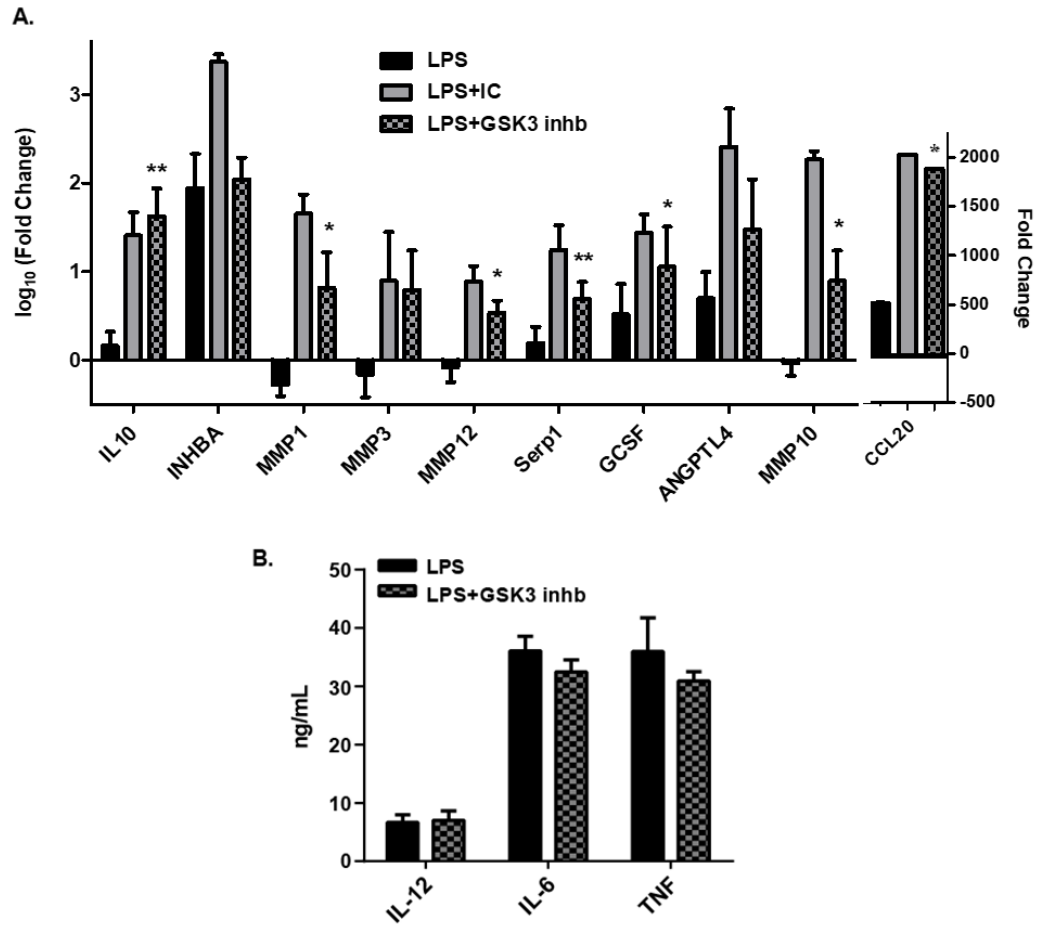
Figure 17. GSK3β inhibition phenocopies IC co-stimulation. (A) HMDMs were stimulated with LPS, LPS+IC, or LPS in the presence of a small molecule inhibitor of GSK3, SB415286 (20 μM). RNA was collected 7 hours after stimulation for qRT-PCR analysis of mRNA transcript levels (fold change is over NS, n=4, bars are standard error of the mean, *p-value<0.05, **p-value<0.01, ***p-value<0.001). (B) Production of inflammatory cytokines 8 hours after stimulation measured by ELISA assay (n=3, error bars are SEM).
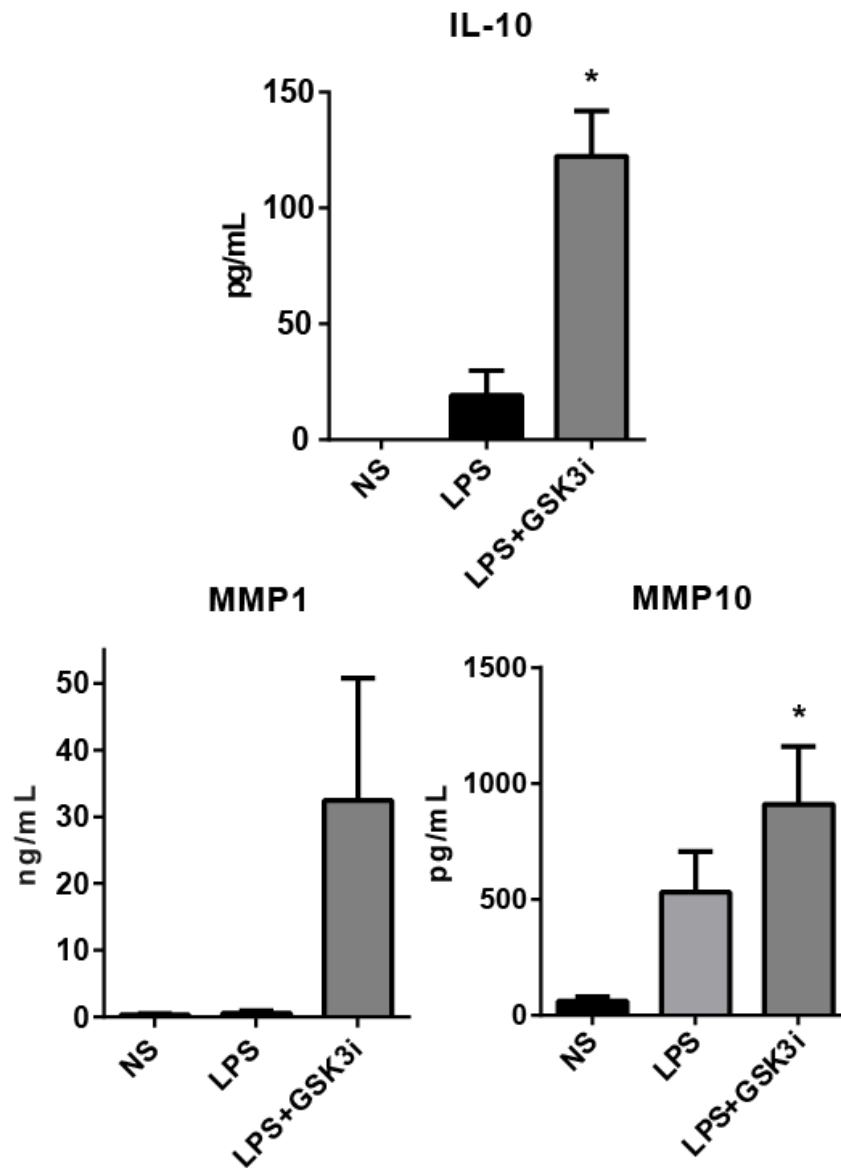
Figure 18. GSK3β-specific inhibition increases protein levels of R-Mφ-IC markers. HMDMs were stimulated with LPS or LPS in the presence of AZ2848, a β isoform-specific inhibitor of GSK3 (750 nM). Supernatants were collected 16 hours after stimulation and analyzed using ELISA (for IL-10) or Luminex analysis of select R-Mφ-IC biomarkers (n=3, bars are standard error of the mean, p-value<0.05).
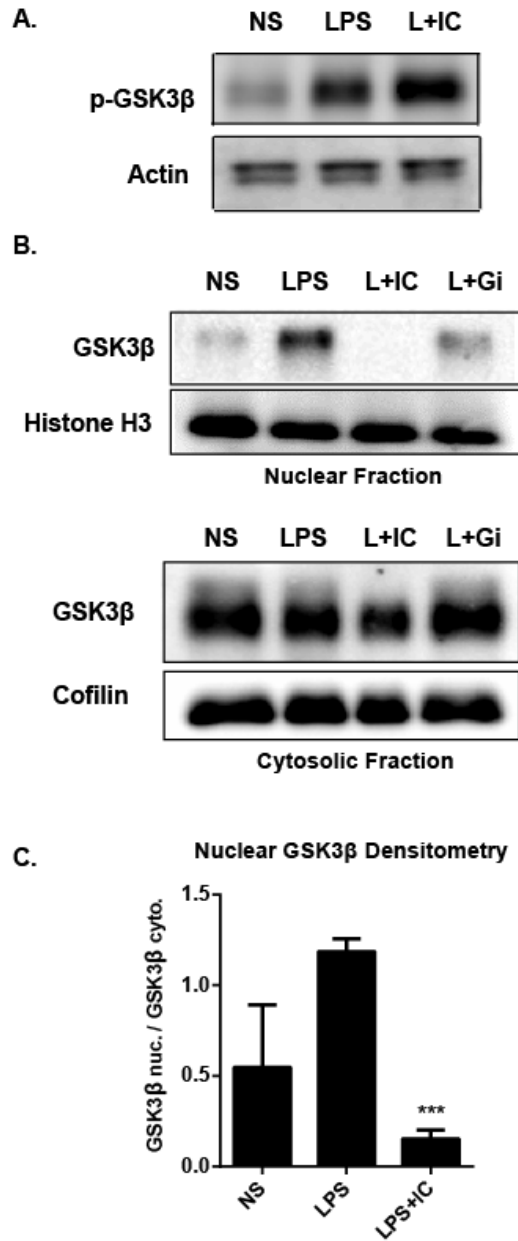
Figure 19. IC co-stimulation inhibits entry of GSK3β into the nucleus. (A) Western blot for phosphorylated GSK3β in whole cell lysates, 30 minutes after activation. (B) Western blotting for total GSK3β in the nuclear and cytosolic fractions of protein lysates collected 30 minutes after stimulation. (C) Densitometry on 3 replicate blots from (B) was calculated using Image J software and normalized to the loading controls before calculating ratio between nuclear and cytosolic GSK3 (n=3, ***p-value<0.001).

lysates. The western blot revealed that while LPS stimulation led to an increase of GSK3β in the nucleus, co-stimulation with IC prevented nuclear translocation, bringing levels down to even lower than those observed in resting cells (Figure 19B). Densitometry analysis (Figure 19C) found this decrease in levels compared to LPS to be statistically significant (n=3, p-value<0.05).

3.6 IPA Diseases and Functions Analysis implicates pathways associated with growth

To determine the functional significance of the differentially expressed genes in R-Mϕ-IC, we uploaded the RNA-seq fold change values from the LPS+IC group compared to LPS treated group into the Ingenuity Pathway Analysis program. The Diseases and Functions report from IPA indicated an up-regulation of genes involved in angiogenesis, proliferation, and tumor vulnerability (Figure 20A), and a down regulation of genes associated with inflammation (Figure 20B). Because the nature of the functions was similar, all predicted functions with a z-score greater than 2 or less than 2 were manually sorted into broader categories (Figure 20, pie charts). Since the diseases and functions available in the IPA knowledge database are based on available literature, the pie charts should be interpreted only as a summary of the functions that have been predicted, and should not be taken to indicate the proportion of gene changes associated with a particular function.

Because even significant overlap in genes can occur between two predicted data sets, the number of unique genes that predicted the 43 activated functions was determined. In total, 1,337 unique genes contributed to the predicted upregulated functions, 754 of which occurred in three cases or fewer. A total of 54 genes were observed in over 50% of the predicted functions. There were 716 unique genes

A.

Pie chart categories: Blood vessel development, Infection, Cell movement, Survival, viability and metabolism, Other, Cancer, Proliferation, differentiation and growth

Bar graph (Activation z-score):
invasion of tumor
invasion of malignant tumor
synthesis of lipid
cell survival
organization of cytoplasm
organization of cytoskeleton
invasion of cells
cell viability
development of cardiovascular system
angiogenesis
vasculogenesis
microtubule dynamics
proliferation of cells
invasion of tumor cell lines
growth of tumor
head and neck cancer
quantity of cells
formation of cells
differentiation of hematopoietic progenitor cells
migration of tumor cells

Activation z-score

B.

Pie chart categories: Vascular disease, Growth, Cancer, Cell Migration, Other, Misc. immune response, Cell death, Inflammation and inflammatory diseases

Bar graph (Activation z-score):
rheumatoid arthritis
rheumatic disease
apoptosis of hematopoietic progenitor cells
hypersensitive reaction
arthritis
arthropathy
cell death
apoptosis of tumor cell lines
apoptosis
glucose metabolism disorder
seizure disorder
inflammation of respiratory system component
necrosis
inflammation of respiratory system
seizures
inflammation of lung
inflammation of body region
inflammation of body cavity
inflammation of organ
organismal death

Activation z-score

Figure 20. RNA sequencing reveals significant changes in global mRNA expression related to immune regulation, angiogenesis, and cancer in R-Mϕ-IC. All DEGs in LI vs LPS, both significantly up and down regulated (FC >=2 or <= -2) were uploaded into the Ingenuity Pathway Analysis Program by Qiagen, and the Diseases and Functions Report was generated. The bar graph represents the top 20 most significantly upregulated (A) and downregulated (B) functions, ranked by z-score. To simplify the visualization, all diseases and functions predicted to be regulated were manually categorized into broader groups (pie chart) in a non-overlapping manner.

73

contributing to the prediction of 33 downregulated functions. 306 of these genes appear in 3 or fewer function data sets, while 48 genes occur in more than half of the downregulated functions. IL-10 appeared in 30 out of the 33. The minimum number of LI-associated genes that contributed to the prediction of a function (up or downregulated) was 38 (invasion of malignant tumor), and the maximum was 1,290 (Cancer). The number of genes used to predict each function is listed in Table 5 along with p-value and z-score.

These predictions are supported by the results of the gene set enrichment analysis (GSEA), which was dominated by gene sets associated with cancer or associated pathways, such as growth factor signaling and hypoxia (Table 4). The IPA analysis suggests a pro-survival, pro-growth, and anti-inflammatory phenotype in the R-Mϕ-IC macrophages compared to M1, consistent with our previous findings.

Table 5. Ingenuity Pathway Analysis Diseases and Functions Report

Diseases or Functions Annotation	p-Value	Activation z-score	# Molecules
invasion of tumor	1.77E-11	4.365	53
invasion of malignant tumor	7.59E-11	3.651	38
synthesis of lipid	9.67E-12	3.64	118
cell survival	8.76E-26	3.498	201
organization of cytoskeleton	3.02E-17	3.445	218
organization of cytoplasm	2.42E-15	3.445	228
invasion of cells	1.91E-21	3.268	141
cell viability	3.50E-23	3.26	176
development of cardiovascular system	7.99E-18	3.172	193
angiogenesis	4.67E-18	3.079	164
vasculogenesis	6.51E-16	3.032	136
microtubule dynamics	1.11E-10	3.019	168
proliferation of cells	1.27E-34	2.867	518
invasion of tumor cell lines	1.30E-13	2.763	80
growth of tumor	1.67E-24	2.702	157
head and neck cancer	7.81E-12	2.668	111
quantity of cells	3.78E-30	2.658	312
formation of cells	3.09E-13	2.592	160
differentiation of hematopoietic progenitor cells	2.04E-10	2.536	62
migration of tumor cells	8.91E-14	2.476	55
growth of epithelial tissue	4.11E-19	2.418	136
differentiation of bone	6.39E-09	2.369	71
viral infection	7.73E-12	2.341	163
cancer	1.44E-38	2.337	1290
differentiation of hematopoietic cells	1.14E-10	2.332	64
differentiation of cells	2.15E-28	2.297	362
formation of cellular protrusions	4.38E-11	2.277	139
mammary tumor	1.36E-12	2.242	236
breast cancer	1.08E-11	2.224	219
growth of neurites	5.48E-09	2.197	77
development of body trunk	2.95E-12	2.19	167
central nervous system tumor	2.58E-09	2.166	132
endothelial cell development	1.62E-11	2.141	70
proliferation of fibroblasts	1.34E-10	2.12	67
migration of cancer cells	2.33E-12	2.107	47
cell movement of tumor cells	1.91E-11	2.104	44
synthesis of DNA	2.88E-11	2.1	73
proliferation of endothelial cells	2.30E-10	2.086	61

growth of connective tissue	1.96E-19	2.07	132
cell cycle progression	2.67E-15	2.06	153
cell movement of fibroblasts	4.87E-09	2.037	39
growth of plasma membrane projections	6.93E-10	2.033	80
metabolism of eicosanoid	1.79E-10	2.012	49
infiltration of cells	6.47E-21	-2.053	98
lymphocyte migration	2.07E-14	-2.059	75
inflammation of liver	4.76E-12	-2.064	59
hypertrophy of heart	3.66E-12	-2.072	69
infiltration by mononuclear leukocytes	9.03E-10	-2.073	40
immune response of phagocytes	3.02E-15	-2.088	52
dermatitis	3.33E-12	-2.09	84
quantity of IgG	1.40E-14	-2.103	56
cell death of tumor cell lines	7.62E-13	-2.134	92
hypoplasia	2.45E-09	-2.139	86
cell death of hematopoietic progenitor cells	1.17E-12	-2.16	52
response of phagocytes	6.85E-14	-2.206	53
chronic inflammatory disorder	3.43E-19	-2.267	177
rheumatoid arthritis	1.17E-15	-2.319	130
rheumatic disease	2.12E-17	-2.343	184
apoptosis of hematopoietic progenitor cells	1.73E-12	-2.404	48
hypersensitive reaction	6.92E-13	-2.414	85
arthritis	1.49E-17	-2.43	170
arthropathy	3.67E-17	-2.468	171
cell death	2.09E-26	-2.469	449
apoptosis of tumor cell lines	3.52E-12	-2.482	76
apoptosis	4.57E-27	-2.579	379
glucose metabolism disorder	1.97E-09	-2.643	182
seizure disorder	1.94E-12	-2.651	89
inflammation of respiratory system component	1.58E-14	-2.709	83
necrosis	2.17E-29	-2.905	347
inflammation of respiratory system	3.82E-15	-2.982	85
seizures	5.77E-14	-3.027	83
inflammation of lung	6.55E-13	-3.168	76
inflammation of body region	5.14E-26	-3.221	190
inflammation of body cavity	1.44E-18	-3.312	135
inflammation of organ	2.60E-25	-3.71	217
organismal death	4.75E-15	-7.687	338

Diseases and functions predicted to be up- or down-regulated in R-Mϕ-IC, ranked by z-score. DEGs in LI vs LPS were uploaded and analyzed in IPA using the Diseases and Functions analysis. "# Molecules" refers to the number of DEGs in the LIvsLPS dataset that contributed to the prediction of that particular function.

In previous studies, murine BMDMs pre-treated with LPS and IC were able to rescue mice from lethal endotoxemia[53], an effect thought to be due in part to the high production of IL-10 secreted by these macrophages. To assess whether similar anti-inflammatory activity could be induced by GSK3β inhibition in macrophages, we sought to utilize the same model. Unfortunately, treatment of BMDMs with GSK3 inhibitor did not result in a drastic increase in IL-10 as was previously observed in HMDMs (Figure 21), despite looking at different time points (Figure 21A), different concentrations of inhibitor (Figure 21B), or different inhibitors (Figure 21C). Because of this, C57 black 6 mice were instead injected intraperitoneally with HMDMs that had been pre-treated with LPS, with or without a GSK3β-specific inhibitor. This injection was followed 2 hours later by injection of a lethal dose of endotoxin, and mice were then monitored for survival. In the mice injected with cells pre-treated with LPS, only 70% had survived by 4 days, whereas mice injected with the LPS+GSK3 inhibitor treated cells survived at a rate of 100% (Figure 22). However, as the p-value was only 0.06, these results are not considered statistically significant.
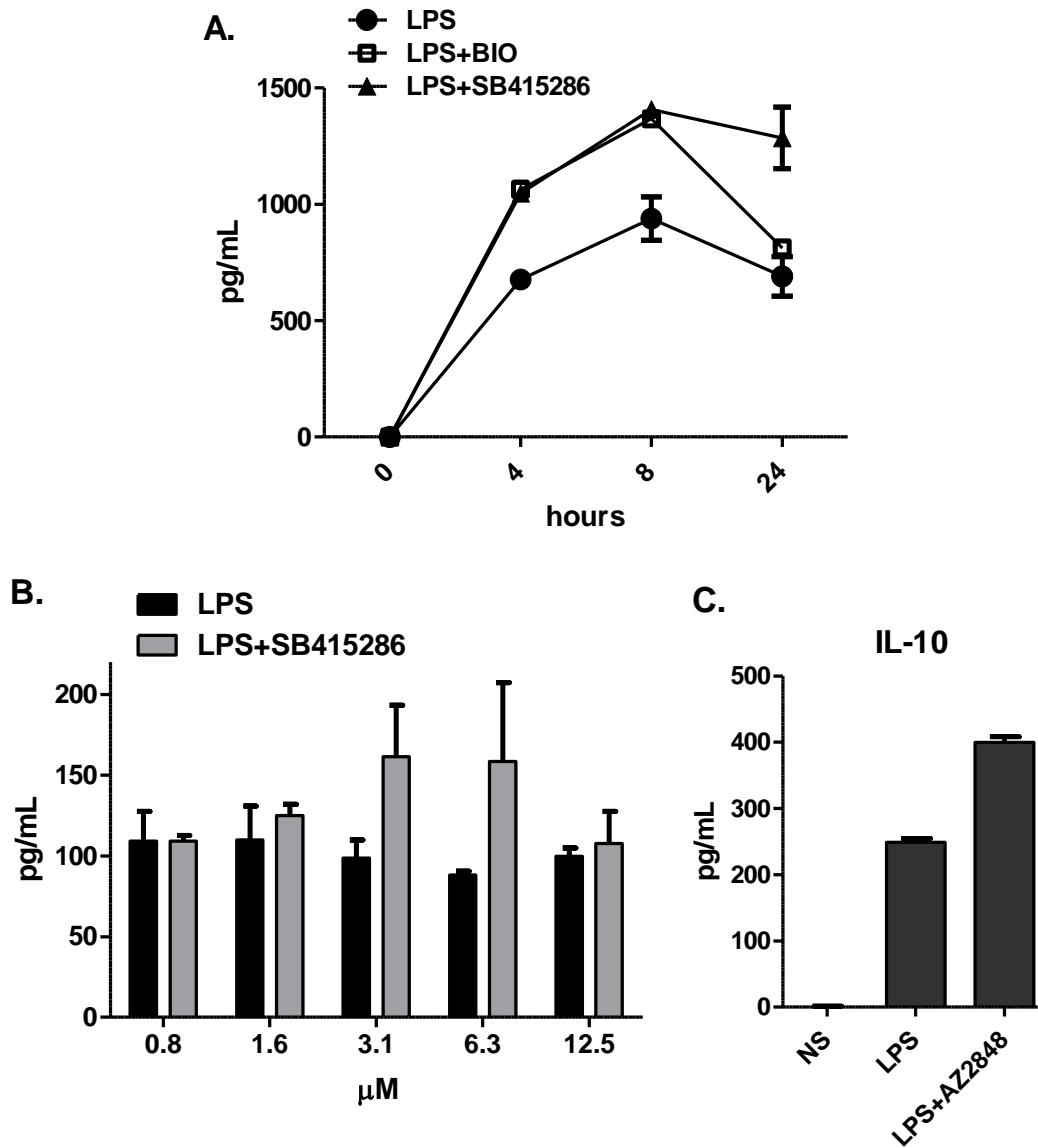
Figure 21. GSK3β inhibition induces only a slight increase in IL-10 in murine macrophages.
BMDMs derived from C57bl/6 mice were treated with LPS with or without an inhibitor of GSK3.
(A) Time course of IL-10 secretion in BMDMs treated with two small-molecule inhibitors of GSK3
(5 µM for each). (B) IL-10 production with GSK3 inhibition at various concentrations, 16 hours after
stimulation. (C) BMDMs were treated with LPS and a potent GSK3β-specific inhibitor (600 nM)
and IL-10 levels were measured by ELISA after 16 h. Values are mean ± standard deviation.
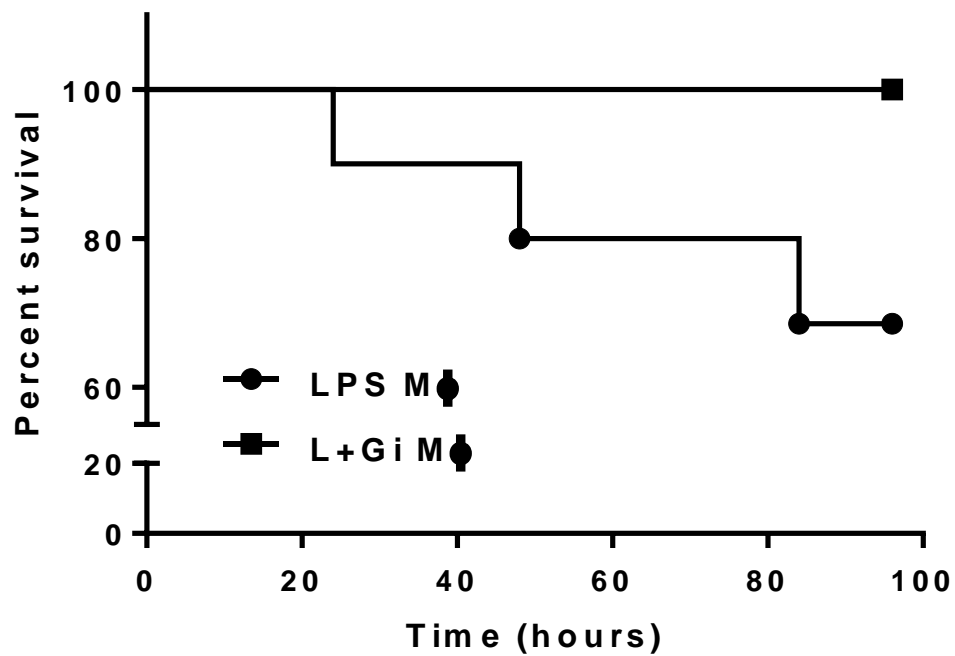
Figure 22. The effect of macrophage-mediated GSK3β inhibition in lethal endotoxemia.
C57bl/6 mice were injected with $2x10^5$ HMDMs pre-treated for 1 hour in culture with 30 ng/mL
LPS (circles), or LPS and GSK3 inhibitor (squares), followed by injection with a lethal dose of
endotoxin two hours later. Graph represents 10 mice per group, with data pooled from 2 independent
experiments (p-value 0.06).

Chapter 4: Discussion

Previous studies of mouse macrophages found that IC co-stimulation could not only suppress IL-12p40, but also increase production of IL-10 and HB-EGF[54,56,57]. This led to the hypothesis that this activation state may play a critical role in tissue repair and the resolution of inflammation. Indeed, injection of LPS+IC stimulated macrophages was able to rescue mice from lethal endotoxemia[53]. These so-called "regulatory" macrophages (R-Mϕ-IC) have a high therapeutic potential, but relevance in humans was still unknown. Using a combination of bioinformatics and functional analyses we have performed the first detailed characterization of this "activation state" in primary human macrophages. Our study proposes that this activation state plays a role in the regulation of inflammation, and that the Akt/GSK3 pathway has an integral part in this activity.

Immune complexes are antigen-IgG antibody complexes used to study the effect of Fc receptor cross-linking in cell culture. Although these complexes do arise naturally within the body under some circumstances, especially in pathological conditions such as lupus, Fc receptor cross-linking is also normally induced in macrophages that have encountered pathogens opsonized with IgG. These IgG molecules cross-link Fcγ receptors and facilitate not only the binding but also the internalization and intracellular fate of IgG-opsonized particles. Here we show that regulatory macrophages have an anti-inflammatory mRNA profile in HMDMs and that IC co-stimulation increases production of molecules involved in healing, survival, and proliferation. This implicates a feedback mechanism wherein antibody production during an infection could not only contribute to the clearance of pathogens, but also to

the resolution of inflammation and tissue remodeling through its effect on macrophage polarization. This idea is supported by a study examining the immune response to chlamydia in B-cell deficient mice, which found that B cells prevented an exaggerated immune response to the infection through induction of immunoregulatory cytokines [145]. Another study found antibodies to be important in the wound healing response through direct binding of antibodies to damaged tissue [146]. The idea that B cells could contribute to tissue healing is an idea that is rarely considered, and has been largely unexplored; nevertheless, some data exists to suggest adaptive immune responses is involved in proper wound healing following inflammation and damage[147–150]. Further studies are needed to uncover the mechanism underlying this observation, to determine the physiological relevance of the R-Mϕ-IC phenotype *in vivo,* and to identify the circumstances under which this phenotype occurs.

4.1 Transcriptomic analysis

As expected, stimulation of human primary macrophages with LPS led to the differential regulation of several thousand genes. The positive association between the two groups compared in Figure 3 indicates that the effect of LPS is similar in both LPS-Mϕ and R-Mϕ-IC. Although LPS had a much greater influence on gene expression than did the addition of IC, immune complexes regulated over 1,000 transcripts. IC can influence LPS-regulated genes in several ways, including amplification or suppression of LPS-induced genes, or restoring suppressed genes to their baseline levels. This ability for IC to modulate LPS-induced gene changes is especially evident when observing the top 10 LPS-upregulated genes, many of which are associated with

inflammation. Despite less than 700 genes being downregulated in R-Mϕ-IC versus LPS-Mϕ, the addition of IC is able to significantly suppress these highly inflammatory LPS-induced transcripts at the RNA level.

R-Mϕ-IC activation leads to the upregulation of 925 transcripts over LPS, 632 of which are also upregulated significantly compared to resting cells. This latter distinction is important for the identification of genes most likely to serve as appropriate biomarkers and that may give this phenotype functional significance. The fact that many of these genes are associated with healing, angiogenesis, and resolution of inflammation led us to consider the possible role of these macrophages in tissue repair. TM4SF1, the most highly upregulated, is a transmembrane protein mainly studied in the context of cancer due to its effect on proliferation and migration of cells[151]. MMP10, also known as stromelysin-2, is a matrix metalloproteinase that has anti-inflammatory effects in vivo[152,153] and is upregulated in ovarian and gastric cancer[154,155]. Table 6 lists the names and functions of some of the top most upregulated genes from Figure 4 that have a potential role in immune regulation. The functional associations of these genes and many others upregulated in R-Mϕ-IC was later confirmed by bioinformatics analyses on gene ontology, both with IPA and GSEA, further suggesting a role for this phenotype in healing.

Table 6. Known immunoregulatory functions of DEGs upregulated in R-Mϕ-IC

Molecule	Log2 FC vs LPS	Functions
TM4SF1	Transmembrane 4 L six family member 1	Induces proliferation and migration of cells[151]
MMP10	Matrix metallopeptidase 10	Extracellular enzyme with anti-inflammatory activity[152,153]
LIF	Leukemia inhibitory factor	Pleiotropic cytokine that influences survival and proliferation dependent on cell type[156]
XIRP1	Xin actin-binding repeat containing 1	Involved in muscle repair and regeneration[157]
MMP3	Matrix metallopeptidase 3	Involved in scar formation, tissue healing, and suppression of inflammation[158–160]
GPR3	G protein-coupled receptor 3	Involved in cell survival and thermogenesis[161,162]
MMP-1	Matrix metallopeptidase 1	Degrades ECM; involved in tissue remodeling and metastasis[163,164]
TNFSF14	Tumor necrosis factor superfamily member 14	Induces proliferation/differentiation[165]; involved in recovery after inflammation[166]
IL-10	Interleukin 10	Anti-inflammatory and immunosuppressive cytokine[29]
DC-STAMP	Dendritic Cell-Specific Transmembrane Protein	Regulates of osteoclast differentiation[167]; increases survival of cancer cells[168]
ANGPTL4	Angiopoietin-like 4	Angiogenic molecule, involved in wound-healing of skin, pro-tumor[169]
INHBA	Inhibin beta A	Forms the homodimer Activin A; pro-wound healing and scar formation, induces regulatory T-cell polarization, has both pro- and anti-inflammatory actions[170]

In order to determine the true physiological role of the R-Mϕ-IC phenotype, several specific biomarkers amenable to multiple measurement techniques must be identified and validated for use in human samples. Although biomarkers for regulatory activation have been identified in mouse, the response to LPS and immune complexes does not overlap 100% between the two species, necessitating species-specific markers. For example, CCR1 was identified as a regulatory marker for murine regulatory macrophages[53], but CCR1 transcript levels were not similarly increased in human R-Mϕ-IC, and were actually decreased compared to resting cells. Here we have identified potential markers of R-Mϕ-IC in HMDMs suitable for two well-known methods of measurement from human samples.

4.2.1 RNAscope markers

To provide a proof-of-concept for identification of these macrophages in tissue, we utilized RNAscope technology, which uses transcript hybridization with fluorescent probes to visually quantify transcripts within fixed tissue and cell culture samples. We found that IC-induced regulatory macrophages can be identified through increased expression of IL10, LIF, and MMP10 transcripts in HMDMs using this technology. Fluorescence intensity appeared to be very high in positive cells whereas other cells remained negative. This heterogeneity may be explained by the requirement for dense clustering of the Fc receptors to induce Syk activation[171], which may not be above threshold in every cell. If used in combination with a macrophage marker such as CD68, we propose this method for identification of regulatory macrophage activation in FFPE tissue sections.

4.2.2 Flow cytometry markers

The identification of protein biomarkers for macrophage activation states represents a challenge due to the dynamic and transient nature of macrophage activation. In this study, we used RNA-sequencing to identify genes for plasma-membrane associated proteins that have a very high fold change increase in R-Mϕ-IC. Due to the complex nature of macrophage activation it is unwise to rely on a single marker, and so a panel of markers, including both up- and down-regulated proteins, is ideal to develop a "signature" for R-Mϕ-IC activation. Through trial-and-error, flow cytometry studies showed that increased CXCR4 and DC-STAMP, along with suppressed CD66b expression were reliable cell surface markers for R-Mϕ-IC activation in human macrophages. Further studies are needed to validate these markers in human tissues.

Dendritic Cell-Specific Transmembrane Protein (DC-STAMP) is a cell surface protein that, despite its name, is expressed also on stimulated macrophages. This protein is mostly known for its role in the regulation of osteoclast differentiation[167], but also appears to increase survival in cancer cells[168]. DC-STAMP has been shown to be regulated by ERK[172], which may explain why its expression is sometimes increased in LPS-stimulated cells, but does not appear to be affected by GSK3 inhibition (data not shown).

C-X-C chemokine receptor type 4 (CXCR-4) is CXC chemokine receptor that binds CXCL4 and is most well-known for its role in the cellular entry of the HIV virus into T cells, as well as its involvement in the recruitment of lymphocytes. CXCR4 is expressed in many cells of the hematopoietic lineage, and has been found to bind

macrophage inhibitory factor (MIF)[173] and extracellular ubiquitin, the latter of which is thought to have an anti-inflammatory effect[174]. CXCR4 expression is associated with the presence and actions of tumor associated macrophages[175], as well as the immunosuppressive phenotype in macrophages seen after sepsis that increases risk for cancer growth[176]. Regulation of CXCR4 expression have been shown to be controlled by calcium signaling[177] and cAMP[178], both of which are thought to be increased after Fc receptor cross-linking in macrophages. As GSK3 inhibition did not increase cell surface levels of CXCR4 (data not shown), this marker is likely controlled through other upstream regulators.

CD66b, also known as CEACAM8, is a GPI-anchored cell surface protein involved in cell adhesion and activation of neutrophils, eosinophils and basophils[179,180]. Very little is known about its function in macrophages, but since it is a marker for granulocytes, it is suggested that this marker be used only in conjunction with a macrophage marker such as CD68. Similar to IC treatment, GSK3 inhibition also suppressed production of CD66b (Figure 23).

Further studies are needed to validate the utility of these markers in human tissue, to (1)
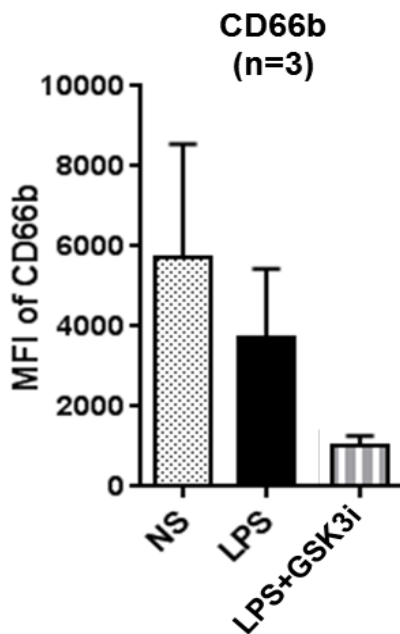

Figure 23. GSK3 inhibition suppresses the surface expression of CD66b. HMDMs were stimulated with LPS with or without GSK3 inhibitor and collected 16 hours later for flow cytometry analysis of candidate biomarkers. MFI for CD66b was calculated using data from 3 donors. Figure was generated by Prabha Chandrasekaran.

assess stability to ensure that the markers are not easily regulated by otherwise inconsequential changes in the environmental milieu; (2) to confirm that expression is induced relatively early and is sustained for a prolonged period; (3) to confirm that expression coincides with the expression of immunoregulatory proteins; (4) to ensure that expression is observed in all types of tissue macrophages (microglia, osteoclasts, etc.) that are capable of undergoing regulatory activation; (5) to ensure that markers are not expressed with IgG antibody alone; (6) to determine if the expression is reliant on the use of LPS or if the marker can be upregulated in the presence of other TLR ligands or inflammatory cytokines; (7) to determine which upstream regulators (ERK, Akt, GSK3, calcium, cAMP, etc) control expression of each marker. Experiments that assess the ability for the potential biomarkers to meet these criteria will strengthen the recommendation for their use in explorative studies in human tissue.

4.3 SOMAscan analysis of secreted proteins

The results of the SOMAscan analysis largely verified our overall impressions from the RNA-sequencing results. Immune complexes are able to broadly suppress several LPS-induced cytokines and chemokines, an observation that may be explained by the upregulation of cyclic AMP in this phenotype. Cyclic AMP is a nucleotide that acts as a second messenger, and in macrophages has been observed to regulate cytokines through its activation of cAMP-response element binding protein (CREB). Here we've shown that cyclic AMP is highly upregulated within minutes of stimulation with immune complexes. This effect of FcR ligation has been previously observed, as treatment of neutrophils with immune complex was also shown to increase cAMP production[181]. Replication of this phenomenon with forskolin, which increases

intracellular levels of cAMP, was able to suppress LPS-induced cytokines, suggesting that the ability for IC to suppress inflammatory cytokines could be mediated through production of cyclic AMP.

The SOMAscan analysis also confirmed the ability for R-Mϕ-IC to produce high amounts of secreted soluble mediators, as shown by a drastic increase in high-count proteins such as the MMPs. The work herein suggests a panel of proteins may be most appropriate for ELISA markers of this phenotype, with IL-10, MMP-1, and activin A being the most abundant. The upregulation of several matrix metalloproteinases suggests that regulatory macrophages could contribute to cell motility, angiogenesis, and tissue remodeling in the context of inflammatory stimuli. The increase in matrix metalloproteinases in particular could have a significant physiological impact, as MMPs are involved not only in degradation of ECM components, but also regulate extracellular signaling molecules[137]. MMP-10 production by macrophages regulates and suppresses immune response following infection[152,153], while MMP-3 and MMP-1 can cleave bFGF and VEGF, releasing their active forms. Not surprisingly then, MMP-1, MMP-3 and MMP-10[182] are associated with tumor metastasis and angiogenesis. Given these actions, regulatory macrophages could inhibit immune responses at the site of inflammation and contribute to resolution and repair. Concordantly, activators of this phenotype could have a deleterious effect on cancer. We look forward to future studies that explore the role of this phenotype in wound healing and chronic disease.

Identifying the major players involved in functional phenotypic switches in activated macrophages is central to our understanding of inflammatory processes. Through our bioinformatics analysis, we found that the upregulated LI genes are associated with HIF, growth factor, Akt/PI3K and ERK signaling pathways. Very little has been done to test Ingenuity Pathway Analysis in its ability to accurately predict upstream regulators. However, the presence of obviously irrelevant regulators such as pharmaceutical drugs on the resulting list of potential regulators suggests that the false positive rate is very high. Another example of a likely false positive is the prediction of TREM1 activation. This receptor appeared several times in the upstream regulators predictions, both in IPA and GSEA. However, the downstream signaling of TREM1 is known to be mediated by ERK, a kinase also found to be activated in R-Mφ-IC through cross-linking of FcRs. This provides a cautionary tale for investigators attempting to draw solid conclusions from bioinformatics data; until an analysis that can accurately predict an aggregated upstream pathway is designed, the prediction of these upstream regulators must be approached with skepticism.

4.4.1 ERK

In previous studies using mouse macrophages, ERK phosphorylation led to transient chromatin remodeling at the IL-10 promoter, which is what accounted for increased production of IL-10 seen after IC treatment [58]. This knowledge was useful during our bioinformatics analysis, as the prediction of ERK involvement gave credence to the software's ability to predict pathways and regulators involved in the phenotype. Indeed, ERK phosphorylation was significantly enhanced in regulatory

macrophages, and inhibition of ERK suppressed the induction of 4 out of the 10 LI marker genes. However, IL-10 did not appear to be affected by ERK inhibition, which is inconsistent with previous results seen in murine macrophages[53]. Nevertheless, the involvement of ERK activation in this phenotype was also supported by a GSEA transcriptional targets analysis which predicted an increase in the activity of AP-1. AP-1 is a transcription factor complex which regulates IL-10 and other LI-associated genes, and which is known to be directly activated by ERK[183]. However, because ERK did not regulate all of the 10 LI marker genes, further studies must be conducted to determine the major transcriptional drivers of the phenotype.

4.4.2 Akt

The upstream regulator analysis provided by IPA was the first to suggest the involvement of the Akt pathway in this phenotype. The Akt pathway is a complex signaling cascade that is remarkably sensitive to the nutritional status of the cell, and can regulate metabolism based on nutrient availability[184]. Akt is also activated by exposure to growth factors, and contributes to survival, increased glucose metabolism, proliferation, transcription factor activation, and in the case of macrophages, cytokine production[185]. Extracellular signaling molecules such as growth factors lead to activation of Akt through their effect on PI3K, which directly phosphorylates Akt[186]. Fc receptor cross-linking is also known to activate PI3K[187], so the increased activation of Akt in the LPS+IC stimulated cells was not entirely unexpected. The effect of Akt inhibition on R-Mϕ-IC biomarkers was striking, as it was clearly involved in the upregulation of almost all LI-induced genes. However, because Akt activation lies

upstream of so many pathways, it became important to determine which Akt substrate was responsible for the gene changes observed in our phenotype.

4.4.3 GSK3

GSK3 is a signaling kinase that is constitutively active in the cell, only becoming inactivated through phosphorylation of its substrate binding site[101]. It was first discovered by studying its effect on glycogen synthase, but was later found to phosphorylate dozens more molecules within the cell[103]. It became heavily studied in the area of neuroscience after it was discovered that lithium worked through inhibition of this kinase. Even more recently, GSK3 was found to have anti-inflammatory activity; in fact, IV injection of the small molecule GSK3 inhibitor SB216763 has been shown to increase survival of endotoxemia in mice[188]. When we observed that IC may increase phosphorylation of GSK3β, we hypothesized that GSK3 was involved in the ability for IC to regulate transcription. Through the use of the small molecule GSK3 inhibitor SB415286, we found that GSK3 inhibition copied the LPS+IC phenotype without also increasing production of inflammatory cytokines. The ability for IC to drastically reduce the levels of GSK3β in the nucleus has a number of implications in transcriptional regulation. GSK3β is itself a transcription factor known to interact with AP-1, CREB, and NFκB, among others[103], and is also involved in the regulation of chromatin remodeling[189]. GSK3β has been found to have an inhibitory effect on AP-1 and CREB, both of which are involved in IL-10 transcriptional control [105,190]. Although GSK3 is now known to be an important regulator of IL-10 in macrophages, this is the first study to show that GSK3β inhibition significantly amplifies LPS-induced transcription of matrix-metalloproteinases in macrophages. Besides its implications in

inflammation, these findings may also explain previous observations that GSK3β inhibition is involved in wound healing and angiogenesis[191,192].

Although further attempts were made to validate the GSK3β phosphorylation seen in the results of the antibody array, only a slight increase in phosphorylation was observed. However, nuclear levels of GSK3β were significantly suppressed by IC co-stimulation. Akt has been shown to inhibit entry of GSK3β into the nucleus[144]. The mechanism for regulation of nuclear translocation has not been thoroughly examined, but one study found that GSK3β contains a bipartite nuclear localization sequence that is normally blocked by the sequestration of GSK3β within protein complexes[193]. Interestingly, this study found that inhibitory phosphorylation at serine 9 was not sufficient to prevent nuclear translocation. Further studies using overexpression of GSK3β are needed to confirm the requirement for GSK3β inhibition for gene regulation following Fc receptor ligation, and to determine the mechanism by which this nuclear translocation is inhibited.

4.4.4 Proposed pathway

Previous studies in mouse established the ability for immune complex to modulate the actions of LPS, generating an anti-inflammatory phenotype that relies on dual signals. In mouse, it was the activation of ERK, as opposed to other MAP kinases, that was able to generate this response. Here we propose that pathways that are minimally or inconsistently activated by TLR signaling (Akt and ERK) are amplified in the presence of IC, thus selectively amplifying the production of TLR-induced immunoregulatory genes. Until thorough studies are done delineating the pathway, the cause-and-effect relationships between these modulators can only be proposed. Given our previous studies in mouse and prevailing evidence in the literature, it is proposed that Akt activation is responsible for GSK3 inhibition in R-Mφ-IC, and that this inhibition allows the independently activated ERK to upregulate immunoregulatory transcripts, possibly through the amplified activation of AP-1 (Illustration 4).
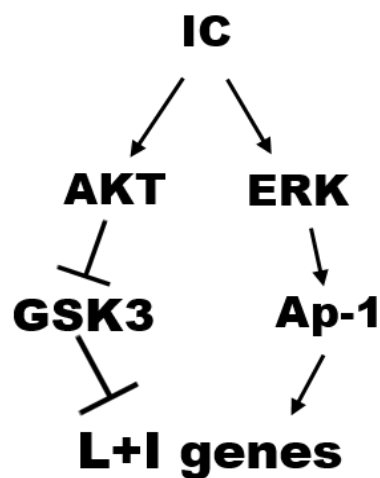
Illustration 4. Proposed pathway for R-Mφ-IC activation.

4.5 *In vivo relevance*

The effect described in this project can be induced by a wide range of biologically relevant substrates. In the past, it was found that IC can modulate the actions of other activators of classical inflammatory pathways in macrophages such as

LTA (a TLR2 agonist) and CD40[194]. Furthermore, the second signal required to modulate inflammation needn't be immune complexes specifically, but rather anything that induces FcγR cross-linking, or theoretically, anything that activates Akt1. Thus, any activator of the Akt1 pathway, such as growth factors, may also act in a similar manner. Delineating the pathways relevant in this phenotype has expanded the potential physiological relevance of our findings to any context that involves the combination of inflammatory stimulus with modulators of the Akt1/GSK3 pathway.

The effects of low-level inflammation are considered a major driver of chronic disease in the developed world. Furthermore, acute inflammation in the context of bacterial sepsis is one of the highest causes of mortality in the United States. For this reason, research into the modulators of inflammation is important to uncovering novel drug targets for anti-inflammatory therapies. In this study, we chose to determine the functional relevance of GSK3 inhibition by using a mouse model of lethal endotoxemia. This model involves injection of mice with high levels of LPS, which induces a lethal cytokine storm. Our results indicate that GSK3β inhibition has an anti-inflammatory effect *in vivo*. These data are supported by multiple studies showing a protective effect of direct treatment with GSK3 inhibitors on LPS endotoxemia[195,196]. Our results go further to suggest that it is the effect of GSK3 inhibition in macrophages specifically that is responsible for this protective effect.

4.6 Conclusion

In sum, our studies reveal the generation of an anti-inflammatory and pro-healing phenotype in activated human macrophages when stimulated with Fc-receptor cross-linking immune complexes. IL-10, MMP-10, and LIF were identified as

biomarkers suitable for identification of this phenotype using RNAscope technology, whereas DC-STAMP could be used as a marker in flow cytometry applications. The anti-inflammatory phenotype observed at the transcript level was also found to translate to the protein level, where IL-10, activin A, and MMP-1 serve as high-abundance ELISA markers for R-Mϕ-IC. The gene changes observed appeared to be induced at least partially by activation of Akt and ERK. GSK3, which is downstream of Akt signaling, is inhibited by blocking of nuclear translocation by treatment with immune complexes. Since inhibition of GSK3 phenocopies the effects of immune complex on upregulated markers, it is suggested that GSK3 plays a role in the generation of this phenotype. Macrophages treated with LPS and a GSK3 inhibitor protected mice from lethal endotoxemia. Given the significance of macrophage activation in both chronic and infectious diseases, we hope that these studies will facilitate clinical and pathological research in humans to determine the role of macrophage phenotypes in chronic and infectious diseases.

Bibliography

1. Alberts B, Johnson A, Lewis J, Raff M, Roberts K, Walter P. *Molecular Biology of the Cell.* 4th ed. New York: Garland Science; 2002. https://www.ncbi.nlm.nih.gov/books/NBK26846/. Accessed May 19, 2017.

2. Hirano M. Evolution of vertebrate adaptive immunity: Immune cells and tissues, and AID/APOBEC cytidine deaminases. *BioEssays*. 2015;37(8):877-887. doi:10.1002/bies.201400178.

3. Kirschning CJ, Bauer S. Toll-like receptors: cellular signal transducers for exogenous molecular patterns causing immune responses. *Int J Med Microbiol*. 2001;291(4):251-260. doi:10.1078/1438-4221-00128.

4. Janeway CA. Approaching the asymptote? Evolution and revolution in immunology. *Cold Spring Harb Symp Quant Biol*. 1989;54(1):1-13. http://www.ncbi.nlm.nih.gov/pubmed/2700931. Accessed June 22, 2017.

5. Janeway CA, Medzhitov R, Preston-Hurlburt P. A human homologue of the Drosophila Toll protein signals activation of adaptive immunity. *Nature*. 1997;388(6640):394-397. doi:10.1038/41131.

6. Elie Metchnikoff | Russian-born biologist | Britannica.com. Encyclopedia Britannica. https://www.britannica.com/biography/Elie-Metchnikoff. Published 2017. Accessed May 19, 2017.

7. Lavin Y, Winter D, Blecher-Gonen R, et al. Tissue-resident macrophage enhancer landscapes are shaped by the local microenvironment. *Cell*. 2014;159(6):1312-1326. doi:10.1016/j.cell.2014.11.018.

8. Noguchi H. ETIOLOGY OF OROYA FEVER : VI. PATHOLOGICAL CHANGES OBSERVED IN ANIMALS EXPERIMENTALLY INFECTED WITH BARTONELLA BACILLIFORMIS. THE DISTRIBUTION OF THE PARASITES IN THE TISSUES. *J Exp Med*. 1927;45(3):437-454. http://www.ncbi.nlm.nih.gov/pubmed/19869264. Accessed May 6, 2017.

9. Nakahara W. THE FUNCTION OF MACROPHAGES IN LOCAL RESISTANCE TO BACTERIAL INFECTIONS. *J Exp Med*. 1925;42(2):201-213. http://www.ncbi.nlm.nih.gov/pubmed/19869046. Accessed May 6, 2017.

10. Gordon S, Plüddemann A, Martinez Estrada F. Macrophage heterogeneity in tissues: phenotypic diversity and functions. *Immunol Rev*. 2014;262(1):36-55. doi:10.1111/imr.12223.

11. Forkner CE. THE ORIGIN OF MONOCYTES IN CERTAIN LYMPH NODES AND THEIR GENETIC RELATION TO OTHER CONNECTIVE TISSUE CELLS. *J Exp Med*. 1930;52(3):385-404. http://www.ncbi.nlm.nih.gov/pubmed/19869772. Accessed May 6, 2017.

12. Weiskopf K, Schnorr PJ, Pang WW, et al. Myeloid Cell Origins, Differentiation, and Clinical Implications. *Microbiol Spectr*. 2016;4(5). doi:10.1128/microbiolspec.MCHD-0031-2016.

13. Geissmann F, Jung S, Littman DR. Blood monocytes consist of two principal subsets with distinct migratory properties. *Immunity*. 2003;19(1):71-82. http://www.ncbi.nlm.nih.gov/pubmed/12871640. Accessed May 20, 2017.

14. Wang H, Melton DW, Porter L, Sarwar ZU, McManus LM, Shireman PK. Altered macrophage phenotype transition impairs skeletal muscle regeneration. *Am J Pathol*. 2014;184(4):1167-1184. doi:10.1016/j.ajpath.2013.12.020.

15. Wolf Y, Boura-Halfon S, Cortese N, et al. Brown-adipose-tissue macrophages control tissue innervation and homeostatic energy expenditure. *Nat Immunol*. 2017;18(6):665-674. doi:10.1038/ni.3746.

16. Gordon S, Martinez-Pomares L. Physiological roles of macrophages. *Pflügers Arch - Eur J Physiol*. 2017;469(3-4):365-374. doi:10.1007/s00424-017-1945-7.

17. Gosselin D, Link VM, Romanoski CE, et al. Environment drives selection and function of enhancers controlling tissue-specific macrophage identities. *Cell*. 2014;159(6):1327-1340. doi:10.1016/j.cell.2014.11.023.

18. Li J, Scherl A, Medina F, et al. Impaired Phagocytosis in Caveolin-1 Deficient Macrophages. *Cell Cycle*. 2005;4(11):1599-1607. doi:10.4161/cc.4.11.2117.

19. Wade BH, Mandell GL. Polymorphonuclear leukocytes: dedicated professional phagocytes. *Am J Med*. 1983;74(4):686-693. http://www.ncbi.nlm.nih.gov/pubmed/6837594. Accessed June 23, 2017.

20. Větvicka V, Fornůsek L, Holub M, Zídková J, Kopecek J. Macrophages of athymic nude mice: Fc receptors, C receptors, phagocytic and pinocytic activities. *Eur J Cell Biol*. 1984;35(1):35-40. http://www.ncbi.nlm.nih.gov/pubmed/6489358. Accessed June 23, 2017.

21. Krause P, Morris V, Greenbaum JA, et al. IL-10-producing intestinal macrophages prevent excessive antibacterial innate immunity by limiting IL-23 synthesis. *Nat Commun*. 2015;6:7055. doi:10.1038/ncomms8055.

22. Cassatella MA, Meda L, Bonora S, Ceska M, Constantin G. Interleukin 10 (IL-

10) inhibits the release of proinflammatory cytokines from human polymorphonuclear leukocytes. Evidence for an autocrine role of tumor necrosis factor and IL-1 beta in mediating the production of IL-8 triggered by lipopolysaccharide. *J Exp Med*. 1993;178(6):2207-2211. http://www.ncbi.nlm.nih.gov/pubmed/8245792. Accessed June 2, 2017.

23. Berg DJ, Davidson N, Kühn R, et al. Enterocolitis and colon cancer in interleukin-10-deficient mice are associated with aberrant cytokine production and CD4(+) TH1-like responses. *J Clin Invest*. 1996;98(4):1010-1020. doi:10.1172/JCI118861.

24. Németh K, Leelahavanichkul A, Yuen PST, et al. Bone marrow stromal cells attenuate sepsis via prostaglandin E(2)-dependent reprogramming of host macrophages to increase their interleukin-10 production. *Nat Med*. 2009;15(1):42-49. doi:10.1038/nm.1905.

25. Amante FH, Stanley AC, Randall LM, et al. A role for natural regulatory T cells in the pathogenesis of experimental cerebral malaria. *Am J Pathol*. 2007;171(2):548-559. doi:10.2353/ajpath.2007.061033.

26. Kühn R, Löhler J, Rennick D, Rajewsky K, Müller W. Interleukin-10-deficient mice develop chronic enterocolitis. *Cell*. 1993;75(2):263-274. http://www.ncbi.nlm.nih.gov/pubmed/8402911. Accessed June 23, 2017.

27. Arai Y, Takanashi H, Kitagawa H, Okayasu I. INVOLVEMENT OF INTERLEUKIN-1 IN THE DEVELOPMENT OF ULCERATIVE COLITIS INDUCED BY DEXTRAN SULFATE SODIUM IN MICE. *Cytokine*. 1998;10(11):890-896. doi:10.1006/cyto.1998.0355.

28. Bogdan C, Paik J, Vodovotz Y, Nathan C. Contrasting mechanisms for suppression of macrophage cytokine release by transforming growth factor-beta and interleukin-10. *J Biol Chem*. 1992;267(32):23301-23308. http://www.ncbi.nlm.nih.gov/pubmed/1429677. Accessed June 23, 2017.

29. Mosser DM, Zhang X. Interleukin-10: new perspectives on an old cytokine. *Immunol Rev*. 2008;226:205-218. doi:10.1111/j.1600-065X.2008.00706.x.

30. GROSS J, LAPIERE CM. Collagenolytic activity in amphibian tissues: a tissue culture assay. *Proc Natl Acad Sci U S A*. 1962;48(6):1014-1022. http://www.ncbi.nlm.nih.gov/pubmed/13902219. Accessed May 17, 2017.

31. Löffek S, Schilling O, Franzke C-W. Biological role of matrix metalloproteinases: a critical balance. *Eur Respir J*. 2011;38(1):191–208. doi:10.1183/09031936.00146510.

32. Kleifeld O, Doucet A, auf dem Keller U, et al. Isotopic labeling of terminal

amines in complex samples identifies protein N-termini and protease cleavage products. *Nat Biotechnol*. 2010;28(3):281-288. doi:10.1038/nbt.1611.

33. Dean RA, Overall CM. Proteomics Discovery of Metalloproteinase Substrates in the Cellular Context by iTRAQTM Labeling Reveals a Diverse MMP-2 Substrate Degradome. *Mol Cell Proteomics*. 2007;6(4):611-623. doi:10.1074/mcp.M600341-MCP200.

34. McQuibban GA, Gong J-H, Wong JP, Wallace JL, Clark-Lewis I, Overall CM. Matrix metalloproteinase processing of monocyte chemoattractant proteins generates CC chemokine receptor antagonists with anti-inflammatory properties in vivo. *Blood*. 2002;100(4):1160-1167. http://www.ncbi.nlm.nih.gov/pubmed/12149192. Accessed June 2, 2017.

35. McQuibban GA, Gong JH, Tam EM, McCulloch CA, Clark-Lewis I, Overall CM. Inflammation dampened by gelatinase A cleavage of monocyte chemoattractant protein-3. *Science*. 2000;289(5482):1202-1206. http://www.ncbi.nlm.nih.gov/pubmed/10947989. Accessed June 2, 2017.

36. Sindrilaru A, Scharffetter-Kochanek K. Disclosure of the Culprits: Macrophages-Versatile Regulators of Wound Healing. *Adv wound care*. 2013;2(7):357-368. doi:10.1089/wound.2012.0407.

37. Caley MP, Martins VLC, O'Toole EA. Metalloproteinases and Wound Healing. *Adv wound care*. 2015;4(4):225-234. doi:10.1089/wound.2014.0581.

38. Gearing AJH, Beckett P, Christodoulou M, et al. Processing of tumour necrosis factor-α precursor by metalloproteinases. *Nature*. 1994;370(6490):555-557. doi:10.1038/370555a0.

39. Mosser DM, Edwards JP. Exploring the full spectrum of macrophage activation. *Nat Rev Immunol*. 2008;8(12):958-969. doi:10.1038/nri2448.

40. Fitzgerald KA, Palsson-McDermott EM, Bowie AG, et al. Mal (MyD88-adapter-like) is required for Toll-like receptor-4 signal transduction. *Nature*. 2001;413(6851):78-83. doi:10.1038/35092578.

41. Cordle SR, Donald R, Read MA, Hawiger J. Lipopolysaccharide induces phosphorylation of MAD3 and activation of c-Rel and related NF-kappa B proteins in human monocytic THP-1 cells. *J Biol Chem*. 1993;268(16):11803-11810. http://www.ncbi.nlm.nih.gov/pubmed/8505309. Accessed June 6, 2017.

42. Zhang FX, Kirschning CJ, Mancinelli R, et al. Bacterial lipopolysaccharide activates nuclear factor-kappaB through interleukin-1 signaling mediators in cultured human dermal endothelial cells and mononuclear phagocytes. *J Biol Chem*. 1999;274(12):7611-7614.

http://www.ncbi.nlm.nih.gov/pubmed/10075645. Accessed June 6, 2017.

43. Gifford GE, Lohmann-Matthes ML. Gamma interferon priming of mouse and human macrophages for induction of tumor necrosis factor production by bacterial lipopolysaccharide. *J Natl Cancer Inst*. 1987;78(1):121-124. http://www.ncbi.nlm.nih.gov/pubmed/3099049. Accessed June 1, 2017.

44. Shi J, Zhao Y, Wang Y, et al. Inflammatory caspases are innate immune receptors for intracellular LPS. *Nature*. 2014;514(7521):187-192. doi:10.1038/nature13683.

45. Ohmori Y, Schreiber RD, Hamilton TA. Synergy between interferon-gamma and tumor necrosis factor-alpha in transcriptional activation is mediated by cooperation between signal transducer and activator of transcription 1 and nuclear factor kappaB. *J Biol Chem*. 1997;272(23):14899-14907. http://www.ncbi.nlm.nih.gov/pubmed/9169460. Accessed June 6, 2017.

46. Grieder FB, Vogel SN. Role of interferon and interferon regulatory factors in early protection against Venezuelan equine encephalitis virus infection. *Virology*. 1999;257(1):106-118. doi:10.1006/viro.1999.9662.

47. Su X, Yu Y, Zhong Y, et al. Interferon-γ regulates cellular metabolism and mRNA translation to potentiate macrophage activation. *Nat Immunol*. 2015;16(8):838-849. doi:10.1038/ni.3205.

48. Stein M, Keshav S, Harris N, Gordon S. Interleukin 4 potently enhances murine macrophage mannose receptor activity: a marker of alternative immunologic macrophage activation. *J Exp Med*. 1992;176(1):287-292. http://www.ncbi.nlm.nih.gov/pubmed/1613462. Accessed June 1, 2017.

49. Corraliza IM, Soler G, Eichmann K, Modolell M. Arginase Induction by Suppressors of Nitric Oxide Synthesis (IL-4, IL-10 and PGE2) in Murine Bone-Marrow-Derived Macrophages. *Biochem Biophys Res Commun*. 1995;206(2):667-673. doi:10.1006/bbrc.1995.1094.

50. Anthony RM, Urban JF, Alem F, et al. Memory TH2 cells induce alternatively activated macrophages to mediate protection against nematode parasites. *Nat Med*. 2006;12(8):955-960. doi:10.1038/nm1451.

51. Lee Y-H, Kim S-N, Kwon H-J, Maddipati KR, Granneman JG. Adipogenic role of alternatively activated macrophages in β-adrenergic remodeling of white adipose tissue. *Am J Physiol - Regul Integr Comp Physiol*. 2016;310(1):R55-R65. doi:10.1152/ajpregu.00355.2015.

52. Troidl C, Möllmann H, Nef H, et al. Classically and alternatively activated macrophages contribute to tissue remodelling after myocardial infarction. *J

Cell Mol Med. 2009;13(9b):3485-3496. doi:10.1111/j.1582-4934.2009.00707.x.

53.   Fleming BD, Chandrasekaran P, Dillon LAL, et al. The generation of macrophages with anti-inflammatory activity in the absence of STAT6 signaling. *J Leukoc Biol*. 2015;98(3):395-407. doi:10.1189/jlb.2A1114-560R.

54.   Sutterwala FS, Noel GJ, Clynes R, Mosser DM. Selective suppression of interleukin-12 induction after macrophage receptor ligation. *J Exp Med*. 1997;185(11):1977-1985. http://www.ncbi.nlm.nih.gov/pubmed/9166427. Accessed May 19, 2017.

55.   Gallo P, Gonçalves R, Mosser DM. The influence of IgG density and macrophage Fc (gamma) receptor cross-linking on phagocytosis and IL-10 production. *Immunol Lett*. 2010;133(2):70-77. doi:10.1016/j.imlet.2010.07.004.

56.   Edwards JP, Zhang X, Frauwirth KA, Mosser DM. Biochemical and functional characterization of three activated macrophage populations. *J Leukoc Biol*. 2006;80(6):1298-1307. doi:10.1189/jlb.0406249.

57.   Edwards JP, Zhang X, Mosser DM. The expression of heparin-binding epidermal growth factor-like growth factor by regulatory macrophages. *J Immunol*. 2009;182(4):1929-1939. doi:10.4049/jimmunol.0802703.

58.   Lucas M, Zhang X, Prasanna V, Mosser DM. ERK activation following macrophage FcgammaR ligation leads to chromatin modifications at the IL-10 locus. *J Immunol*. 2005;175(1):469-477. http://www.ncbi.nlm.nih.gov/pubmed/15972681. Accessed February 26, 2017.

59.   Vogel C, Marcotte EM. Insights into the regulation of protein abundance from proteomic and transcriptomic analyses. *Nat Rev Genet*. 2012;13(4):227-232. doi:10.1038/nrg3185.

60.   Xue J, Schmidt S V, Sander J, et al. Transcriptome-based network analysis reveals a spectrum model of human macrophage activation. *Immunity*. 2014;40(2):274-288. doi:10.1016/j.immuni.2014.01.006.

61.   Kawai T, Akira S. The role of pattern-recognition receptors in innate immunity: update on Toll-like receptors. *Nat Immunol*. 2010;11(5):373-384. doi:10.1038/ni.1863.

62.   Anderson K V, Jürgens G, Nüsslein-Volhard C. Establishment of dorsal-ventral polarity in the Drosophila embryo: genetic studies on the role of the Toll gene product. *Cell*. 1985;42(3):779-789. http://www.ncbi.nlm.nih.gov/pubmed/3931918. Accessed June 21, 2017.

63.   Lemaitre B, Nicolas E, Michaut L, Reichhart JM, Hoffmann JA. The dorsoventral regulatory gene cassette spätzle/Toll/cactus controls the potent antifungal response in Drosophila adults. *Cell*. 1996;86(6):973-983. http://www.ncbi.nlm.nih.gov/pubmed/8808632. Accessed June 1, 2017.

64.   Christmas P. Toll-Like Receptors: Sensors that Detect Infection. *Nat Educ 3(9)85*. 2010;3(9):85.

65.   Alexopoulou L, Holt AC, Medzhitov R, Flavell RA. Recognition of double-stranded RNA and activation of NF-kappaB by Toll-like receptor 3. *Nature*. 2001;413(6857):732-738. doi:10.1038/35099560.

66.   Diebold SS, Kaisho T, Hemmi H, Akira S, Reis e Sousa C. Innate Antiviral Responses by Means of TLR7-Mediated Recognition of Single-Stranded RNA. *doi.org*. 2004;303(5663):1529-1531. doi:10.1126/science.1093616.

67.   Akira S, Hemmi H, Takeuchi O, et al. A Toll-like receptor recognizes bacterial DNA. *Nature*. 2000;408(6813):740-745. doi:10.1038/35047123.

68.   Oganesyan G, Saha SK, Guo B, et al. Critical role of TRAF3 in the Toll-like receptor-dependent and -independent antiviral response. *Nature*. 2006;439(7073):208-211. doi:10.1038/nature04374.

69.   O'Neill LAJ, Golenbock D, Bowie AG. The history of Toll-like receptors — redefining innate immunity. *Nat Rev Immunol*. 2013;13(6):453-460. doi:10.1038/nri3446.

70.   Fitzgerald KA, Rowe DC, Barnes BJ, et al. LPS-TLR4 Signaling to IRF-3/7 and NF-κB Involves the Toll Adapters TRAM and TRIF. *J Exp Med*. 2003;198(7). http://jem.rupress.org/content/198/7/1043. Accessed July 26, 2017.

71.   Takahashi K, Kawai T, Kumar H, Sato S, Yonehara S, Akira S. Cutting Edge: Roles of Caspase-8 and Caspase-10 in Innate Immune Responses to Double-Stranded RNA. *J Immunol*. 2006;176(8). http://www.jimmunol.org/content/176/8/4520. Accessed July 26, 2017.

72.   Everts B, Amiel E, Huang SC-C, et al. TLR-driven early glycolytic reprogramming via the kinases TBK1-IKKε supports the anabolic demands of dendritic cell activation. *Nat Immunol*. 2014;15(4):323-332. doi:10.1038/ni.2833.

73.   Cohen HB, Briggs KT, Marino JP, Ravid K, Robson SC, Mosser DM. TLR stimulation initiates a CD39-based autoregulatory mechanism that limits macrophage inflammatory responses. *Blood*. 2013;122(11):1935-1945.

102

doi:10.1182/blood-2013-04-496216.

74. Hamidzadeh K, Christensen SM, Dalby E, Chandrasekaran P, Mosser DM. Macrophages and the Recovery from Acute and Chronic Inflammation. *Annu Rev Physiol*. 2017;79(1):567-592. doi:10.1146/annurev-physiol-022516-034348.

75. Wang Q, Dziarski R, Kirschning CJ, Muzio M, Gupta D. Micrococci and Peptidoglycan Activate TLR2 MyD88 IRAK TRAF NIK IKK NF- B Signal Transduction Pathway That Induces Transcription of Interleukin-8. *Infect Immun*. 2001;69(4):2270-2276. doi:10.1128/IAI.69.4.2270-2276.2001.

76. Mercurio F, Manning AM. NF-kB as a primary regulator of the stress response. *Oncogene*. 1999;18:6163-6171.

77. Maguire O, Collins C, O'Loughlin K, Miecznikowski J, Minderman H. Quantifying nuclear p65 as a parameter for NF-κB activation: Correlation between ImageStream cytometry, microscopy, and Western blot. *Cytometry A*. 2011;79(6):461-469. doi:10.1002/cyto.a.21068.

78. Baeuerle PA, Baltimore D. A 65-kappaD subunit of active NF-kappaB is required for inhibition of NF-kappaB by I kappaB. *Genes Dev*. 1989;3(11):1689-1698. http://www.ncbi.nlm.nih.gov/pubmed/2691328. Accessed June 6, 2017.

79. Roff M, Thompson J, Rodriguez MS, et al. Role of IkappaBalpha ubiquitination in signal-induced activation of NFkappaB in vivo. *J Biol Chem*. 1996;271(13):7844-7850. http://www.ncbi.nlm.nih.gov/pubmed/8631829. Accessed June 2, 2017.

80. Cao S, Zhang X, Edwards JP, Mosser DM. NF- B1 (p50) Homodimers Differentially Regulate Pro- and Anti-inflammatory Cytokines in Macrophages. *J Biol Chem*. 2006;281(36):26041-26050. doi:10.1074/jbc.M602222200.

81. Lawrence T. The nuclear factor NF-kappaB pathway in inflammation. *Cold Spring Harb Perspect Biol*. 2009;1(6):a001651. doi:10.1101/cshperspect.a001651.

82. Beemiller P, Zhang Y, Mohan S, et al. A Cdc42 activation cycle coordinated by PI 3-kinase during Fc receptor-mediated phagocytosis. *Mol Biol Cell*. 2010;21(3):470-480. doi:10.1091/mbc.E08-05-0494.

83. Androulidaki A, Iliopoulos D, Arranz A, et al. The kinase Akt1 controls macrophage response to lipopolysaccharide by regulating microRNAs. *Immunity*. 2009;31(2):220-231. doi:10.1016/j.immuni.2009.06.024.

84.   Arranz A, Doxaki C, Vergadi E, et al. Akt1 and Akt2 protein kinases differentially contribute to macrophage polarization. *Proc Natl Acad Sci U S A*. 2012;109(24):9517-9522. doi:10.1073/pnas.1119038109.

85.   Hoshino R, Chatani Y, Yamori T, et al. Constitutive activation of the 41-/43-kDa mitogen-activated protein kinase signaling pathway in human tumors. *Oncogene*. 1999;18(3):813-822. doi:10.1038/sj.onc.1202367.

86.   Luo Y, Pollard JW, Casadevall A. Fcγ Receptor Cross-linking Stimulates Cell Proliferation of Macrophages via the ERK Pathway. 2009. doi:10.1074/jbc.M109.037168.

87.   Kolanus W, Romeo C, Seed B. Lineage-independent activation of immune system effector function by myeloid Fc receptors. *EMBO J*. 1992;11(13):4861-4868. http://www.ncbi.nlm.nih.gov/pubmed/1464313. Accessed May 29, 2017.

88.   Mócsai A, Ruland J, Tybulewicz VLJ. The SYK tyrosine kinase: a crucial player in diverse biological functions. *Nat Rev Immunol*. 2010;10(6):387-402. doi:10.1038/nri2765.

89.   Darby C, Geahlen RL, Schreiber AD. Stimulation of macrophage Fc gamma RIIIA activates the receptor-associated protein tyrosine kinase Syk and induces phosphorylation of multiple proteins including p95Vav and p62/GAP-associated protein. *J Immunol*. 1994;152(11):5429-5437. http://www.ncbi.nlm.nih.gov/pubmed/8189062. Accessed August 28, 2016.

90.   Indik ZK, Park JG, Pan XQ, Schreiber AD. Induction of phagocytosis by a protein tyrosine kinase. *Blood*. 1995;85(5):1175-1180. http://www.ncbi.nlm.nih.gov/pubmed/7858249. Accessed June 9, 2017.

91.   Rajnavölgyi E, Reth M, Uher F, Miklós K, Gergely J, Rajewsky K. Fc-dependent effector functions of idiotype-anti-idiotype immune complexes. *Mol Immunol*. 1984;21(2):127-136. http://www.ncbi.nlm.nih.gov/pubmed/6608663. Accessed June 9, 2017.

92.   Lach-Trifilieff E, Menear K, Schweighoffer E, Tybulewicz VL, Walker C. Syk-deficient eosinophils show normal interleukin-5-mediated differentiation, maturation, and survival but no longer respond to FcgammaR activation. *Blood*. 2000;96(7):2506-2510. http://www.ncbi.nlm.nih.gov/pubmed/11001904. Accessed June 9, 2017.

93.   Ericson SG, Zhao Y, Gao H, et al. Interleukin-6 Production by Human Neutrophils After Fc-Receptor Cross-Linking or Exposure to Granulocyte Colony-Stimulating Factor. *Blood*. 1998;91(6). http://www.bloodjournal.org/content/91/6/2099?sso-checked=true. Accessed

June 11, 2017.

94. Marois L, Vaillancourt M, Paré G, et al. CIN85 Modulates the Down-regulation of FcγRIIa Expression and Function by c-Cbl in a PKC-dependent Manner in Human Neutrophils. *J Biol Chem*. 2011;286(17):15073-15084. doi:10.1074/jbc.M110.213660.

95. Young JD-E, Cohn ZA. Role of granule proteins in lymphocyte-mediated killing. *J Cell Biochem*. 1986;32(2):151-167. doi:10.1002/jcb.240320207.

96. Takai T. Roles of Fc receptors in autoimmunity. *Nat Rev Immunol*. 2002;2(8):580-592. doi:10.1038/nri856.

97. Lin J, Kurilova S, Scott BL, et al. TIRF imaging of Fc gamma receptor microclusters dynamics and signaling on macrophages during frustrated phagocytosis. *BMC Immunol*. 2016;17(1):5. doi:10.1186/s12865-016-0143-2.

98. Nimmerjahn F, Ravetch J V. Fcγ receptors as regulators of immune responses. *Nat Rev Immunol*. 2008;8(1):34-47. doi:10.1038/nri2206.

99. Crowley MT, Costello PS, Fitzer-Attas CJ, et al. A critical role for Syk in signal transduction and phagocytosis mediated by Fcgamma receptors on macrophages. *J Exp Med*. 1997;186(7):1027-1039. http://www.ncbi.nlm.nih.gov/pubmed/9314552. Accessed June 9, 2017.

100. Hamerman JA, Tchao NK, Lowell CA, Lanier LL. Enhanced Toll-like receptor responses in the absence of signaling adaptor DAP12. *Nat Immunol*. 2005;6(6):579-586. doi:10.1038/ni1204.

101. Frame S, Cohen P, Biondi RM, et al. A common phosphate binding site explains the unique substrate specificity of GSK3 and its inactivation by phosphorylation. *Mol Cell*. 2001;7(6):1321-1327. doi:10.1016/S1097-2765(01)00253-2.

102. EMBI N, RYLATT DB, COHEN P. Glycogen Synthase Kinase-3 from Rabbit Skeletal Muscle. *Eur J Biochem*. 2005;107(2):519-527. doi:10.1111/j.1432-1033.1980.tb06059.x.

103. Sutherland C, Calum. What Are the bona fide GSK3 Substrates? *Int J Alzheimers Dis*. 2011;2011:505607. doi:10.4061/2011/505607.

104. Beurel E, Michalek SM, Jope RS. Innate and adaptive immune responses regulated by glycogen synthase kinase-3 (GSK3). *Trends Immunol*. 2010;31(1):24-31. doi:10.1016/j.it.2009.09.007.

105. Hu X, Paik PK, Chen J, et al. IFN-gamma suppresses IL-10 production and

synergizes with TLR2 by regulating GSK3 and CREB/AP-1 proteins. *Immunity*. 2006;24(5):563-574. doi:10.1016/j.immuni.2006.02.014.

106.   Nandan D, Camargo de Oliveira C, Moeenrezakhanlou A, et al. Myeloid Cell IL-10 Production in Response to Leishmania Involves Inactivation of Glycogen Synthase Kinase-3β Downstream of Phosphatidylinositol-3 Kinase. *J Immunol*. 2011;188(1).

107.   Lee H-C, Lin Y-Z, Lai Y-T, et al. Glycogen synthase kinase 3 beta in somites plays a role during the angiogenesis of zebrafish embryos. *FEBS J*. 2014;281(19):4367-4383. doi:10.1111/febs.12942.

108.   Paramesha M, Ramesh CK, Krishna V, Kumar Swamy HM, Aditya Rao SJ, Hoskerri J. Effect of dehydroabietylamine in angiogenesis and GSK3-β inhibition during wound healing activity in rats. *Med Chem Res*. 2015;24(1):295-303. doi:10.1007/s00044-014-1110-1.

109.   Vincent J-L, Marshall JC, Ñamendys-Silva SA, et al. Assessment of the worldwide burden of critical illness: the Intensive Care Over Nations (ICON) audit. *Lancet Respir Med*. 2014;2(5):380-386. doi:10.1016/S2213-2600(14)70061-X.

110.   Torio CM, Andrews RM. National Inpatient Hospital Costs: The Most Expensive Conditions by Payer, 2011: Statistical Brief #160. Healthcare Cost and Utilization Project (HCUP) Statistical Briefs. https://www.hcup-us.ahrq.gov/reports/statbriefs/sb160.jsp. Published 2013. Accessed May 1, 2017.

111.   Kang C-I, Song J-H, Chung DR, et al. Risk factors and pathogenic significance of severe sepsis and septic shock in 2286 patients with gram-negative bacteremia. *J Infect*. 2011;62(1):26-33. doi:10.1016/j.jinf.2010.10.010.

112.   Schulte W, Bernhagen J, Bucala R, Bucala R. Cytokines in sepsis: potent immunoregulators and potential therapeutic targets--an updated view. *Mediators Inflamm*. 2013;2013:165974. doi:10.1155/2013/165974.

113.   Kalil AC, Opal SM. Sepsis in the Severely Immunocompromised Patient. *Curr Infect Dis Rep*. 2015;17(6):32. doi:10.1007/s11908-015-0487-4.

114.   Lv S, Han M, Yi R, Kwon S, Dai C, Wang R. Anti-TNF-α therapy for patients with sepsis: a systematic meta-analysis. *Int J Clin Pract*. 2014;68(4):520-528. doi:10.1111/ijcp.12382.

115.   Martin GS. Sepsis, severe sepsis and septic shock: changes in incidence, pathogens and outcomes. *Expert Rev Anti Infect Ther*. 2012;10(6):701-706. doi:10.1586/eri.12.50.

116. Bozza FA, Salluh JI, Japiassu AM, et al. Cytokine profiles as markers of disease severity in sepsis: a multiplex analysis. *Crit Care*. 2007;11(2):R49. doi:10.1186/cc5783.

117. Mehta A, Brewington R, Chatterji M, et al. Infection-induced modulation of m1 and m2 phenotypes in circulating monocytes: role in immune monitoring and early prognosis of sepsis. *Shock*. 2004;22(5):423-430. http://www.ncbi.nlm.nih.gov/pubmed/15489634. Accessed July 14, 2017.

118. Remick DG. Pathophysiology of sepsis. *Am J Pathol*. 2007;170(5):1435-1444. doi:10.2353/ajpath.2007.060872.

119. Angus DC, Linde-Zwirble WT, Lidicker J, Clermont G, Carcillo J, Pinsky MR. Epidemiology of severe sepsis in the United States: analysis of incidence, outcome, and associated costs of care. *Crit Care Med*. 2001;29(7):1303-1310. http://www.ncbi.nlm.nih.gov/pubmed/11445675. Accessed June 8, 2017.

120. Bolger AM, Lohse M, Usadel B. Trimmomatic: a flexible trimmer for Illumina sequence data. *Bioinformatics*. 2014;30(15):2114-2120. doi:10.1093/bioinformatics/btu170.

121. Kent WJ, Sugnet CW, Furey TS, et al. The human genome browser at UCSC. *Genome Res*. 2002;12(6):996-1006. doi:10.1101/gr.229102. Article published online before print in May 2002.

122. Trapnell C, Pachter L, Salzberg SL. TopHat: discovering splice junctions with RNA-Seq. *Bioinformatics*. 2009;25(9):1105-1111. doi:10.1093/bioinformatics/btp120.

123. Anders S, McCarthy DJ, Chen Y, et al. Count-based differential expression analysis of RNA sequencing data using R and Bioconductor. *Nat Protoc*. 2013;8(9):1765-1786. doi:10.1038/nprot.2013.099.

124. Bolstad BM, Irizarry RA, Astrand M, Speed TP. A comparison of normalization methods for high density oligonucleotide array data based on variance and bias. *Bioinformatics*. 2003;19(2):185-193. http://www.ncbi.nlm.nih.gov/pubmed/12538238. Accessed May 4, 2017.

125. Smyth GK. Linear Models and Empirical Bayes Methods for Assessing Differential Expression in Microarray Experiments. *Stat Appl Genet Mol Biol*. 2004;3(1):1-25. doi:10.2202/1544-6115.1027.

126. Ritchie ME, Phipson B, Wu D, et al. limma powers differential expression analyses for RNA-sequencing and microarray studies. *Nucleic Acids Res*. 2015;43(7):e47-e47. doi:10.1093/nar/gkv007.

127.   Kramer A, Green J, Pollard J, Tugendreich S. Causal analysis approaches in Ingenuity Pathway Analysis. *Bioinformatics*. 2014;30(4):523-530. doi:10.1093/bioinformatics/btt703.

128.   Subramanian A, Tamayo P, Mootha VK, et al. Gene set enrichment analysis: a knowledge-based approach for interpreting genome-wide expression profiles. *Proc Natl Acad Sci U S A*. 2005;102(43):15545-15550. doi:10.1073/pnas.0506580102.

129.   Xie X, Lu J, Kulbokas EJ, et al. Systematic discovery of regulatory motifs in human promoters and 3' UTRs by comparison of several mammals. *Nature*. 2005;434(7031):338-345. doi:10.1038/nature03441.

130.   Rasband WS. ImageJ. 2016. https://imagej.nih.gov/ij/. Accessed May 1, 2017.

131.   Livak KJ, Schmittgen TD. Analysis of Relative Gene Expression Data Using Real-Time Quantitative PCR and the 2−ΔΔCT Method. *Methods*. 2001;25(4):402-408. doi:10.1006/meth.2001.1262.

132.   Alasoo K, Martinez FO, Hale C, et al. Transcriptional profiling of macrophages derived from monocytes and iPS cells identifies a conserved response to LPS and novel alternative transcription. *Sci Rep*. 2015;5(1):12524. doi:10.1038/srep12524.

133.   Beyer M, Mallmann MR, Xue J, et al. High-Resolution Transcriptome of Human Macrophages. Zirlik A, ed. *PLoS One*. 2012;7(9):e45466. doi:10.1371/journal.pone.0045466.

134.   Björkbacka H, Fitzgerald KA, Huet F, et al. The induction of macrophage gene expression by LPS predominantly utilizes Myd88-independent signaling cascades. *Physiol Genomics*. 2004;19(3). http://physiolgenomics.physiology.org/content/19/3/319.long#sec-10. Accessed April 11, 2017.

135.   Damstrup L, Kuwada SK, Dempsey PJ, et al. Amphiregulin acts as an autocrine growth factor in two human polarizing colon cancer lines that exhibit domain selective EGF receptor mitogenesis. *Br J Cancer*. 1999;80(7):1012-1019. doi:10.1038/sj.bjc.6690456.

136.   Mittal R, Patel AP, Debs LH, et al. Intricate Functions of Matrix Metalloproteinases in Physiological and Pathological Conditions. *J Cell Physiol*. 2016;231(12):2599-2621. doi:10.1002/jcp.25430.

137.   Van Lint P, Libert C. Chemokine and cytokine processing by matrix metalloproteinases and its effect on leukocyte migration and inflammation. *J

Leukoc Biol. 2007;82(6):1375-1381. doi:10.1189/jlb.0607338.

138.   Le Y, Zhou Y, Iribarren P, Wang JM. Cellular & Molecular Immunology Chemokines and Chemokine Receptors: Their Manifold Roles in Homeostasis and Disease. 2004;1(2). http://www.cmi.ustc.edu.cn/1/2/95.pdf. Accessed June 11, 2017.

139.   Damås JK, Landrø L, Fevang B, et al. Homeostatic chemokines CCL19 and CCL21 promote inflammation in human immunodeficiency virus-infected patients with ongoing viral replication. *Clin Exp Immunol*. 2009;157(3):400-407. doi:10.1111/j.1365-2249.2009.03976.x.

140.   Alvarez E, Piccio L, Mikesell RJ, et al. CXCL13 is a biomarker of inflammation in multiple sclerosis, neuromyelitis optica, and other neurological conditions. *Mult Scler*. 2013;19(9):1204-1208. doi:10.1177/1352458512473362.

141.   Hayari Y, Kukulansky T, Gloherson A. Regulation of thymocyte proliferative response by macrophage-derived prostaglandin E2 and inter leukin 1. *Eur J Immunol*. 1985;15(1):43-47. doi:10.1002/eji.1830150109.

142.   Xaus J, Mirabet M, Lloberas J, et al. IFN-gamma up-regulates the A2B adenosine receptor expression in macrophages: a mechanism of macrophage deactivation. *J Immunol*. 1999;162(6):3607-3614. http://www.ncbi.nlm.nih.gov/pubmed/10092821. Accessed June 12, 2017.

143.   Cross DAE, Alessi DR, Cohen P, Andjelkovich M, Hemmings BA. Inhibition of glycogen synthase kinase-3 by insulin mediated by protein kinase B. *Nature*. 1995;378(6559):785-789. doi:10.1038/378785a0.

144.   Bechard M, Dalton S. Subcellular Localization of Glycogen Synthase Kinase 3 Controls Embryonic Stem Cell Self-Renewal. *Mol Cell Biol*. 2009;29(8):2092-2104. doi:10.1128/MCB.01405-08.

145.   Buendía AJ, Del Río L, Ortega N, et al. B-cell-deficient mice show an exacerbated inflammatory response in a model of Chlamydophila abortus infection. *Infect Immun*. 2002;70(12):6911-6918. doi:10.1128/iai.70.12.6911-6918.2002.

146.   Nishio N, Ito S, Suzuki H, Isobe K-I. Antibodies to wounded tissue enhance cutaneous wound healing. *Immunology*. 2009;128(3):369-380. doi:10.1111/j.1365-2567.2009.03119.x.

147.   Nosbaum A, Prevel N, Truong H-A, et al. Cutting Edge: Regulatory T Cells Facilitate Cutaneous Wound Healing. *J Immunol*. 2016;196(5):2010-2014. doi:10.4049/jimmunol.1502139.

148. Hofmann U, Frantz S. Role of Lymphocytes in Myocardial Injury, Healing, and Remodeling After Myocardial Infarction. *Circ Res*. 2015;116(2):354-367. doi:10.1161/CIRCRESAHA.116.304072.

149. Könnecke I, Serra A, El Khassawna T, et al. T and B cells participate in bone repair by infiltrating the fracture callus in a two-wave fashion. *Bone*. 2014;64:155-165. doi:10.1016/j.bone.2014.03.052.

150. Yang S, Ding W, Feng D, et al. Loss of B cell regulatory function is associated with delayed healing in patients with tibia fracture. *APMIS*. 2015;123(11):975-985. doi:10.1111/apm.12439.

151. Huang Y-K, Fan X-G, Qiu F. TM4SF1 Promotes Proliferation, Invasion, and Metastasis in Human Liver Cancer Cells. *Int J Mol Sci*. 2016;17(5):661. doi:10.3390/ijms17050661.

152. McMahan RS, Birkland TP, Smigiel KS, et al. Stromelysin-2 (MMP10) Moderates Inflammation by Controlling Macrophage Activation. *J Immunol*. 2016;197(3):899-909. doi:10.4049/jimmunol.1600502.

153. Koller FL, Dozier EA, Nam KT, et al. Lack of MMP10 exacerbates experimental colitis and promotes development of inflammation-associated colonic dysplasia. *Lab Investig*. 2012;92(12):1749-1759. doi:10.1038/labinvest.2012.141.

154. Xu J, E C, Yao Y, Ren S, Wang G, Jin H. Matrix metalloproteinase expression and molecular interaction network analysis in gastric cancer. *Oncol Lett*. 2016;12(4):2403-2408. doi:10.3892/ol.2016.5013.

155. Ke X, Zhang S, Wu M, et al. Tumor-associated macrophages promote invasion via Toll-like receptors signaling in patients with ovarian cancer. *Int Immunopharmacol*. 2016;40:184-195. doi:10.1016/j.intimp.2016.08.029.

156. Nicola NA, Babon JJ. Leukemia inhibitory factor (LIF). *Cytokine Growth Factor Rev*. 2015;26(5):533-544. doi:10.1016/j.cytogfr.2015.07.001.

157. Al-Sajee D, Nissar AA, Coleman SK, et al. Xin-deficient mice display myopathy, impaired contractility, attenuated muscle repair and altered satellite cell functionality. *Acta Physiol*. 2015;214(2):248-260. doi:10.1111/apha.12455.

158. Johnson JL, Dwivedi A, Somerville M, George SJ, Newby AC. Matrix Metalloproteinase (MMP)-3 Activates MMP-9 Mediated Vascular Smooth Muscle Cell Migration and Neointima Formation in Mice. *Arterioscler Thromb Vasc Biol*. 2011;31(9):e35-e44. doi:10.1161/ATVBAHA.111.225623.

159. Sahin H, Tholema N, Petersen W, Raschke MJ, Stange R. Impaired biomechanical properties correlate with neoangiogenesis as well as VEGF and MMP-3 expression during rat patellar tendon healing. *J Orthop Res*. 2012;30(12):1952-1957. doi:10.1002/jor.22147.

160. Takimoto K, Kawashima N, Suzuki N, et al. Down-regulation of Inflammatory Mediator Synthesis and Infiltration of Inflammatory Cells by MMP-3 in Experimentally Induced Rat Pulpitis. *J Endod*. 2014;40(9):1404-1409. doi:10.1016/j.joen.2014.04.001.

161. Tanaka S, Miyagi T, Dohi E, et al. Developmental expression of GPR3 in rodent cerebellar granule neurons is associated with cell survival and protects neurons from various apoptotic stimuli. *Neurobiol Dis*. 2014;68:215-227. doi:10.1016/j.nbd.2014.04.007.

162. Godlewski G, Jourdan T, Szanda G, et al. Mice lacking GPR3 receptors display late-onset obese phenotype due to impaired thermogenic function in brown adipose tissue. *Sci Rep*. 2015;5:14953. doi:10.1038/srep14953.

163. Pardo A, Selman M. MMP-1: the elder of the family. *Int J Biochem Cell Biol*. 2005;37(2):283-288. doi:10.1016/j.biocel.2004.06.017.

164. Juncker-Jensen A, Deryugina EI, Rimann I, et al. Tumor MMP-1 Activates Endothelial PAR1 to Facilitate Vascular Intravasation and Metastatic Dissemination. *Cancer Res*. 2013;73(14):4196-4211. doi:10.1158/0008-5472.CAN-12-4495.

165. Heo S-K, Noh E-K, Gwon G-D, et al. LIGHT (TNFSF14) Increases the Survival and Proliferation of Human Bone Marrow-Derived Mesenchymal Stem Cells. Kerkis I, ed. *PLoS One*. 2016;11(11):e0166589. doi:10.1371/journal.pone.0166589.

166. Krause P, Zahner SP, Kim G, Shaikh RB, Steinberg MW, Kronenberg M. The Tumor Necrosis Factor Family Member TNFSF14 (LIGHT) Is Required for Resolution of Intestinal Inflammation in Mice. *Gastroenterology*. 2014;146(7):1752-1762.e4. doi:10.1053/j.gastro.2014.02.010.

167. Chiu Y-H, Ritchlin CT. DC-STAMP: A Key Regulator in Osteoclast Differentiation. *J Cell Physiol*. 2016;231(11):2402-2407. doi:10.1002/jcp.25389.

168. Zeng XX, Chu TJ, Yuan JY, et al. Transmembrane 7 superfamily member 4 regulates cell cycle progression in breast cancer cells. *Eur Rev Med Pharmacol Sci*. 2015;19(22):4353-4361. http://www.ncbi.nlm.nih.gov/pubmed/26636523. Accessed June 12, 2017.

169. Guo L, Li S-Y, Ji F-Y, et al. Role of Angptl4 in vascular permeability and inflammation. *Inflamm Res*. 2014;63(1):13-22. doi:10.1007/s00011-013-0678-0.

170. de Kretser DM, O'Hehir RE, Hardy CL, Hedger MP. The roles of activin A and its binding protein, follistatin, in inflammation and tissue repair. *Mol Cell Endocrinol*. 2012;359(1-2):101-106. doi:10.1016/j.mce.2011.10.009.

171. Lin J, Kurilova S, Scott BL, et al. TIRF imaging of Fc gamma receptor microclusters dynamics and signaling on macrophages during frustrated phagocytosis. *BMC Immunol*. 2016;17(1):5. doi:10.1186/s12865-016-0143-2.

172. Oh JH, Lee NK. Up-Regulation of RANK Expression via ERK1/2 by Insulin Contributes to the Enhancement of Osteoclast Differentiation. *Mol Cells*. 2017;40(5):371-377. doi:10.14348/molcells.2017.0025.

173. Rajasekaran D, Gröning S, Schmitz C, et al. Macrophage Migration Inhibitory Factor-CXCR4 Receptor Interactions. *J Biol Chem*. 2016;291(30):15881-15895. doi:10.1074/jbc.M116.717751.

174. Majetschak M. Extracellular ubiquitin: immune modulator and endogenous opponent of damage-associated molecular pattern molecules. *J Leukoc Biol*. 2011;89(2):205-219. doi:10.1189/jlb.0510316.

175. Ba H, Li B, Li X, et al. Transmembrane tumor necrosis factor-α promotes the recruitment of MDSCs to tumor tissue by upregulating CXCR4 expression via TNFR2. *Int Immunopharmacol*. 2017;44:143-152. doi:10.1016/j.intimp.2016.12.028.

176. Mota JM, Leite CA, Souza LE, et al. Post-Sepsis State Induces Tumor-Associated Macrophage Accumulation through CXCR4/CXCL12 and Favors Tumor Progression in Mice. *Cancer Immunol Res*. 2016;4(4):312-322. doi:10.1158/2326-6066.CIR-15-0170.

177. Cristillo AD, Bierer BE. Regulation of CXCR4 expression in human T lymphocytes by calcium and calcineurin. *Mol Immunol*. 2003;40(8):539-553. http://www.ncbi.nlm.nih.gov/pubmed/14563373. Accessed June 26, 2017.

178. CRISTILLO AD, Highbarger HC, Dewar RL, Dimitrov DS, Golding H, Bierer BE. Up-regulation of HIV coreceptor CXCR4 expression in human T lymphocytes is mediated in part by a cAMP-responsive element. *FASEB J*. 2002;16(3):354-364. doi:10.1096/fj.01-0744com.

179. Schröder AK, Uciechowski P, Fleischer D, Rink L. Crosslinking of CD66b on Peripheral Blood Neutrophils Mediates the Release of Interleukin-8 from

Intracellular Storage. *Hum Immunol*. 2006;67(9):676-682. doi:10.1016/j.humimm.2006.05.004.

180. Yoon J, Terada A, Kita H. CD66b regulates adhesion and activation of human eosinophils. *J Immunol*. 2007;179(12):8454-8462. http://www.ncbi.nlm.nih.gov/pubmed/18056392. Accessed June 26, 2017.

181. Wang J, Brown EJ. Immune Complex-induced Integrin Activation and L-plastin Phosphorylation Require Protein Kinase A. *J Biol Chem*. 1999;274:24349-24356. http://www.jbc.org/content/274/34/24349.full.pdf. Accessed June 12, 2017.

182. Justilien V, Regala RP, Tseng I-C, et al. Matrix metalloproteinase-10 is required for lung cancer stem cell maintenance, tumor initiation and metastatic potential. *PLoS One*. 2012;7(4):e35040. doi:10.1371/journal.pone.0035040.

183. Frost JA, Geppert TD, Cobb MH, Feramisco JR. A requirement for extracellular signal-regulated kinase (ERK) function in the activation of AP-1 by Ha-Ras, phorbol 12-myristate 13-acetate, and serum. *Proc Natl Acad Sci U S A*. 1994;91(9):3844-3848. http://www.ncbi.nlm.nih.gov/pubmed/8170999. Accessed June 9, 2017.

184. Song G, Ouyang G, Bao S. The activation of Akt/PKB signaling pathway and cell survival. *J Cell Mol Med*. 2005;9(1):59-71. http://www.ncbi.nlm.nih.gov/pubmed/15784165. Accessed June 12, 2017.

185. Lee YG, Lee J, Byeon SE, et al. Functional role of Akt in macrophage-mediated innate immunity. *Front Biosci (Landmark Ed*. 2011;16:517-530. http://www.ncbi.nlm.nih.gov/pubmed/21196185. Accessed June 9, 2017.

186. Brennan P, Babbage JW, Burgering BM, Groner B, Reif K, Cantrell DA. Phosphatidylinositol 3-kinase couples the interleukin-2 receptor to the cell cycle regulator E2F. *Immunity*. 1997;7(5):679-689. http://www.ncbi.nlm.nih.gov/pubmed/9390691. Accessed June 9, 2017.

187. Marshall JG, Booth JW, Stambolic V, et al. Restricted accumulation of phosphatidylinositol 3-kinase products in a plasmalemmal subdomain during Fc gamma receptor-mediated phagocytosis. *J Cell Biol*. 2001;153(7):1369-1380. http://www.ncbi.nlm.nih.gov/pubmed/11425868. Accessed February 27, 2017.

188. Martin M, Rehani K, Jope RS, Michalek SM. Toll-like receptor-mediated cytokine production is differentially regulated by glycogen synthase kinase 3. *Nat Immunol*. 2005;6(8):777-784. doi:10.1038/ni1221.

189. Park SH, Park-Min K-H, Chen J, Hu X, Ivashkiv LB. Tumor necrosis factor

induces GSK3 kinase–mediated cross-tolerance to endotoxin in macrophages. *Nat Immunol*. 2011;12(7):607-615. doi:10.1038/ni.2043.

190. Götschel F, Kern C, Lang S, et al. Inhibition of GSK3 differentially modulates NF-κB, CREB, AP-1 and β-catenin signaling in hepatocytes, but fails to promote TNF-α-induced apoptosis. *Exp Cell Res*. 2008;314(6):1351-1366. doi:10.1016/j.yexcr.2007.12.015.

191. Kim H-S, Skurk C, Thomas SR, et al. Regulation of angiogenesis by glycogen synthase kinase-3beta. *J Biol Chem*. 2002;277(44):41888-41896. doi:10.1074/jbc.M206657200.

192. Karrasch T, Spaeth T, Allard B, Jobin C. PI3K-Dependent GSK3ß(Ser9)-Phosphorylation Is Implicated in the Intestinal Epithelial Cell Wound-Healing Response. Harwood AJ, ed. *PLoS One*. 2011;6(10):e26340. doi:10.1371/journal.pone.0026340.

193. Meares GP, Jope RS. Resolution of the nuclear localization mechanism of glycogen synthase kinase-3: functional effects in apoptosis. *J Biol Chem*. 2007;282(23):16989-17001. doi:10.1074/jbc.M700610200.

194. Gerber JS, Mosser DM. Reversing Lipopolysaccharide Toxicity by Ligating the Macrophage Fcγ Receptors. *J Immunol*. 2001;166(11). http://www.jimmunol.org/content/166/11/6861.long. Accessed July 19, 2017.

195. Dugo L, Collin M, Allen DA, et al. Inhibiting glycogen synthase kinase 3beta in sepsis. *Novartis Found Symp*. 2007;280:128-42-6, 160-164. http://www.ncbi.nlm.nih.gov/pubmed/17380792. Accessed September 30, 2016.

196. Martin M, Rehani K, Jope RS, Michalek SM. Toll-like receptor-mediated cytokine production is differentially regulated by glycogen synthase kinase 3. *Nat Immunol*. 2005;6(8):777-784. doi:10.1038/ni1221.